

THE UNIVERSITY OF MICHIGAN
COLLEGE OF ENGINEERING
Department of Meteorology and Oceanography

Technical Report

NONLINEAR ASPECTS OF THE LARGE-SCALE MOTION IN THE ATMOSPHERE

Chien-hsiung Yang

Aksel C. Wiin-Nielsen
Project Director

ORA Project 08759

supported by:

NATIONAL SCIENCE FOUNDATION
GRANT NO. GA-841
WASHINGTON, D.C.

administered through:

OFFICE OF RESEARCH ADMINISTRATION ANN ARBOR

November 1967

This report was also a dissertation submitted by the first author in partial fulfillment of the requirements for the degree of Doctor of Philosophy in The University of Michigan, 1967.

TABLE OF CONTENTS

	Page
LIST OF TABLES	v
LIST OF FIGURES	vii
ABSTRACT	x
1. INTRODUCTION	1
1.1 An Outline of the Study	1
1.2 Observational Studies of Atmospheric Energetics	2
1.3 An Analytical Study of Nonlinear Effects of Baro- clinic Stability	9
2. FORMULATION AND DERIVATION	16
2.1 Fundamental Equations	16
2.2 Equations for Energies of Zonal Mean and Eddies	18
2.2.1 Kinetic Energy	19
2.2.2 Available Potential Energy	22
2.3 Equations in the Wave-Number Domain	24
2.4 Tendency Equations for the Energies of the nth Component	27
2.4.1 Kinetic Energy	27
2.4.2 Available Potential Energy	35
2.5 Physical Interpretation	36
2.6 Computation Procedure	39
3. RESULTS	44
3.1 Introduction	44
3.1.1 Analysis and Synthesis	44
3.1.2 A Brief Description of the General Circula- tion Observed During the Period	46
3.2 Annual Averages	47
3.3 Annual Variations	59
3.4 Decomposition of Exchanges and Influxes in the Time Domain	73
3.5 Decomposition of Exchanges Among Waves into Ele- mentary Interactions	85
3.6 A Flow Diagram of Atmospheric Energy	90

TABLE OF CONTENTS (Concluded)

	Page
4. AN ANALYTICAL STUDY OF NONLINEAR EFFECTS IN WEAK BAROCLINIC INSTABILITY	96
4.1 Model	96
4.2 Linearized Theory	100
4.3 Curve of Critical Stability	103
4.4 System of Nonlinear Equations	105
4.5 Simplification of the Nonlinear Problem of Stability in the Limit of $c_i \rightarrow 0$	110
4.6 Numerical Results	130
5. CONCLUDING REMARKS	142
5.1 Conjectures	142
5.2 Justifications	144
5.3 Opportunities	146
BIBLIOGRAPHY	148
APPENDIX	
A. RELATIONSHIPS BETWEEN COMPLEX AND REAL EXPRESSIONS	151
B. MONTHLY AVERAGES AND STANDARD ERRORS OF EXCHANGES AND INFLUXES	159
C. MONTHLY MEANS OF ZONAL WIND AND ZONAL TEMPERATURE	167
D. ZONAL INDICES	172

LIST OF TABLES

Table		Page
1	List of Transform Pairs	25
2	Static Stability, $\bar{\sigma}(10^{-6} \text{ kg}^{-2} \text{ m}^4 \text{ sec}^2)$	42
3	Flow of Kinetic Energy Due to the Interaction Among Waves	67
4	Flow of Potential Energy Due to the Interaction Among Waves	68
5	Compositions of Exchanges and Influxes of Kinetic Energy in the Time Domain---Annual Averages, Total Atmosphere (unit: $\text{ergs cm}^{-2} \text{ sec}^{-1}$)	76
6	Compositions of Exchanges and Influxes of Available Potential Energy in the Time Domain---Annual Averages, Total Atmosphere (unit: $\text{ergs cm}^{-2} \text{ sec}^{-1}$)	76
7	Compositions of Exchanges and Influxes of Kinetic Energy in the Time Domain---Annual Averages, Individual Layers (unit: $\text{ergs cm}^{-2} \text{ sec}^{-1} \text{ cb}^{-1}$)	82
8	Compositions of Exchanges and Influxes of Available Potential Energy in the Time Domain---Annual Averages, Individual Layers (unit: $\text{ergs cm}^{-2} \text{ sec}^{-1} \text{ cb}^{-1}$)	83
9	Compositions of Exchanges and Influxes of Energies of the Zonal Mean in the Time Domain---Annual Averages, Individual Layers ($\text{ergs cm}^{-2} \text{ sec}^{-1} \text{ cb}^{-1}$)	86
10	Decomposition of Kinetic-Energy Exchanges into Elementary Interactions, Averages of 58 Sets of Observations in March, 1963 for the Total Atmosphere (unit: $\text{ergs cm}^{-2} \text{ sec}^{-1}$)	91
11	Monthly Averages of Quantities Evaluated from Energy Balance (unit: $\text{erg cm}^{-2} \text{ sec}^{-1}$)	94
12	Critical Wind Shear (m sec^{-1})	132
13	Value of $\epsilon_1(10^{-13} \text{ m}^{-3} \text{ sec})$ on the Critical Stability	134
14	Value of μ_S/v_S (10 msec^{-1})	135

LIST OF TABLES (Concluded)

Table		Page
B1	Monthly Means and Their Standard Errors of $C(K_Z, K_n)$	160
B2	Monthly Means and Their Standard Errors of $\sum_m C(K_m, K_n)$	161
B3	Monthly Means and Their Standard Errors of $F(K_E)$	162
B4	Monthly Means and Their Standard Errors of $C(E_Z, E_n)$	163
B5	Monthly Means and Their Standard Errors of $\sum_m C(E_m, E_n)$	164
B6	Monthly Means and Their Standard Errors of $F(E_n)$	165
B7	Monthly Means and Their Standard Errors of $F(K_Z)$ and $F(E_Z)$	166

LIST OF FIGURES

Figure	Page
1. Vertical resolution of the computation.	41
2. Annual averages of exchanges and influxes of kinetic energy ($\text{erg cm}^{-2} \text{sec}^{-1}$) in the total atmosphere (0~100 cb).	48
3. Annual averages of exchanges and influxes of available potential energy ($\text{erg cm}^{-2} \text{sec}^{-1}$) in the total atmosphere (10~100 cb).	49
4. A comparison between the results obtained by Saltzman and Teweles (1964) and those of the present study on the kinetic energy exchanges at 500 mb (unit: $\text{erg cm}^{-2} \text{sec}^{-1}$).	52
5. Vertical variations of exchanges and influxes of eddy kinetic energy ($\text{erg cm}^{-2} \text{sec}^{-1} \text{cb}^{-1}$).	54
6. Vertical variations of exchanges and influxes of eddy available potential energy ($\text{erg cm}^{-2} \text{sec}^{-1} \text{cb}^{-1}$).	55
7. Vertical variations of exchanges and influxes of kinetic and available potential energies of the zonal mean ($\text{erg cm}^{-2} \text{sec}^{-1} \text{cb}^{-1}$).	56
8(A). $C(K_Z, K_E)$ ($\text{erg cm}^{-2} \text{sec}^{-1}$) in the total atmosphere (0~100 cb).	60
8(B). $C(K_Z, K_E)$ ($\text{erg cm}^{-2} \text{sec}^{-1}$) in the individual layers.	60
9(A). $C(E_Z, E_E)$ ($\text{erg cm}^{-2} \text{sec}^{-1}$) in the total atmosphere (10-100 cb).	62
9(B). $C(E_Z, E_E)$ ($\text{erg cm}^{-2} \text{sec}^{-1} \text{cb}^{-1}$) in the individual layers.	62
10(A). $C(K_{E'}, K_E)$ ($\text{erg cm}^{-2} \text{sec}^{-1}$) in the total atmosphere (0-100 cb).	64
10(B). $C(K_{E'}, K_E)$ ($\text{erg cm}^{-2} \text{sec}^{-1} \text{cb}^{-1}$) in the individual layers.	64
11(A). $C(E_{E'}, E_E)$ ($\text{erg cm}^{-2} \text{sec}^{-1}$) in the total atmosphere (10-100 cb).	65

LIST OF FIGURES (Continued)

Figure	Page
11(B). $C(E_E, E_E)$ ($\text{erg cm}^{-2} \text{ sec}^{-1} \text{ cb}^{-1}$) in the individual layers.	65
12(A). $F(K_E)$ ($\text{erg cm}^{-2} \text{ sec}^{-1}$) in the total atmosphere (0-100 cb).	70
12(B). $F(K_E)$ ($\text{erg cm}^{-2} \text{ sec}^{-1} \text{ cb}^{-1}$) in the individual layers.	70
13(A). $F(E_E)$ ($\text{erg cm}^{-2} \text{ sec}^{-1}$) in the total atmosphere (10-100 cb).	71
13(B). $F(E_E)$ ($\text{erg cm}^{-2} \text{ sec}^{-1} \text{ cb}^{-1}$) in the individual layers.	71
14(A). Exchanges and influxes of energies of the zonal mean in the total atmosphere ($\text{erg cm}^{-2} \text{ sec}^{-1}$).	72
14(B). Exchanges and influxes of energies of the zonal mean in the individual layers ($\text{erg cm}^{-2} \text{ sec}^{-1} \text{ cb}^{-1}$).	72
15. Compositions of $C(K_Z, K_E)$ ($\text{erg cm}^{-2} \text{ sec}^{-1}$) in the total atmosphere (0-100 cb).	78
16. Compositions of $C(E_Z, E_E)$ ($\text{erg cm}^{-2} \text{ sec}^{-1}$) in the total atmosphere (10-100 cb).	78
17. Compositions of $C(K_E, K_E)$ ($\text{erg cm}^{-2} \text{ sec}^{-1}$) in the total atmosphere (0-100 cb).	79
18. Compositions of $C(E_E, E_E)$ ($\text{erg cm}^{-2} \text{ sec}^{-1}$) in the total atmosphere (100-100 cb).	79
19. Compositions of $F(K_E)$ ($\text{erg cm}^{-2} \text{ sec}^{-1}$) in the total atmosphere (0-100 cb).	80
20. Compositions of $F(K_E)$ ($\text{erg cm}^{-2} \text{ sec}^{-1}$) in the total atmosphere (10-100 cb).	80
21. Compositions of exchanges and influxes of energies of the zonal mean ($\text{erg cm}^{-2} \text{ sec}^{-1}$) in the total atmosphere.	87
22. Flow diagram of the atmospheric energy, averaged over a year from February, 1963 to January, 1964 for the region north of 20°N.	95

LIST OF FIGURES (Concluded)

Figure	Page
23. A two-level quasi-geostrophic baroclinic model.	96
24. Variations of $ A_M ^2$ with time.	119
25. Variations of c_i , ϵ_i , $ A_M^\infty $, $ A_S^\infty $ with $\Delta U_S = U_S - U_{SC}$. $K_V = k \times 10^5 \text{ m}^2 \text{ sec}^{-1}$, $H = 0$.	136
26. Variations of c_i , ϵ_i , $ A_M^\infty $, $ A_S^\infty $ with $\Delta U_S = U_S - U_{SC}$. $K_V = k \times 10^5 \text{ m}^2 \text{ sec}^{-1}$, $H = 4 \times 10^{-7} \text{ sec}^{-1}$.	138
27. Initial segments of trajectories in the $(-A_{SC}, A_M ^2)$ -plane.	140
28. A schematic diagram of the distributions of energy and energy exchanges in the atmosphere. The ordinate is energy in the unit of watt m^{-2} .	145

ABSTRACT

Nonlinear aspects of the large-scale motion in the atmosphere are studied observationally in the energy exchanges among the harmonic components and analytically in the effects of nonlinear interactions upon the growth of baroclinic waves.

In the observational study the energy exchanges arising from the horizontal advections of momentum and heat by the nondivergent component of the geostrophic motion are calculated in the region north of 20°N diagnostically from the observations of the heights of isobaric surface taken daily during the period from February, 1963 to January, 1964.

The major conclusions which can be drawn from the study are:

(i) There is a "predominant" mode of energy exchange which prevails in the atmosphere. Such a predominant mode of energy is well represented by the pattern obtained from the averages of the exchanges over a year.

(ii) In the predominant mode of energy exchange available potential energy is transferred from the motion of larger scale to that of smaller scale in the troposphere, while the reverse transfer of a smaller magnitude takes place in the lower stratosphere. On the other hand, kinetic energy is transferred from the eddies to the zonal mean flow throughout the atmosphere and largely in the layer close to the jet-stream level. The transfer of kinetic energy from the cyclone waves to both the larger and smaller scales of motion plays an important role in the exchanges of kinetic energy.

(iii) The exchanges and influxes are generally greater in winter than in summer and major deviations from the predominant mode of the exchange pattern occur mainly in summer. The influx of zonal kinetic energy from the tropics in the upper atmosphere is important in sustaining the zonal flow by augmenting the transfer from the eddy kinetic energy.

(iv) The exchanges involving the intermediate and smaller scales of motion are largely due to the presence of the rapidly fluctuating component of the motion, whereas the exchanges among the motion of larger scale arise from the slowly fluctuating and stationary components of the motion.

In the analytical study the development of baroclinic waves superimposed upon a constant parallel flow in a rectangular region of the β -plane is investigated by including the most important nonlinear interactions. The horizontal eddy diffusion and Newtonian cooling are assumed to be the mechanism responsible for dissipation of energy.

The method employed is that of Stuart and Watson (1960) in which the amplification factor of the amplitude of the wave disturbance is used as the small parameter of the system and is thus applied to the basic wind shear which is slightly different from the critical value.

It is shown that in such a model the initial nonlinear effect appears in the eddy heat transport which modifies the parallel shear flow and that the modification of the parallel shear flow interacts with the wave disturbance in such a way as to inhibit the amplitude of the latter from growing indefinitely with time.

It is furthermore shown that insofar as the secondary nonlinear interactions may be neglected such nonlinear interactions result in the amplitude of the wave disturbance and of the modification of the basic shear flow that tend asymptotically to equilibrium values. These equilibrium values are computed numerically by using values of the parameters typical of the real atmosphere and are shown to be small compared with those observed in the atmosphere.

Numerical integrations are also carried out on a number of examples to illustrate the variations of these amplitudes with time while approaching the equilibrium values. It is seen in these examples that the amplitudes are slowly varying functions of time and that the variations are well within the range of those observed in the real atmosphere.

1. INTRODUCTION

1.1 AN OUTLINE OF THE STUDY

The presence of the nonlinear terms in the Navier-Stokes equations of motion is well known. In the large-scale atmospheric flow, even after due account is taken of the major characteristics that are of meteorological interest (see, for example, Charney (1960)), the nonlinear terms that represent the horizontal advection of momentum (or vorticity) are seen to be of the same order of magnitude as the rate of local change of momentum (or vorticity). This implies that, as long as our concern is the variation of the flow, such nonlinear terms play a role of fundamental importance, and understanding of their modi operandi is essential for a satisfactory description of the phenomena associated with the flow.

Initiated by this recognition, the first phase of the work was devoted to an observational study of the nonlinear aspects of the large-scale flow in the atmosphere as they appeared in energy exchanges, with the hope that such an investigation would reveal the relative importance of the nonlinear aspects in comparison with others that have become known through similar studies by others. An attempt was then made, in the second phase, to carry out an analytical study on a relatively simple model of the large-scale atmospheric flow in which the effect of non-linearity is accounted for. This was accomplished by an investigation of

the initial effects of nonlinear interactions on the behavior of a baroclinically unstable parallel flow.

1.2 OBSERVATIONAL STUDIES OF ATMOSPHERIC ENERGETICS

Based on the classical work of Lorenz (1955), in which he introduced the concept of available potential energy and derived a set of equations depicting the energy cycle in the atmosphere, the field of atmospheric energetics has enjoyed a constant growth in the number of related studies over the past decade. Excellent reviews and summaries have since been published (Krueger, Winston and Haines (1965), Oort (1964), Wiin-Nielsen (1964)).

Considering energy as being distributed into a number of compartments by the decomposition of a flow into its zonal and eddy motions and by a differentiation between various forms of energy, e.g., available potential and kinetic energies, the major concern of most of these studies has been centered around the magnitudes of energy in and the rates of exchange of energy among these individual compartments. The results of these studies have revealed many important features of the atmospheric energy cycle that seem to prevail in the region outside the tropics in the Northern Hemisphere. For example, it is well recognized by now that the dominant mode of energy transfer in the atmosphere has energy flow from zonal potential to zonal kinetic energy via eddy potential and eddy kinetic energy, in that order. Since, in principle, there is no upper limit to the number of distinctive compartments among

which energy can be partitioned and exchanges may be considered, analysis of this nature may be carried out to investigate further details of the exchange processes by increasing the number of compartments. Wiin-Nielsen's work (1964), in which kinetic energy is partitioned into the vertical-mean zonal flow, vertical-mean eddy flow, vertical-shear zonal flow, and vertical-shear eddy flow, is such an example.

Saltzman (1957), on the other hand, derived formulas for major exchange processes which involve both available potential and kinetic energies and occur among all the compartments obtained by a Fourier analysis in longitude of a given flow. In such a formulation exchange processes may be classified into two categories. To the first category belong all the exchange processes arising from the linear terms in the equations of motion and the thermodynamic equation. These may be termed as the one-component exchanges in the sense that the formula for such an exchange involves only one wave component. Such processes as generation of potential energy, conversion between potential and kinetic energies, and dissipation of kinetic energy by friction all belong to this category. They refer to the processes that result in changes of the form of energy. To the second category belong all the exchange processes arising from the nonlinear terms in the equations of motion and the thermodynamic equation. These can be further subdivided into two kinds, namely the two-component and three-component exchanges. A two-component exchange arises from interactions between the zonal motion and a single wave component in the eddy motion, or from interactions between a wave

component and its first harmonic in the eddy motion. The conversion of available potential energy from the zonal mean to eddies is an example of the first type of the two-component exchange. On the other hand, a three-component exchange arises from interactions among three wave components, and the formula for such an exchange involves three wave numbers. The three-component exchange and the two-component exchange between harmonics result in redistribution of energy in the eddy motion. The three-component exchange can be distinguished by its conservation property from both the one- and two-component exchanges. Suppose A, B, and C form a triad of compartments in which a three-component exchange can take place. If the gains in A, B, and C due to such a three-component exchange are denoted respectively by $G(A;B,C)$, $G(B;C,A)$, and $G(C;A,B)$, the conservation property states that

$$G(A;B,C) + G(B;C,A) + G(C;A,B) = 0$$

in contrast to

$$G(A;B) + G(B;A) = 0$$

which holds for the one- or two-component exchange. Thus, while knowledge of the gain in one compartment is sufficient to determine the one- or two-component exchange, it is no longer so in a three-component exchange. $G(A;B,C)$ alone does not tell how much of it comes from B rather than C.

The use of Saltzman's formulas in an observational study was first reported by Saltzman and Fleisher (1960), in which gains of kinetic energy in individual components due to the two- and three-component exchanges were computed for the first 15 components of the eddy motion of the geostrophic flow at the 50-cb level observed daily in the year of 1952. The study was later extended by Saltzman and Teweles (1964) to cover a 9-year period extending from 1955 to 1964. By enlarging the size of the sample they were able to reduce the magnitudes of probable errors in the values of annual and seasonal means of the gains in the individual wave components. The principal conclusions drawn from these results are: (1) that all the 15 components in the eddy motion transfer kinetic energy to the zonal motion, (2) that among the components in the eddy motion those with wave number $n = 2$ and $5 \sim 10$ act as sources of kinetic energy for the rest, and (3) that the magnitude of gain (positive or negative) due to the three-component exchange is comparable with that due to the two-component exchange with the zonal motion in most of the wave components. The first conclusion agrees with the well-known notion that the atmosphere tends to have the eddy motion supply kinetic energy to the zonal motion. The third seems to document the importance of the three-component exchange relative to the two-component exchange. In the second conclusion, the source at wave number 2 has been interpreted as being due to a strong forced conversion of energy on the scale of the major continents and oceans, while the sources in wave numbers from 5 to 10 have been considered as an observational verification of

the theorems by Fjørtoft (1953) on energy transfer in two-dimensional, nondivergent flows. With regard to the latter, since Fjørtoft's theorems are based on spherical harmonics and the results of Saltzman-Teweles were obtained using the Fourier analysis in longitude, such an agreement seems to imply that the structure of eddies in the mid-troposphere tends to be isotropic in the mean when its projection on an isobaric surface is considered.

The work presented in this study is an extension of the studies by Saltzman et al., to a higher vertical resolution and also to available potential energy, with the intention of studying the vertical variations and obtaining better estimates for the total atmosphere of the magnitudes of such exchange processes. Considering the two- and three-component exchanges involving only the horizontal motion, the rates of change in both kinetic and available potential energies for the zonal mean and for each of the first 15 components in the eddies are calculated diagnostically from the distribution of the nondivergent component of the flow on each of eight isobaric surfaces, where daily observations at 00Z are available, for the period of a year from February 1963 to January 1964. The area covered extends from 20° to 85° latitude in the Northern Hemisphere. In computing the exchanges in available potential energy, specific volume, which is obtained from the vertical gradient of the stream function with the aid of the thermal-wind approximation, is employed instead of temperature. The derivation of the formulas for the exchanges is provided in Chapter 2 and a detailed analysis of the

results of the observational study in Chapter 3. However, a short summary of the major conclusions is given in the following paragraphs.

Speaking in terms of the annual averages for the total atmosphere, the results show that in the exchanges of kinetic energy all the wave components except wave number 3 in the eddies give up energy to the zonal motion and the components with wave number 2 and 5 ~ 11 act as sources for the rest through the exchanges among waves. Wave number 2 distinguishes itself from others as the largest sources both in the exchange with the zonal motion and in the exchange among waves. In the exchanges of available potential energy, on the other hand, all the wave components are fed by the zonal mean, while the components with wave number 2 ~ 5 and 7 act as sources for the others through interactions among waves. In both forms of energy the energy fluxes through the boundaries in the eddies are small compared to those in the zonal mean; nevertheless, the effect of such fluxes in the net gains of the individual wave components cannot be totally dismissed.

With regard to the vertical variation, the largest exchange in kinetic energy takes place in the region close to the jet-stream level, while the largest exchange in available potential energy occurs in the middle of the troposphere. Each of these seems to coincide with the level where the maximum amount of the energy itself is observed. There is a definite indication that the direction of transfer in the available potential energy exchanges in the lower stratosphere is opposite

to that in the troposphere. Contributions to the exchanges by long waves increase with height while those by short waves decrease.

In the kinetic-energy exchange due to interactions among waves, the medium-wave group (wave number $n = 6 \sim 10$) acts as a source for both the long-wave ($n = 1 \sim 5$) and short-wave ($n = 11 \sim 15$) groups in the troposphere, as Saltzman and Fleisher (loc. cit.) found on the 50-cb level in 1952, but there is very little gain in the short-wave group in the lower troposphere. In the lower stratosphere, however, the source tends to be displaced toward the long-wave group with both medium- and short-wave groups becoming the sink. In the available potential energy exchange due to interactions among waves, the long-wave group is definitely the source to the others in the troposphere, but becomes the sink in the lower stratosphere.

Almost all of the exchanges among waves are found to be carried out by the fast-transient waves throughout the entire atmosphere. The contributions to the exchanges by the slow-transient and stationary waves are found to increase with height and become important only in the exchange with the zonal mean. See Section 3.4 for the definition of the terms, "fast-transient," "slow-transient," and "stationary" waves.

While there are considerable variations in magnitude of the transfers due to these exchanges in the course of a year, the deviations in direction from that of the annual averages are mostly confined to the summer months.

1.3 AN ANALYTICAL STUDY OF NONLINEAR EFFECTS ON BAROCLINIC STABILITY

In the linearized theory of stability the perturbations imposed on an equilibrium flow are assumed to be infinitesimally small and, in the differential system governing the fluid motion, nonlinear terms in the perturbation quantities are neglected in comparison with the linear ones. The stability of an equilibrium flow is then defined with respect to such small perturbations. If the differential system under consideration is autonomous and if the equilibrium flow is stationary, the linearized equations of the stability problem admit solutions whose time dependence is given by an exponential function. The equilibrium flow is said to be unstable if there exists a perturbation which grows without limit in the course of time. On the other hand, if all the perturbations tend to zero as time tends to infinity, it is said to be stable. In the limiting case, in which there exists a perturbation which remains of constant amplitude while all others tend to zero in the course of time, the equilibrium flow is said to be neutral.

With such classifications made of an equilibrium flow on the basis of a linearized analysis the following questions seem to arise immediately:

(1) How small should a perturbation be in order that an equilibrium flow remains stable as predicted by the linearized theory? Or, posed differently, would an equilibrium flow remain stable with respect to a perturbation of small but finite amplitude in the stable regime?

(2) What are the immediate effects of a growing perturbation as its amplitude tends to grow with time to such an extent that the linearized theory is no longer valid?

An attempt is made in this study to see whether answers to the above questions can be obtained in cases where the rate of amplification (or damping) is sufficiently small by investigating the asymptotic behavior of the nonlinear effects using an approach originally developed by Stuart and Watson (1960) in the problem of baroclinic stability.

The problem of baroclinic stability is in this study formulated by using the two-level quasi-geostrophic model with a constant static stability on a β -plane, in which the stationary flow consists of constant parallel vertical-mean and vertical-shear flows. Such a model has been the object of many investigations that are based on the linearized theory. To cite a few, Phillips (1954) discussed the stability property of an adiabatic and frictionless atmosphere so modeled and Holopainen (1961) considered the effect of surface friction on the stability, while the study by Haltiner and Caverly (1965) dealt with the structure of the disturbances under the influence of surface friction. Wiin-Nielsen, Vernekar and Yang (1967) recently considered a model which incorporates surface friction and diabatic heating, both of which are assumed of linear nature, with the main emphasis on the energetics of the model.

The results of stability studies of the model may be said to consist of the following: (1) the frequency equation is quadratic; (2) the stability properties may be described on a (k, U_s) -plane, where k is the wave number of the travelling disturbance and U_s the speed of the stationary shear flow; (3) the unstable regime, in which only one of the

two admissible wave disturbances for a given wave number amplifies, is confined to the long-wave side of a certain critical wave number k_C , with the critical wind shear increasing asymptotically to infinity as $k \rightarrow k_C$ and $k \rightarrow 0$, and (4) the value of the critical wave number is determined by the field parameters of the model, while the critical wind shear is a function of the field parameters and the wave number of the disturbance. In this model, if the atmosphere is assumed to be of infinite transverse extent, as was done in most of the studies quoted above, the amplitude of the disturbances may be considered independent of the transverse coordinate and, hence, there would be no nonlinear effects of the disturbances.

For the purpose of introducing certain effects of interactions among disturbances, therefore, the transverse variation in the amplitudes of the wave disturbances is introduced by confining the atmosphere to a channel of finite width and by restraining the normal velocities at the boundaries to be zero. On the other hand, the periodicity of the atmospheric motion around a latitude is replaced by the imposition of the condition that the variation of the stream functions in the longitudinal direction should be cyclic with a given finite length. These two conditions will confine the atmosphere horizontally to a rectangle on the β -plane and also to limit the eigenfunctions to a denumerable set. It then follows from the result of the linearized theory that there exists only a finite number of modes of disturbance that are capable of leading to instability.

Horizontal eddy diffusion with constant diffusivities is assumed to be the mechanism responsible for dissipating both kinetic and available potential energies of wave disturbances. The type of diabatic heating that has been used by Wiin-Nielsen, Vernekar and Yang (loc. cit.) is also incorporated in the model. Such diabatic heating may be considered as a crude approximation to the heat exchange that takes place between the atmosphere and the earth's surface.

The method of Stuart and Watson developed in connection with a study of nonlinear effects in the two-dimensional stability problem is concerned with the asymptotic behavior of the time-dependent component of the amplitude of a periodic solution in a region of weak instability (or stability). It considers the problem of superimposing a wave disturbance of a prescribed mode (the fundamental disturbance) with a small but not infinitesimal amplitude on a parallel stationary flow. The nonlinear interactions in such a perturbed flow are then seen to start with a modification of the parallel flow and a generation of the first harmonics of the fundamental mode, both of which arise from interactions among the fundamental disturbances themselves, and proceed to cascade both up and down the harmonic scale. Representing, then, the stream function by a Fourier series in the coordinate along the direction of the parallel flow and assuming the amplitude function of each Fourier component separable in time and the transversal coordinate, one obtains a nonlinear ordinary differential equation for the time-dependent amplitude of the fundamental mode by the method of perturbation with the

amplification factor as the small parameter. The solution is then sought of such an equation with the terminal condition that: (i) if the amplification factor is positive (supercritical condition) the solution behaves as an exponentially increasing function as $t \rightarrow \infty$ or, (ii) if the amplification factor is negative (subcritical condition) the solution tends to an exponentially decreasing function as $t \rightarrow \infty$.

The analysis presented in this study (Chapter 4) stops at the first approximation, taking only the most important nonlinear effects into consideration, in applying the method of Stuart and Watson. It will be seen that, on account of the constant stationary flows assumed, the analysis is much simpler than that of Poiseuille or Couette flow and the first nonlinear effect appears only in a modification of the basic vertical-shear flow caused by the eddy heat transport, which, in turn, changes the energy transfer from the parallel flow into the fundamental disturbances and also produces a new mode of disturbance by interacting with the fundamental disturbances.

When c_i is very small, e.g. of the order of $.1 \text{ msec}^{-1}$ or less, the equation for the square amplitude of the fundamental disturbance in the vertical-mean flow is found to be of the form

$$\frac{d|A|^2}{dt} = 2\alpha_x c_i |A|^2 - 2\alpha_x \epsilon_i |A|^4$$

which is the same as that obtained by Stuart in the plane Poiseuille flow. It takes the form of the equation for a logistic curve and gives the limiting equilibrium amplitude as $t \rightarrow \infty$ if $\epsilon_i > 0$ in the supercrit-

ical condition ($c_i > 0$) and as $t \rightarrow -\infty$ if $\epsilon_i < 0$ in the subcritical condition ($c_i < 0$). Within the realm of the approximations made, if ϵ_i is of magnitude not less than order unity at the limit $c_i \rightarrow 0$, such an equilibrium amplitude may be considered to have a real significance. On the other hand, even when ϵ_i is found to be of magnitude less than order unity so that the value of the limiting amplitude no longer carries any real significance, the variation of the amplitude as prescribed by the above equation may still be considered as representing the behavior of the disturbance over a greater range of time than that of the linearized theory.

The numerical computation with the use of typical values in the real atmosphere for the field parameters show that the nonlinear effect included in the present analysis can indeed make a travelling wave-disturbance, which has been found to grow exponentially with time in the linearized theory, to attain a finite amplitude. However, the values of such limiting or equilibrium amplitudes are found to be small in comparison with what is generally observed in the real atmosphere.

When c_i is in the order of 1 msec^{-1} , the equation for the square amplitude of the fundamental disturbance in the vertical-mean flow takes the form

$$\frac{d|A|^2}{dt} = 2\alpha_x c_i |A|^2 \left(1 - \frac{\epsilon_i}{c_i} \int_{t_0}^t |A|^2 \exp(-\gamma(t-\tau)) d\tau \right) .$$

An investigation on the behavior of the solution, carried out on a system of differential equations which is equivalent to the above equation, reveals that when $c_i > 0$, $\epsilon_i > 0$ the solution tends asymptotically to

the equilibrium value c_i/ϵ_i as time goes to infinity with a undulatory variation. On the other hand, when $c_i < 0$, $\epsilon_i < 0$ the solution may be shown to decay, if the initial value of $|A|^2$ does not exceed the limiting value $|c_i|/|\epsilon_i|$, but may grow without a bound if the initial value of $|A|^2$ exceeds $|c_i|/|\epsilon_i|$. It may therefore be concluded that even in this case the limiting value c_i/ϵ_i for the unstable disturbance represents a stable limit while the limiting value $|c_i|/|\epsilon_i|$ for the stable disturbance remains unstable.

The results of the numerical integration of the last equation using the Runge-Kutta method show that the maximum values of the amplitude may reach a value comparable to those observed in the real atmosphere.

2. FORMULATION AND DERIVATION

2.1 FUNDAMENTAL EQUATIONS

The large-scale motion in the atmosphere, when it is considered on the time scale of a day or so, is known to be quasi-horizontal, quasi-nondivergent and quasi-adiabatic. For the purpose of studying the inherent behavior of a system from the viewpoint of diagnosis rather than prognosis as is being attempted in the present study, it is believed that there are more advantages than sacrifices in stripping the system of elements of lesser importance. The scope of the study has therefore been confined from the beginning to what is thought of as the minimal essence. Thus, only the part of the atmospheric motion that is horizontal, nondivergent and adiabatic is considered.

The system of equations governing the nondivergent, adiabatic, frictionless atmospheric motion consists of (i) two equations for the horizontal motion, (ii) the hydrostatic equation, (iii) the continuity equation, and (iv) the thermodynamic energy equation. These equations are presented below in the spherical coordinates (λ, ϕ, p) , where λ is the longitude, ϕ the latitude, and p the pressure.

(i) The equations of the horizontal motion are:

$$u_t + \frac{u}{a \cos \phi} u_\lambda + \frac{v}{a} u_\phi = - \frac{g}{a \cos \phi} z_\lambda + v \left(f + \frac{u \tan \phi}{a} \right) \quad (2.1)$$

$$v_t + \frac{u}{a \cos \phi} v_\lambda + \frac{v}{a} v_\phi = - \frac{g}{a} z_\phi - u \left(f + \frac{u \tan \phi}{a} \right) \quad (2.2)$$

(ii) The hydrostatic equation is

$$z_p = -\frac{\alpha}{g} . \quad (2.3)$$

(iii) The continuity equation is

$$\frac{1}{a \cos \phi} u_\lambda + \frac{1}{a} v_\phi - \frac{\tan \phi}{a} v = 0 . \quad (2.4)$$

(iv) The thermodynamic energy equation is

$$\alpha_t + \frac{u}{a \cos \phi} \alpha_\lambda + \frac{v}{a} \alpha_\phi = 0 \quad (2.5)$$

in which

u = the λ -component of the velocity

v = the ϕ -component of the velocity

a = the radius of earth

g = the acceleration of gravity

z = the height from the ground

f = the Coriolis parameter

α = the specific volume

and the subscripts denote the differentiations.

The mean kinetic energy per unit area of the atmosphere bounded by

$$0 \leq \lambda \leq 2\pi, \quad \phi_S \leq \phi \leq \phi_N, \quad p_1 \leq p \leq p_2$$

is, with the aid of the hydrostatic equation (2.3), given by

$$K = \frac{1}{g} \frac{1}{2\pi a^2 (\sin \phi_N - \sin \phi_S)} \int_{p_1}^{p_2} \int_{\phi_S}^{\phi_N} \int_0^{2\pi} \frac{(u^2 + v^2)}{2} a^2 \cos \phi \, d\lambda d\phi dp$$

which will be written as

$$K = \frac{1}{g} \frac{1}{\sin(\phi_N) - \sin(\phi_S)} \int_{p_1}^{p_2} \int_{\phi_S}^{\phi_N} \bar{k} \cos \phi \, d\phi dp \quad (2.6)$$

with

$$\bar{k} = \frac{1}{2\pi} \int_0^{2\pi} \frac{(u^2 + v^2)}{2} \, d\lambda . \quad (2.7)$$

Similarly, the mean available potential energy per unit area in the same volume may be written as

$$E = \frac{1}{g} \frac{1}{\sin \phi_N - \sin \phi_S} \int_{p_1}^{p_2} \int_{\phi_S}^{\phi_N} \bar{e} \cos \phi \, d\phi dp \quad (2.8)$$

with

$$\bar{e} = \frac{1}{2\pi} \int_0^{2\pi} \frac{1}{\bar{\sigma}} \frac{\alpha^{*2}}{2} \, d\lambda \quad (2.9)$$

where $\bar{\sigma} = \sigma(p)$ is the static stability which is assumed to be a function of pressure only throughout the atmosphere and α^* is the deviation of specific volume from the isobaric average.

2.2 EQUATIONS FOR ENERGIES OF ZONAL MEAN AND EDDIES

By decomposing u , v , α^* into the zonally-averaged components and the deviations from these averages as

$$\begin{aligned} u &= \bar{u} + u' \\ v &= \bar{v} + v' \\ \alpha^* &= \bar{\alpha}^* + \alpha^{*'} \end{aligned} \quad (2.10)$$

where

$$\bar{f} = \frac{1}{2\pi} \int_0^{2\pi} f \, d\lambda$$

for any f , both kinetic and available potential energy may be expressed as sums of two components, namely, the energy of the zonally-averaged state and that of the deviation from the zonally-averaged state which will be referred to as the "eddies" for brevity. In short,

$$\begin{aligned} \bar{k} &= k_Z + k_E \\ \bar{e} &= e_Z + e_E \end{aligned} \tag{2.11}$$

where

$$\begin{aligned} k_Z &= \frac{1}{2} (\overline{u^2 + v^2}) \\ k_E &= \frac{1}{2} (\overline{u'^2 + v'^2}) \\ e_Z &= \frac{1}{\sigma} \overline{\alpha^{*2}} \\ e_E &= \frac{1}{\sigma} \overline{\alpha^{* \prime 2}} \end{aligned} \tag{2.12}$$

In the following the equation for each of the four components in (2.12) will be derived from the fundamental equations presented in Section 2.1.

2.2.1 Kinetic Energy

By multiplying Eqs. (2.1) and (2.2) by u and v , respectively, and integrating around a latitude circle, we obtain

$$\begin{aligned} \left(\frac{u^2}{2} \right)_t &= - \frac{u}{a \cos \phi} \left(\frac{u^2}{2} \right)_\phi - \frac{v}{a} \left(\frac{u^2}{2} \right)_\phi + \overline{fuv} + \frac{\tan \phi}{a} \overline{u^2 v} \\ &\quad - \frac{1}{a \cos \phi} \overline{u(gz)_\lambda} \end{aligned}$$

$$\left(\overline{\frac{v^2}{2}}\right)_t = -\frac{u}{a \cos \phi} \left(\overline{\frac{v^2}{2}}\right)_\lambda - \frac{v}{a} \left(\overline{\frac{v^2}{2}}\right)_\phi - f\overline{uv} - \frac{\tan \phi}{a} \overline{u^2 v} - \frac{1}{a} \overline{v(gz)}_\phi$$

in which

$$\begin{aligned} \frac{u}{a \cos \phi} \left(\overline{\frac{u^2}{2}}\right)_\lambda + \frac{v}{a} \left(\overline{\frac{u^2}{2}}\right)_\phi &= \frac{1}{a \cos \phi} \left(\overline{\frac{u^2 v}{2} \cos \phi}\right)_\phi \\ &- \frac{u^2}{2} \left\{ \frac{1}{a \cos \phi} \left(\frac{\partial u}{\partial \lambda} + \frac{\partial (v \cos \phi)}{\partial \phi} \right) \right\} \\ &= \frac{1}{a \cos \phi} \left(\overline{\frac{u^2 v}{2} \cos \phi}\right)_\phi \end{aligned}$$

and

$$\begin{aligned} \frac{u}{a \cos \phi} \left(\overline{\frac{v^2}{2}}\right)_\lambda + \frac{v}{a} \left(\overline{\frac{v^2}{2}}\right)_\phi &= \frac{1}{a \cos \phi} \left(\overline{\frac{v^2 v}{2} \cos \phi}\right)_\phi \\ &- \frac{v^2}{2} \left\{ \frac{1}{a \cos \phi} \left(\frac{\partial u}{\partial \lambda} + \frac{\partial (v \cos \phi)}{\partial \phi} \right) \right\} \\ &= \frac{1}{a \cos \phi} \left(\overline{\frac{v^2 v}{2} \cos \phi}\right)_\phi \end{aligned}$$

on account of the continuity equation (2.4). By adding them together,

we therefore obtain

$$(\overline{k})_t = -\frac{1}{a \cos \phi} \left[\left(\overline{\frac{u^2 v}{2}} + \overline{\frac{v^2 v}{2}} \right) \cos \phi \right]_\phi - \frac{1}{a \cos \phi} \overline{u(gz)}_\lambda - \frac{1}{a} \overline{v(gz)}_\phi.$$

Substituting

$$\frac{\overline{u^2 v}}{2} = \left(\frac{\overline{u^2}}{2} + \frac{\overline{u'^2}}{2} \right) \overline{v} + \frac{\overline{u'^2 v'}}{2} + \overline{u u' v'}$$

$$\frac{\overline{v^2 v}}{2} = \left(\frac{\overline{v^2}}{2} + \frac{\overline{v'^2}}{2} \right) \overline{v} + \frac{\overline{v'^2 v'}}{2} + \overline{v v' v'}$$

$$\overline{u(gz)_\lambda} = \overline{u'(gz')_\lambda}$$

$$\overline{v(gz)_\phi} = \overline{\bar{v}(g\bar{z})_\phi} + \overline{v'(gz')_\phi}$$

into the above equation, we have

$$\begin{aligned} (\bar{k})_t &= -\frac{1}{a \cos \phi} \left[\left\{ \left(\frac{\bar{u}^2}{2} + \frac{\bar{v}^2}{2} \right) \bar{v} + \left(\frac{u'^2 + v'^2}{2} \right) \bar{v} \right. \right. \\ &\quad \left. \left. + \frac{(u'^2 + v'^2)v'}{2} + \bar{u}(u'v') + \bar{v}(v'^2) \right\} \cos \phi \right]_\phi \quad (2.13) \\ &\quad - \frac{1}{a \cos \phi} [g(\bar{z}\bar{v} + z'v') \cos \phi]_\phi . \end{aligned}$$

Next, by substituting Eq. (2.4) into Eqs. (2.1) and (2.2) we have

$$(u)_t = -\frac{1}{a \cos \phi} [(u^2)_\lambda + (uv \cos \phi)_\phi] + v \left(f + \frac{\tan \phi}{a} u \right) - \frac{1}{a \cos \phi} (gz)_\lambda$$

$$(v)_t = -\frac{1}{a \cos \phi} [(uv)_\lambda + (v^2 \cos \phi)_\phi] - u \left(f + \frac{\tan \phi}{a} u \right) - \frac{1}{a} (gz)_\phi .$$

By multiplying \bar{u} to $(u)_t$, \bar{v} to $(v)_t$ and integrating the sum of the results around a latitude circle we arrive at

$$\begin{aligned} (kz)_t &= -\frac{1}{a \cos \phi} [(\bar{u} \bar{u} \bar{v} + \bar{v} \bar{v}^2) \cos \phi]_\phi \\ &\quad + \frac{1}{2} [\bar{u} \bar{v} (\bar{u})_\phi + \bar{v}^2 (\bar{v})_\phi] + \frac{\tan \phi}{a} (\bar{u} \bar{u} \bar{v} - \bar{v} \bar{u}^2) \\ &\quad - \frac{\bar{v}}{a} (g\bar{z})_\phi . \end{aligned}$$

By decomposing in the fashion of $\bar{u} \bar{v} = \bar{u} \bar{v} + \bar{u}' \bar{v}'$ and by making use of

$[\bar{v} \cos \phi]_\phi = 0$, we may then write the above equation as

$$\begin{aligned}
(k_Z)_t &= -\frac{1}{a \cos \phi} \left[\left(\frac{\bar{u}^2}{2} + \frac{\bar{v}^2}{2} \right) \bar{v} + \bar{u}(\overline{u'v'}) \right. \\
&\quad \left. + \overline{v'(v'^2)} \right] \cos \phi - \frac{1}{a \cos \phi} (g\bar{z}\bar{v} \cos \phi) \phi \\
&\quad + \left\{ \overline{u'v'} \frac{\cos \phi}{a} \left(\frac{\bar{u}}{\cos \phi} \right) \phi + \overline{v'^2} \frac{1}{a} (\bar{v}) \phi \right. \\
&\quad \left. - \overline{u'^2} \frac{\tan \phi}{a} \bar{v} \right\}. \tag{2.14}
\end{aligned}$$

Finally, by subtracting (2.14) from (2.13) we obtain

$$\begin{aligned}
(k_E)_t &= -\frac{1}{a \cos \phi} \left[\left(\frac{\overline{u'^2+v'^2}}{2} \right) \bar{v} + \frac{\overline{(u'^2+v'^2)v'}}{2} \right] \cos \phi \\
&\quad - \frac{1}{a \cos \phi} (g\bar{z}'\bar{v}' \cos \phi) \phi \\
&\quad - \left\{ \overline{u'v'} \frac{\cos \phi}{a} \left(\frac{\bar{u}}{\cos \phi} \right) \phi + \overline{v'^2} \frac{1}{a} (\bar{v}) \phi \right. \\
&\quad \left. - \overline{u'^2} \frac{\tan \phi}{a} \bar{v} \right\}. \tag{2.15}
\end{aligned}$$

2.2.2 Available Potential Energy

When the change with time of the isobaric average of specific volume is neglected, we have from Eq. (2.5) that

$$\alpha_t^* + \frac{u}{a \cos \phi} \alpha_\lambda^* + \frac{v}{a} \alpha_\phi^* = 0.$$

By multiplying α^* and integrating around a latitude circle we obtain

$$\begin{aligned}
\left(\frac{\overline{\alpha^{*2}}}{2}\right)_t &= -\frac{u}{a \cos \phi} \left(\frac{\alpha^{*2}}{2}\right)_\lambda - \frac{v}{a} \left(\frac{\alpha^{*2}}{2}\right)_\phi \\
&= -\frac{1}{a \cos \phi} \left[\left(\frac{u\alpha^{*2}}{2}\right)_\lambda + \left(\frac{v\alpha^{*2} \cos \phi}{2}\right)_\phi \right] \\
&\quad + \frac{\alpha^{*2}}{2} \frac{1}{a \cos \phi} [(u)_\lambda + (v \cos \phi)_\phi] \\
&= -\frac{1}{a \cos \phi} \left(\frac{v\alpha^{*2} \cos \phi}{2}\right)_\phi
\end{aligned}$$

so that

$$\begin{aligned}
\bar{\sigma}(\bar{e})_t = \left(\frac{\overline{\alpha^{*2}}}{2}\right)_t &= -\frac{1}{a \cos \phi} \left[\left(\frac{\overline{\alpha^{*2}}}{2} \bar{v} \cos \phi\right)_\phi \right. \\
&\quad \left. + (\overline{\alpha^*} \bar{v}' \overline{\alpha^{*'}} \cos \phi)_\phi + \left(\frac{\overline{\alpha^{*12}}}{2} \bar{v}' \cos \phi\right)_\phi \right]. \quad (2.16)
\end{aligned}$$

Next, by multiplying $\overline{\alpha^*}$ and integrating around a latitude circle,

it follows that

$$\begin{aligned}
\bar{\sigma}(e_Z)_t = \left(\frac{\overline{\alpha^{*2}}}{2}\right)_t &= -\frac{\overline{\alpha^*}}{a \cos \phi} \overline{u(\alpha^*)}_\lambda - \frac{\overline{\alpha^*}}{a} \overline{v(\alpha^*)}_\phi \\
&= -\frac{\overline{\alpha^*}}{a \cos \phi} \left\{ \overline{u'(\alpha^{*'})}_\lambda + \bar{v} \cos \phi (\overline{\alpha^*})_\phi + \overline{v'(\alpha^{*'})}_\phi \cos \phi \right\} \\
&= -\frac{1}{a \cos \phi} \left\{ \left(\frac{\overline{\alpha^{*2}}}{2} \bar{v} \cos \phi\right)_\phi + (\overline{\alpha^*} \bar{v}' \overline{\alpha^{*'}} \cos \phi)_\phi \right. \\
&\quad \left. - (\bar{v}' \overline{\alpha^{*'}} \cos \phi) (\overline{\alpha^*})_\phi \right\}. \quad (2.17)
\end{aligned}$$

By subtracting (2.17) from (2.16), we obtain

$$\begin{aligned}
\bar{\sigma}(e_E)_t &= -\frac{1}{a \cos \phi} \left(\frac{\overline{\alpha^{*12}}}{2} \bar{v}' \cos \phi\right)_\phi \\
&\quad + \frac{1}{a \cos \phi} \bar{v}' \overline{\alpha^{*'}} \cos \phi (\overline{\alpha^*})_\phi. \quad (2.18)
\end{aligned}$$

2.3 EQUATIONS IN THE WAVE-NUMBER DOMAIN

We now define the Fourier transform $F(n; \phi, p, t)$ of a real variable $f(\lambda, \phi, p, t)$ by

$$F(n; \phi, p, t) = \frac{1}{2\pi} \int_0^{2\pi} f(\lambda, \phi, p, t) e^{-in\lambda} d\lambda \quad (2.19)$$

so that

$$f(\lambda, \phi, p, t) = \sum_{n=-\infty}^{\infty} F(n; \phi, p, t) e^{in\lambda} \quad (2.20)$$

where f satisfies the requirements that it should be piecewise differentiable in the interval $0 \leq \lambda \leq 2\pi$, a condition which all the relevant variables in Eqs. (2.1)-(2.5) are assumed to fulfill. $F(n; \phi, p, t)$ will be referred to as the n th component of $f(\lambda, \phi, p, t)$.

It then follows from the convolution theorem that for any two functions f, g with the Fourier transforms $F(n), G(n)$, respectively, we have

$$\sum_{m=-\infty}^{\infty} G(m)F(n-m) = \frac{1}{2\pi} \int_0^{2\pi} [f(\lambda)g(\lambda)] e^{-in\lambda} d\lambda \quad (2.21)$$

and, in particular, Parseval's theorem which states that

$$\sum_{n=-\infty}^{\infty} |F(n)|^2 = \frac{1}{2\pi} \int_0^{2\pi} f^2(\lambda) d\lambda. \quad (2.22)$$

Table 1 lists the symbols of transform pairs of the relevant variables in Eqs. (2.1)-(2.5).

TABLE 1

LIST OF TRANSFORM PAIRS

Variable	u	v	α	z
Transform	U	V	A	Z

The Fourier transforms of Eqs. (2.1)-(2.5) are obtained by multiplying each equation by $(2\pi)^{-1} e^{-in\lambda}$ and integrating around a latitude circle. It may be readily verified that they are:

(i) The equations of horizontal motion:

$$U_t(n) = - \sum_{m=-\infty}^{\infty} \left[\frac{im}{a \cos \phi} U(m)U(n-m) + \frac{1}{a} U_{\phi}(m)V(n-m) - \frac{\tan \phi}{a} U(m)V(n-m) \right] \\ - i \frac{ng}{a \cos \phi} Z(n) + fV(n) \quad (2.23)$$

$$V_t(n) = - \sum_{m=-\infty}^{\infty} \left[\frac{im}{a \cos \phi} V(m)U(n-m) + \frac{1}{a} V_{\phi}(m)V(n-m) + \frac{\tan \phi}{a} U(m)U(n-m) \right] \\ - \frac{g}{a} Z_{\phi}(n) - fU(n) . \quad (2.24)$$

(ii) The hydrostatic equation:

$$Z_p(n) = - \frac{1}{g} A(n) . \quad (2.25)$$

(iii) The continuity equation:

$$i \frac{n}{a \cos \phi} U(n) + \frac{1}{a} V_{\phi}(n) - \frac{\tan \phi}{a} V(n) = 0 . \quad (2.26)$$

(iv) The thermodynamic energy equation:

$$A_t(n) = - \sum_{m=-\infty}^{\infty} \left[\frac{im}{a \cos \phi} A(m)U(n-m) + \frac{1}{a} A_{\phi}(m)V(n-m) \right] . \quad (2.27)$$

It follows from Eq. (2.22) that the energies defined in Eqs. (2.7) and (2.9) can be expressed in terms of the Fourier transforms as

$$\bar{k} = \frac{1}{2} [U^2(o) + V^2(o)] + \sum_{n=1}^{\infty} (|U(n)|^2 + |V(n)|^2)$$

and

$$\bar{e} = \frac{1}{2} \frac{1}{\sigma} A^{*2}(o) + \sum_{n=1}^{\infty} \frac{1}{\sigma} |A^*(n)|^2$$

or by defining

$$k_Z = \frac{1}{2} [U^2(o) + V^2(o)] \quad (2.28)$$

$$k_n = |U(n)|^2 + |V(n)|^2 \quad (2.29)$$

$$e_Z = \frac{1}{2} \frac{1}{\sigma} A^{*2}(o) \quad (2.30)$$

$$e_n = \frac{1}{\sigma} |A^*(n)|^2 \quad (2.31)$$

as

$$\bar{k} = k_Z + \sum_{n=1}^{\infty} k_n \quad (2.32)$$

$$\bar{e} = e_Z + \sum_{n=1}^{\infty} e_n \quad (2.33)$$

where k_Z and e_Z are the kinetic and available potential energy of the zonal mean, respectively, and k_n , e_n are the kinetic and available potential energy of the n th component of the eddies respectively.

2.4 TENDENCY EQUATIONS FOR THE ENERGIES OF THE n th COMPONENT

2.4.1 Kinetic Energy

The expression for $(k_n)_t$ can be derived as follows. Multiplying Eq. (2.23) by $U(-n)$ the equation for $U_t(-n)$ by $U(n)$ and adding the resulting equations, we obtain

$$\begin{aligned}
 |U(n)|_t^2 = & - \sum_{\substack{m=-\infty \\ m \neq 0}}^{\infty} \left[\frac{im}{a \cos \phi} U(m) \{U(n-m)U(-n) + U(-n-m)U(n)\} \right. \\
 & + \frac{1}{a} U_\phi(m) \{V(n-m)U(-n) + V(-n-m)U(n)\} \\
 & \left. - \frac{\tan \phi}{a} U(m) \{V(n-m)U(-n) + V(-n-m)U(n)\} \right] \\
 & - \frac{ing}{a \cos \phi} \{Z(n)U(-n) - Z(-n)U(n)\} \\
 & + f \{V(n)U(-n) + V(-n)U(n)\} \\
 & - \frac{1}{a} U_\phi(0) \{V(n)U(-n) + V(-n)U(n)\} \\
 & + \frac{\tan \phi}{a} U(0) \{V(n)U(-n) + V(-n)U(n)\} . \tag{2.34}
 \end{aligned}$$

We shall consider first the terms under the summation over m . The second and third terms together may be written as

$$\begin{aligned}
 & \frac{1}{a \cos \phi} [V(n-m)U(-n) + V(-n-m)U(n)] [U(m) \cos \phi]_\phi \\
 & = \frac{1}{a \cos \phi} \{U(-n) [U(m)V(n-m) \cos \phi]_\phi + U(n) [U(m)V(-n-m) \cos \phi]_\phi\} \\
 & \quad - \frac{1}{a} \{U(-n)U(m)V_\phi(n-m) + U(n)U(m)V_\phi(-n-m)\}
 \end{aligned}$$

so that the summation becomes

$$\begin{aligned}
& - \sum_{\substack{m=-\infty \\ m \neq 0}}^{\infty} \left[\frac{im}{a \cos \phi} U(m) \{U(n-m)U(-n)+U(-n-m)U(n)\} \right. \\
& \quad + \frac{1}{a \cos \phi} \{U(-n)[U(m)V(+n-m)\cos \phi]_{\phi} + U(n)[U(m)V(-n-m)\cos \phi]_{\phi}\} \\
& \quad \left. - \frac{1}{a} U(m) \{V_{\phi}(n-m)U(-n)+V_{\phi}(-n-m)U(n)\} \right] .
\end{aligned}$$

If, now, the use is made of the transform of the continuity equation in the form of

$$\begin{aligned}
i \frac{(n-m)}{a \cos \phi} U(n-m) + \frac{1}{a} V_{\phi}(n-m) - \frac{\tan \phi}{a} V(n-m) &= 0 \\
i \frac{(-n-m)}{a \cos \phi} U(-n-m) + \frac{1}{a} V_{\phi}(-n-m) - \frac{\tan \phi}{a} V(-n-m) &= 0 \quad (2.35)
\end{aligned}$$

in the above equations, we obtain

$$\begin{aligned}
& - \sum_{m=-\infty}^{\infty} \left[\frac{in}{a \cos \phi} U(m) \{U(-n)U(n-m)-U(n)U(-n-m)\} \right. \\
& \quad - \frac{\tan \phi}{a} U(m) \{U(-n)V(+n-m)+U(n)V(-n-m)\} \\
& \quad \left. + \frac{1}{a \cos \phi} \{U(-n)[U(m)V(n-m)\cos \phi]_{\phi} + U(n)[U(m)V(-n-m)\cos \phi]_{\phi}\} \right] .
\end{aligned}$$

Next, the term second to the last of Eq. (2.34) may be written as

$$\begin{aligned}
& -\{U(-n)V(n)+U(n)V(-n)\} \frac{\cos \phi}{a} \left[\frac{U(o)}{\cos \phi} \right]_{\phi} \\
& + \{U(-n)V(n)+U(n)V(-n)\} U(o) \frac{\tan \phi}{a} .
\end{aligned}$$

Consequently, Eq. (2.34) may now be rewritten as

$$\begin{aligned}
(|U(n)|^2)_t &= - \sum_{\substack{m=-\infty \\ m \neq 0}}^{\infty} \left[\frac{in}{a \cos \phi} U(m) \{U(-n)U(n-m) - U(n)U(-n-m)\} \right. \\
&\quad \left. + \frac{1}{a \cos \phi} \{U(-n)[U(m)V(n-m)\cos \phi]_{\phi} + U(n)[U(m)V(-n-m)\cos \phi]_{\phi}\} \right] \\
&\quad - \{U(-n)V(n) + U(n)V(-n)\} \frac{\cos \phi}{a} \left[\frac{U(0)}{\cos \phi} \right]_{\phi} \\
&\quad - \frac{ing}{a \cos \phi} \{Z(n)U(-n) - Z(-n)U(n)\} \\
&\quad + \left\{ f + \frac{\tan \phi}{a} U(0) \right\} \{V(n)U(-n) + V(-n)U(n)\} \\
&\quad + \frac{\tan \phi}{a} \sum_{m=-\infty}^{\infty} U(m) \{V(n-m)U(-n) + V(-n-m)U(n)\} \quad (2.36)
\end{aligned}$$

in which the last term may be rewritten as

$$\frac{\tan \phi}{a} \left[\sum_{m=-\infty}^{\infty} U(m) \{V(n-m)U(-n)\} + \sum_{m=-\infty}^{\infty} U(m) \{V(-n-m)U(n)\} \right]$$

so that if $m' = n-m$ (or $m = n-m'$) in the first and $m' = -n-m$ (or $m = -n-m'$) in the second are substituted, it becomes

$$\begin{aligned}
&\frac{\tan \phi}{a} \left[\sum_{m'=-\infty}^{\infty} U(n-m')V(m')U(-n) + \sum_{m'=-\infty}^{\infty} U(-n-m')V(m')U(n) \right] \\
&= \frac{\tan \phi}{a} \{U(n)U(-n) + U(-n)U(n)\}V(0) \\
&\quad + \frac{\tan \phi}{a} \sum_{\substack{m=-\infty \\ m \neq 0}}^{\infty} V(m) \{U(n-m)U(-n) + U(-n-m)U(n)\} .
\end{aligned}$$

Therefore, Eq. (2.36) becomes

$$\begin{aligned}
(|U(n)|^2)_t &= -\frac{\cos \phi}{a} \left[\frac{U(o)}{\cos \phi} \right]_{\phi} \{V(n)U(-n)+V(-n)U(n)\} \\
&- i \frac{ng}{a \cos \phi} \{Z(n)U(-n)-Z(-n)U(n)\} \\
&+ \frac{\tan \phi}{a} V(o) \{U(n)U(-n)+U(-n)U(n)\} \\
&+ \left\{ f + \frac{\tan \phi}{a} U(o) \right\} \{V(n)U(-n)+V(-n)U(n)\} \\
&- \sum_{\substack{m=-\infty \\ m \neq 0}}^{\infty} \left[\frac{in}{a \cos \phi} U(m) \{U(n-m)U(-n)-U(-n-m)U(n)\} \right. \\
&+ \frac{1}{a \cos \phi} \{U(-n)[U(m)V(n-m)\cos \phi]_{\phi} \\
&\quad \left. + U(n)[U(m)V(-n-m)\cos \phi]_{\phi} \right. \\
&\left. - \frac{\tan \phi}{a} V(m) \{U(n-m)U(-n)+U(-n-m)U(n)\} \right] . \quad (2.37)
\end{aligned}$$

Similarly, from Eq. (2.24) and the corresponding equation for $V_t(-n)$ we obtain

$$\begin{aligned}
(|V(n)|^2)_t &= - \sum_{\substack{m=-\infty \\ m \neq 0}}^{\infty} \left[\frac{im}{a \cos \phi} V(m) \{U(n-m)V(-n)+U(-n-m)V(n)\} \right. \\
&+ \frac{1}{a} V_{\phi}(m) \{V(n-m)V(-n)+V(-n-m)V(n)\} \\
&\left. + \frac{\tan \phi}{a} U(m) \{U(n-m)V(-n)+U(-n-m)V(n)\} \right] \\
&- \frac{g}{a} \{Z_{\phi}(+n)V(-n)+Z_{\phi}(-n)V(n)\} \\
&- \left\{ f + \frac{\tan \phi}{a} U(o) \right\} \{U(n)V(-n)+U(-n)V(n)\} \\
&- \frac{1}{a} V_{\phi}(o) \{V(n)V(-n)+V(-n)V(n)\} \quad (2.38)
\end{aligned}$$

in which the terms under summation can be rewritten as

$$\begin{aligned}
& \frac{im}{a \cos \phi} V(m) \{U(+n-m)V(-n)+U(-n-m)V(n)\} \\
& + \frac{1}{a \cos \phi} \{V(-n)[V(m)V(n-m)\cos \phi]_{\phi}+V(n)[V(m)V(-n-m)\cos \phi]_{\phi}\} \\
& - \frac{1}{a} V(m) \{V_{\phi}(n-m)V(-n)+V_{\phi}(-n-m)V(n)\} \\
& + \frac{\tan \phi}{a} V(m) \{V(n-m)V(-n)+V(-n-m)V(n)\}
\end{aligned}$$

so that if the use is made of the continuity equations (2.35), Eq.

(2.38) becomes

$$\begin{aligned}
(|V(n)|^2)_t &= - \frac{ig}{a} \{Z_{\phi}(n)V(-n)+Z_{\phi}(-n)V(n)\} \\
& - \frac{1}{a} V_{\phi}(o) \{V(n)V(-n)+V(-n)V(n)\} \\
& - \left\{ f + \frac{\tan \phi}{a} U(o) \right\} \{U(n)V(-n)+U(-n)V(n)\} \\
& - \sum_{\substack{m=-\infty \\ m \neq 0}}^{\infty} \left[\frac{im}{a \cos \phi} V(n) \{U(n-m)V(-n)-U(-n-m)V(n)\} \right. \\
& + \frac{1}{a \cos \phi} \{V(-n)[V(m)V(n-m)\cos \phi]_{\phi} \\
& \quad \left. +V(n)[V(m)V(-n-m)\cos \phi]_{\phi}\} \right. \\
& \left. + \frac{\tan \phi}{a} U(m) \{U(n-m)V(-n)+U(-n-m)V(n)\} \right]
\end{aligned} \tag{2.39}$$

Adding (2.37) and (2.39) we obtain

$$\begin{aligned}
(k_n)_t = & -g \left[\frac{in}{a \cos \phi} \{Z(n)U(-n) - Z(-n)U(n)\} + \frac{1}{a} \{Z_\phi(n)V(-n) + Z_\phi(n)V(n)\} \right] \\
& - \frac{\cos \phi}{a} \left[\frac{U(o)}{a \cos \phi} \right]_\phi \{V(n)U(-n) + V(-n)U(n)\} \\
& - \frac{1}{a} V_\phi(o) \{V(n)V(-n) + V(-n)V(n)\} + \frac{\tan \phi}{a} V(o) \{U(n)U(-n) + U(-n)U(n)\} \\
& + \sum_{\substack{m=-\infty \\ m \neq 0}}^{\infty} \left[\frac{1}{a \cos \phi} U(m) \{U(n-m)(-in)U(-n) + U(-n-m)(in)U(n)\} \right. \\
& + \frac{1}{a \cos \phi} V(m) \{U(n-m)(-in)V(-n) + U(-n-m)(in)V(n)\} \\
& - \frac{1}{a \cos \phi} \{U(-n)[U(m)V(n-m)\cos \phi\}_\phi + U(n)[U(m)V(-n-m)\cos \phi\}_\phi \\
& - \frac{1}{a \cos \phi} \{V(-n)[V(m)V(n-m)\cos \phi\}_\phi + V(n)[V(m)V(-n-m)\cos \phi\}_\phi \\
& + \frac{\tan \phi}{a} V(m) \{U(n-m)U(-n) + U(-n-m)U(n)\} \\
& \left. - \frac{\tan \phi}{a} U(m) \{U(n-m)V(-n) + U(-n-m)V(n)\} \right]. \tag{2.40}
\end{aligned}$$

Integrating Eq. (2.25) with respect to $\sin \phi$ from ϕ_S to ϕ_N and noting that

$$\begin{aligned}
& \int_{\phi_S}^{\phi_N} \left[-\frac{1}{a \cos \phi} \{U(-n)[U(m)V(n-m)\cos \phi\}_\phi + U(n)[U(m)V(-n-m)\cos \phi\}_\phi \right. \\
& \left. - \frac{1}{a \cos \phi} \{V(-n)[V(m)V(n-m)\cos \phi\}_\phi + V(n)[V(m)V(-n-m)\cos \phi\}_\phi \right] \cos \phi d\phi \\
& = -\frac{1}{a} \left[\{U(m)[V(n-m)U(-n) + V(-n-m)U(n)] \right. \\
& \quad \left. + V(m)[V(n-m)V(-n) + V(-n-m)V(n)] \} \cos \phi \right]_{\phi_S}^{\phi_N} \\
& + \frac{1}{a} \int_{\phi_S}^{\phi_N} \left[U(m) \{V(n-m)U_\phi(-n) + V(-n-m)U_\phi(n)\} \right. \\
& \quad \left. + V(m) \{V(n-m)V_\phi(-n) + V(-n-m)V_\phi(n)\} \right] \cos \phi d\phi
\end{aligned}$$

and that

$$\begin{aligned}
& \frac{i n}{a \cos \phi} \{Z(n)U(-n)-Z(-n)U(n)\} + \frac{1}{a} \{Z_{\phi}(n)V(-n)+Z_{\phi}(-n)V(n)\} \\
&= \frac{i n}{a \cos \phi} \{Z(n)U(-n)-Z(-n)U(n)\} + \frac{1}{a} \{Z(n)V(-n)+Z(-n)V(n)\}_{\phi} \\
&\quad - \frac{1}{a} \{Z(n)V_{\phi}(-n)+Z(-n)V_{\phi}(n)\} \\
&= \frac{1}{a} \{Z(n)V(-n)+Z(-n)V(n)\}_{\phi} - \left[Z(n) \left\{ \frac{1}{a \cos \phi} (-i n)U(-n) + \frac{1}{a} V_{\phi}(-n) \right\} \right. \\
&\quad \left. + Z(-n) \left\{ \frac{1}{a \cos \phi} (i n)U(n) + \frac{1}{a} V_{\phi}(n) \right\} \right] \\
&= \frac{1}{a} \{Z(n)V(-n)+Z(-n)V(n)\}_{\phi} - \frac{\tan \phi}{a} \{Z(n)V(-n)+Z(-n)V(n)\}
\end{aligned}$$

so that

$$\begin{aligned}
& \int_{\phi_S}^{\phi_N} \frac{1}{a} \{Z(n)V(-n)+Z(-n)V(n)\}_{\phi} \cos \phi \, d\phi \\
&\quad - \int_{\phi_S}^{\phi_N} \frac{\tan \phi}{a} \{Z(n)V(-n)+Z(-n)V(n)\} \cos \phi \, d\phi \\
&= \frac{1}{a} \left[\{Z(n)V(-n)+Z(-n)V(n)\} \cos \phi \right]_{\phi_S}^{\phi_N}
\end{aligned}$$

we arrive at

$$\begin{aligned}
& \left[\int_{\phi_S}^{\phi_N} k_n \cos \phi \, d\phi \right]_t = (K_n)_t \\
& = - \int_{\phi_S}^{\phi_N} \left\{ \frac{\cos \phi}{a} \left[\frac{U(o)}{\cos \phi} \right]_{\phi} \Phi_{uv}(n) + \frac{1}{a} V_{\phi}(o) \Phi_{vv}(n) \right. \\
& \quad \left. - \frac{\tan \phi}{a} V(o) \Phi_{uu}(n) \right\} \cos \phi \, d\phi \\
& + \int_{\phi_S}^{\phi_N} \sum_{\substack{m=-\infty \\ m \neq 0}}^{\infty} \left\{ U(m) \left[\frac{1}{a \cos \phi} \Psi_{uu\lambda}(m,n) + \frac{1}{a} \Psi_{vu\phi}(m,n) \right. \right. \\
& \quad \left. \left. - \frac{\tan \phi}{a} \Psi_{uv}(m,n) \right] \right. \\
& \quad \left. + V(m) \left[\frac{1}{a \cos \phi} \Psi_{uv\lambda}(m,n) + \frac{1}{a} \Psi_{vv\phi}(m,n) + \frac{\tan \phi}{a} \Psi_{uu}(m,n) \right] \right\} \cos \phi \, d\phi \\
& - \frac{1}{a} \left[\sum_{\substack{m=-\infty \\ m \neq 0}}^{\infty} \{ U(m) \Psi_{vu}(m,n) + V(m) \Psi_{vv}(m,n) \} \cos \phi \right]_{\phi_S}^{\phi_N} \\
& - \frac{g}{a} \left[\Phi_{vz}(n) \cos \phi \right]_{\phi_S}^{\phi_N} \tag{2.41}
\end{aligned}$$

in which

$$\Phi_{fg}(n) = F(n)G(-n) + F(-n)G(n) \tag{2.42}$$

$$\Psi_{fg}(m,n) = F(n-m)G(-n) + F(-n-m)G(n) \tag{2.43}$$

where F,G are the Fourier transforms of f,g respectively.

2.4.2 Available Potential Energy

It follows from Eq. (2.18) that

$$\begin{aligned}
(|A^*(n)|^2)_t &= - \sum_{\substack{m=-\infty \\ m \neq 0}}^{\infty} \left[\frac{\text{im}}{a \cos \phi} A^*(m) \{U(n-m)A^*(-n) + U(-n-m)A^*(n)\} \right. \\
&\quad \left. + \frac{1}{a} A_{\phi}^*(m) \{V(n-m)A^*(-n) + V(-n-m)A^*(n)\} \right] \\
&\quad - \frac{1}{a} A_{\phi}^*(0) \{V(n)A^*(-n) + V(-n)A^*(n)\} . \tag{2.44}
\end{aligned}$$

Writing the terms under the summation as

$$\begin{aligned}
&\frac{\text{im}}{a \cos \phi} A^*(m) \{U(n-m)A^*(-n) + U(-n-m)A^*(n)\} \\
&+ \frac{1}{a \cos \phi} \{A^*(-n) [A^*(m)V(n-m) \cos \phi]_{\phi} + A^*(n) [A^*(m)V(-n-m) \cos \phi]_{\phi}\} \\
&- \frac{1}{a} \{A^*(m) [V_{\phi}(n-m)A^*(-n) + V_{\phi}(-n-m)A^*(n)]\} \\
&+ \frac{\tan \phi}{a} \{A^*(m) [V(n-m)A^*(-n) + V(-n-m)A^*(n)]\}
\end{aligned}$$

and using the transforms of the continuity equations (2.35) to rewrite

them as

$$\begin{aligned}
&\frac{\text{im}}{a \cos \phi} A^*(m) \{U(n-m)A^*(-n) + U(-n-m)A^*(n)\} \\
&+ \frac{1}{a \cos \phi} \{A^*(-n) [A^*(m)V(n-m) \cos \phi]_{\phi} + A^*(n) [A^*(m)V(-n-m) \cos \phi]_{\phi}\} \\
&+ \frac{i(n-m)}{a \cos \phi} A^*(m) [U(n-m)A^*(-n)] \\
&+ \frac{i(-n-m)}{a \cos \phi} A^*(m) [U(-n-m)A^*(n)] \\
&= \frac{1}{a \cos \phi} A^*(m) \{U(n-m)(in)A^*(-n) + U(-n-m)(-in)A^*(n)\} \\
&+ \frac{1}{a \cos \phi} \{A^*(-n) [A^*(m)V(n-m) \cos \phi]_{\phi} + A^*(n) [A^*(m)V(-n-m) \cos \phi]_{\phi}\}
\end{aligned}$$

so that Eq. (2.44) becomes

$$\begin{aligned}
(|A^*(n)|^2)_t &= -\frac{1}{a} A_\phi^*(o) \{V(n)A^*(-n) + V(-n)A^*(n)\} \\
&+ \sum_{\substack{m=-\infty \\ m \neq 0}}^{\infty} \left[\frac{1}{a \cos \phi} A^*(m) \{U(n-m)(-in)A^*(-n) + U(-n-m)(in)A^*(n)\} \right. \\
&\left. - \frac{1}{a \cos \phi} \{A^*(-n)[A^*(m)V(n-m)\cos \phi]_\phi + A^*(n)[A^*(m)V(-n-m)\cos \phi]_\phi \} \right]
\end{aligned}$$

which, when integrated with respect to $\sin \phi$ from ϕ_S to ϕ_N , gives

$$\begin{aligned}
\int_{\phi_S}^{\phi_N} e_n \cos \phi \, d\phi &= (E_n)_t \\
&= - \int_{\phi_S}^{\phi_N} \left\{ \frac{1}{\sigma} \frac{1}{a} A_\phi^*(o) \Phi_{v\alpha^*}(n) \right\} \cos \phi \, d\phi \\
&+ \int_{\phi_S}^{\phi_N} \frac{1}{\sigma} \sum_{\substack{m=-\infty \\ m \neq 0}}^{\infty} A^*(m) \left\{ \frac{1}{a \cos \phi} \Psi_{u\alpha^*}(m,n) + \frac{1}{a} \Psi_{v\alpha^*}(m,n) \right\} \cos \phi \, d\phi \\
&- \frac{1}{a} \frac{1}{\sigma} \left[\sum_{\substack{m=-\infty \\ m \neq 0}}^{\infty} A^*(m) \Psi_{v\alpha^*}(m,n) \cos \phi \right]_{\phi_S}^{\phi_N} \tag{2.45}
\end{aligned}$$

in which the symbols Φ, Ψ are the same as those defined in (2.42) and (2.43) respectively.

2.5 PHYSICAL INTERPRETATION

In Eq. (2.41), the first integral

$$\begin{aligned}
- \int_{\phi_S}^{\phi_N} \left\{ \frac{\cos \phi}{a} \left[\frac{U(o)}{\cos \phi} \right]_\phi \Phi_{uv}(n) + \frac{1}{a} V_\phi(o) \Phi_{vv}(n) - \frac{\tan \phi}{a} V(o) \Phi_{uu}(n) \right\} \cos \phi \, d\phi \\
= C(K_Z, K_n) \tag{2.46}
\end{aligned}$$

represents the conversion from the zonal kinetic energy into the kinetic energy of the n th component through the work of Reynolds stresses against the zonal velocity gradients. It is readily seen by a reference to Eq. (2.12) that

$$\sum_n C(K_Z, K_n) = C(K_Z, K_E) . \quad (2.47)$$

The second integral

$$\begin{aligned} & \int_{\phi_S}^{\phi_N} \sum_{\substack{m=-\infty \\ m \neq 0}}^{\infty} \left\{ U(m) \left[\frac{1}{a \cos \phi} \Psi_{uu\lambda}(m, n) + \frac{1}{a} \Psi_{vu\phi}(m, n) - \frac{\tan \phi}{a} \Psi_{uv}(m, n) \right] \right. \\ & \quad \left. + V(m) \left[\frac{1}{a \cos \phi} \Psi_{uv\lambda}(m, n) + \frac{1}{a} \Psi_{vv\phi}(m, n) + \frac{\tan \phi}{a} \Psi_{uu}(m, n) \right] \right\} \cos \phi \, d\phi \\ & = \sum_{\substack{m=-\infty \\ m \neq 0, n}}^{\infty} C(K_m, K_n) \end{aligned} \quad (2.48)$$

represents the transfer of kinetic energies of other wave components into that of the n th component through the nonlinear wave interaction.

A reference to Eq. (2.12) shows that

$$\sum_n \sum_m C(K_m, K_n) = 0 . \quad (2.49)$$

There are two kinds of net fluxes in Eq. (2.41). The first, which is given by

$$\left[\frac{1}{a} \sum_{\substack{m=-\infty \\ m \neq 0}}^{\infty} \{ U(m) \Psi_{vu}(m, n) + V(m) \Psi_{vv}(m, n) \} \cos \phi \right]_{\phi_S}^{\phi_N} = F_3(K_n) \quad (2.50)$$

represents the flux arising from the nonlinear interactions among the waves, while the second, which is given by

$$\left[\frac{1}{a} \Phi_{vZ}(n) \cos \phi \right]_{\phi_S}^{\phi_N} = F_1(K_n) \quad (2.51)$$

represents the rate of work done by the potential at the boundaries.

Obviously

$$\sum_n F(K_n) = \sum_n (F_1(K_n) + F_3(K_n)) = F(K_E) \quad (2.52)$$

which is given by the flux terms in Eq. (2.14).

Similarly, in Eq. (2.45), the first integral

$$- \int_{\phi_S}^{\phi_N} \frac{1}{a} \left\{ \frac{1}{\sigma} A^*(0) \Phi_{v\alpha^*}(n) \right\} \cos \phi \, d\phi = C(E_Z, E_n) \quad (2.53)$$

represents the conversion of the zonal available potential energy into the available potential energy of the nth component and

$$\sum_n C(E_Z, E_n) = C(E_Z, E_E) . \quad (2.54)$$

The second integral

$$\int_{\phi_S}^{\phi_N} \frac{1}{\sigma} \sum_{\substack{m=-\infty \\ m \neq 0}}^{\infty} A^*(m) \left\{ \frac{1}{a \cos \phi} \Psi_{u\alpha^*}(m, n) + \frac{1}{a} \Psi_{v\alpha^*}(m, n) \right\} \cos \phi \, d\phi \\ = \sum_m C(E_m, E_n) \quad (2.55)$$

defines the transfer of available potential energies of other wave components into that of the nth component through wave interaction. Here, again, as in Eq. (2.49)

$$\sum_n \sum_m C(E_m, E_n) = 0 . \quad (2.56)$$

The boundary flux

$$\left[\frac{1}{a} \frac{1}{\sigma} \sum_{\substack{m=-\infty \\ m \neq 0}}^{\infty} A^*(m) \Psi_{v\alpha^*}(m, n) \cos \phi \right]_{\phi_S}^{\phi_N} = F(E_n) \quad (2.57)$$

gives the net flux through the boundaries due to the nonlinear interaction.

With the symbols introduced above, Eqs. (2.41) and (2.45) may be written as

$$(K_n)_t = C(K_Z, K_n) + \sum_m C(K_m, K_n) - F(K_n) \quad (2.58)$$

$$(E_n)_t = C(E_Z, E_n) + \sum_m C(E_m, E_n) - F(E_n) . \quad (2.59)$$

2.6 COMPUTATION PROCEDURE

The nondivergent flow is obtained from the geostrophic stream function Ψ which is defined as the solution of the differential equation

$$\nabla^2 \Psi = \frac{g}{f} \nabla^2 z - g \nabla(1/f) \cdot \nabla z$$

subject to the boundary condition that the wind is geostrophic and normal at the boundary of the octagonal region covered by the JNWP 1977 point grid. The values of the Fourier coefficients up to $N = 15$ of this stream function evaluated at latitudes between 20°N and 87.5°N with a 2.5° interval on each of eight isobaric surfaces, namely, 100-, 85-, 70-, 50-, 30-, 20-, 15-, and 10-cb have been provided by the National Center for Atmospheric Research for the input of the subsequent computation.

The specific volume is approximated by

$$\alpha = -f_0 \Psi_p$$

instead of being evaluated with the use of the hydrostatic equation (2.3) from the geopotential.

Differentiations and integrations with respect to both latitude and pressure are replaced respectively by centered finite differences and sums. Thus, a set of the Fourier components of each of the velocity components, specific volume and their first derivatives are defined at every latitude from 22.5°N to 85°N with 2.5° interval, with the set at latitude ϕ representing the mean in the belt between $\phi+1.25^{\circ}$ and $\phi-1.25^{\circ}$ on each of the eight isobaric surfaces.

In the calculation of kinetic energy exchanges the values on each isobaric surface are assumed to represent the mean values of the layer which extends half way to both of the adjacent levels where observations are available, and are weighted accordingly by the thickness of the layer to give the corresponding values in that layer.

On the other hand, in the calculation of available potential energy exchanges the mean specific volume in the layer between two adjacent levels is obtained from the difference of the stream functions and the mean velocity in the layer is defined as the average of those on the bounding surfaces. The values of exchanges obtained from these mean values of the layer are then weighted by the thickness of the layer.

Figure 1 shows the vertical resolution of the computational scheme described above.

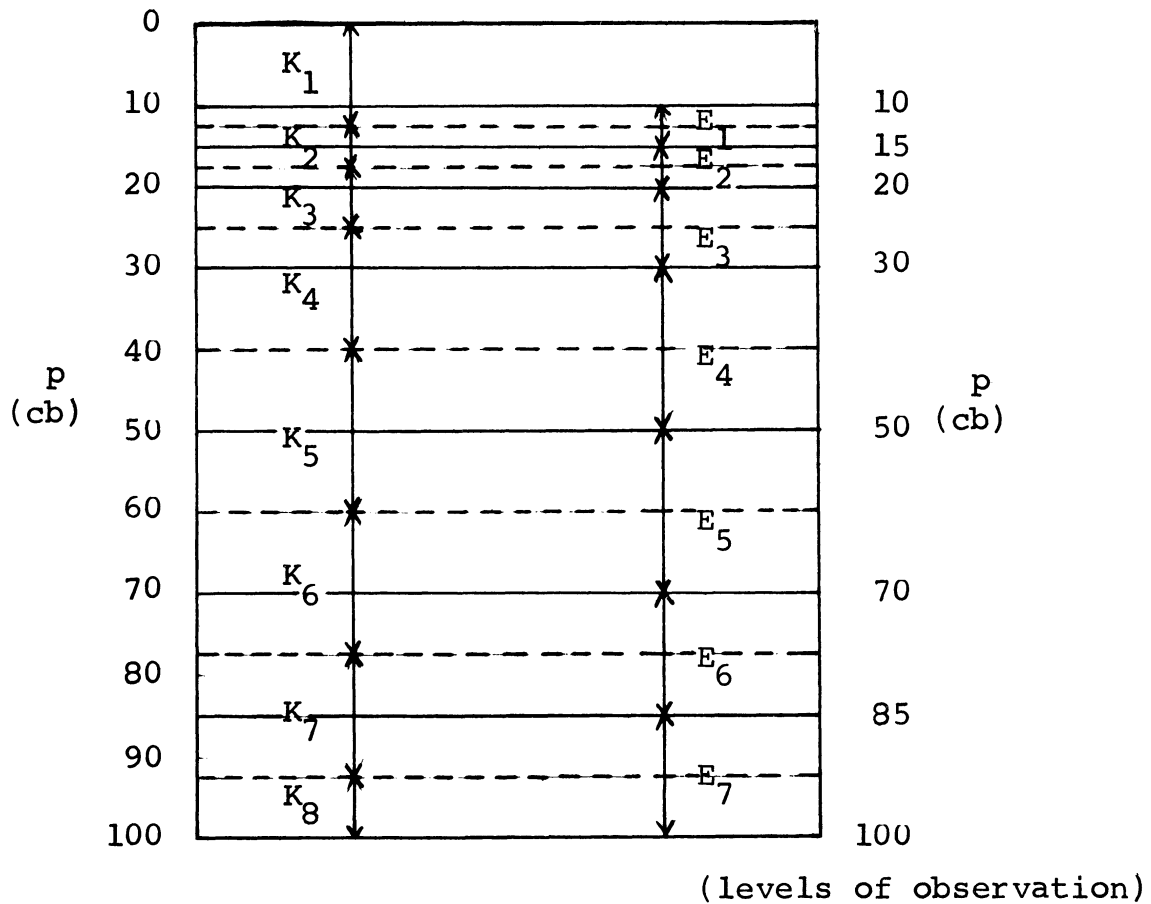


Fig. 1. Vertical resolution of the computation.

The values of static stability in the individual layers are computed by linear interpolation from those calculated by Gates (1960) for the months of January and July. The January values are used in the winter months of December, January and February, and the July values in the summer months of June, July, and August, while the averages of the January and July values are chosen to represent those in the rest of the year. Table 2 lists the values of static stability used in the computation.

TABLE 2

STATIC STABILITY, $\bar{\sigma}(10^{-6} \text{ kg}^{-2} \text{ m}^4 \text{ sec}^2)$

Layer (cb)	Winter	Spring & Fall	Summer
10 ~ 15	91.4	95.7	100
15 ~ 20	54.5	42.8	31.0
20 ~ 30	17.9	13.3	8.73
30 ~ 50	3.73	3.70	3.66
50 ~ 70	2.26	2.23	2.20
70 ~ 85	2.24	1.77	1.30
85 ~ 100	1.88	1.75	1.62

Lastly, the expressions for $\Phi_{fg}(n)$ and $\sum_m H(m)\Psi_{fg}(m,n)$, where f , g , and h have the Fourier transforms F , G , and H , respectively, in terms of their cosine and sine coefficients may be shown to be given by (see Appendix A)

$$\begin{aligned} \Phi_{fg}(n) &= \frac{1}{2} [F_C(n)G_C(n) + F_S(n)G_S(n)] \\ \sum_{\substack{m=-\infty \\ m \neq 0}}^{\infty} H(m)\Psi_{fg}(m,n) &= (1/4)G_C(n) \left[\sum_{m=1}^{\infty} \{H_C(m)F_C(n+m) + H_S(m)F_S(n+m)\} \right. \\ &\quad + \sum_{m=1}^{n-1} \{H_C(m)F_C(n-m) - H_S(m)F_S(n-m)\} \\ &\quad + \left. \sum_{m=n+1}^{\infty} \{H_C(m)F_C(m-n) + H_S(m)F_S(m-n)\} + 2H(0)F_C(n) \right] \\ &\quad + (1/4)G_S(n) \left[\sum_{m=1}^{\infty} \{H_C(m)F_C(n+m) - H_S(m)F_S(n+m)\} \right. \\ &\quad + \sum_{m=1}^{n-1} \{H_C(m)F_S(n-m) + H_S(m)F_C(n-m)\} \\ &\quad + \left. \sum_{m=n+1}^{\infty} \{H_S(m)F_C(m-n) - H_C(m)F_S(m-n)\} + 2H(0)F_S(n) \right] \end{aligned}$$

where subscripts c and s denote the cosine and sine coefficients respectively.

While there are no apparent constraints that may be applied to check the values of $C(K_Z, K_n)$ and $F(K_n)$ (or $C(E_Z, E_n)$ and $F(E_n)$) obtained from Eqs. (2.46) and (2.50) (or Eqs. (2.53) and (2.57)), Eqs. (2.49) and (2.56) must be satisfied by the sums of all the conversions due to wave interactions. In practice, however, because of the finite differences employed in defining the values of derivatives of the velocity components, these sums generally yield values that are different from zero. With the assumptions that such nonzero sums are fundamentally errors arising from the finite differences and that the errors are equally distributed among all waves, the value of the conversion due to wave interaction in a wave component is defined to be the value obtained from Eq. (2.48) (or Eq. (2.55)) minus a correction which is the value of the sum divided by the number of wave components. The same procedure was used earlier by Saltzman and Fleisher (1960) and although it appears as a case of over-simplification, as will be shown later (Section 3.5) in the decomposition of the nonlinear exchanges, the method seems well justified, at least in the absence of alternatives that may suggest a further improvement.

3. RESULTS

3.1 INTRODUCTION

3.1.1 Analysis and Synthesis

On each set of available observations taken daily at 00Z, two exchanges, one between a wave component and the zonal mean and the other between a wave component and all other wave components, and the net flux through the latitudinal boundaries are computed for each of the 15 wave components in each layer in both kinetic and available potential energies. In computing the kinetic energy flux the component containing $\Phi_{VZ}(n)$ on the boundary is neglected in view of the boundary condition imposed on the stream function. In addition, the net fluxes of kinetic and available potential energies of the zonal mean are also computed. Monthly averages and standard errors of these quantities are obtained from the daily values in each month and the annual averages are defined to be the averages of the 12 monthly values. The tables in Appendix B present the monthly statistics for the entire atmosphere.

The values of the standard errors that measure the intra-monthly variabilities of the quantities indicate that there is a definite decrease in the variability toward the short-wave end in all quantities and that the variability of the three-component interaction, as represented by the exchanges among waves and the net fluxes of individual wave components, is generally greater than that of the two-component interac-

tion as given by the exchanges between individual waves and the zonal mean and the net fluxes of the energies of the zonal mean.

On account of the high level of variabilities both within a month and between months, on the one hand, and because of difficulty in examining the results in terms of individual wave components, on the other, most of the analyses are carried out in terms of a number of combinations both in wave-number and in layer. The choices of such syntheses are dictated by physical reasoning and precedents and are compromised by convenience. Thus, in the wave-number domain, the 15 wave components are grouped into three wave groups, each consisting of five components, as long- ($n = 1...5$), medium- ($n = 6...10$), and short-wave ($n = 11...15$) groups. Such a grouping seems to be the simplest and also to be in conformity with the results of investigations of the linear baroclinic instability, e.g., Phillips (1954), that show that the degree of instability is greatest in the medium waves with the decrease on both ends. It is also the grouping used by Saltzman and Fleisher (1960) in their study of kinetic-energy exchanges at 50 cb. Along the vertical, on the other hand, the tropopause and proximity to the ground seem to be the natural objects of consideration. Therefore, by placing the mean level of the tropopause at the 20-cb level and dividing the troposphere into two, the whole atmosphere is divided into three layers, namely, the lower stratosphere, the upper troposphere and the lower troposphere.

3.1.2 A Brief Description of the General Circulation Observed During the Period

No attempt will be made to relate the results of computation on the exchanges and influxes of the energies quantitatively with the atmospheric motion. Nevertheless, a brief description of the general circulation observed from a conventional standpoint is inserted here to help a proper viewing of the results.

The monthly-mean cross sections of the zonal wind and the zonally-averaged temperature are collected in Appendix C. The seasonal-normal cross section of wind and temperature are also entered in the middle month of each season. The seasonal normals of the zonal wind are obtained at 5-degree intervals on 85-, 70-, 50-, 30-, 20-, and 10-cb levels from the Normal Charts issued by the Office of the Chief of Naval Operations (1959), while the seasonal normals of the zonally-averaged temperature are taken from the tables by Goldie, Moore, and Austin (1957) and by J. London (1957).

The zonal indices in the subtropical ($20^{\circ} \sim 35^{\circ}\text{N}$), temperate ($35^{\circ} \sim 55^{\circ}\text{N}$), and polar ($55^{\circ} \sim 70^{\circ}\text{N}$) belts defined on the 70-cb level in the Western Hemisphere are chosen to represent the intra-monthly variations of the zonal wind in different regions of the Northern Hemisphere. The time series of the 5-day means of the zonal indices that have been compiled by the Extended Forecast Division of the U.S. Weather Bureau are presented in Appendix D.

While there are only small deviations from the normals in the distributions of the zonally-averaged temperature throughout the year, the

wind distributions exhibit a subtropical jet which is stronger than the normal through the entire period. Its positive anomaly is much larger in winter than in summer. In the middle latitudes the westerlies are weaker than the normal during most of the winter months, but above the normal during the summer months as the subtropical jet moves northward. The polar vortex in high latitudes is stronger than the normal throughout the year except during May.

The frequency and amplitude of the intra-monthly fluctuations of the zonal wind may be seen in the time-series of the zonal indices to the extent they appear on the 70-cb level on the 5-day means. The abnormality of the winter 1962-1963 is exhibited in the extremely low index of the temperate belt and the extremely high index of the subtropical belt, both of which persist through the period between late December and early February. The recovery to the high index in middle latitudes takes place rather rapidly but irregularly in the second half of February. Rapid and small fluctuations in the high-index cycle of March are followed by slow and large fluctuations in the rest of the spring. In the period between early June and late September the fluctuations are generally moderate in both frequency and amplitude. Starting in early October, however, the amplitude of the fluctuations becomes extremely large and the frequency increases toward the end of the period.

3.2 ANNUAL AVERAGES

The annual averages of exchanges and influxes of kinetic and available potential energies are presented in Figs. 2 and 3. The vertical

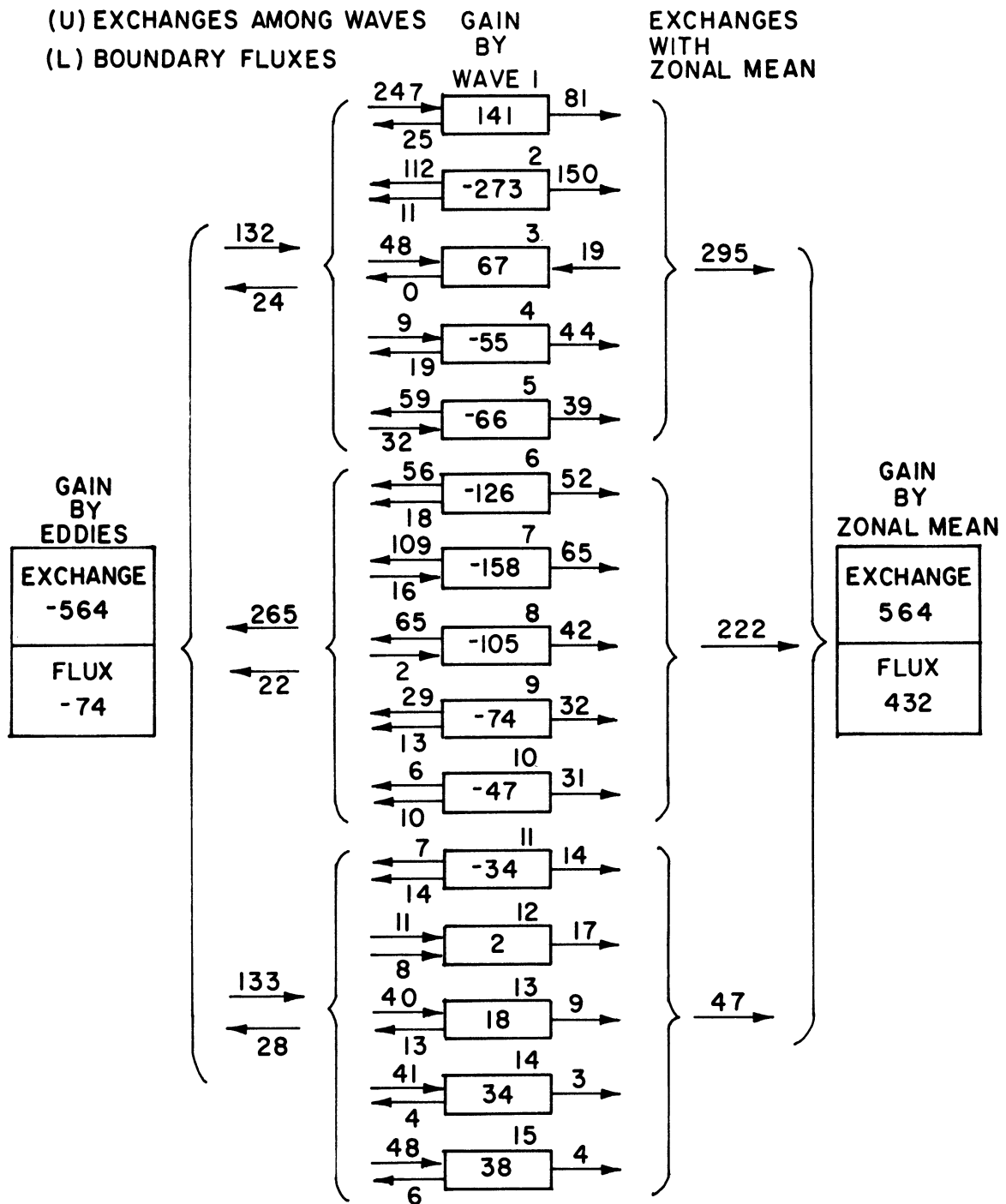


Fig. 2. Annual averages of exchanges and influxes of kinetic energy ($\text{erg cm}^{-2} \text{sec}^{-1}$) in the total atmosphere (0~100 cb).

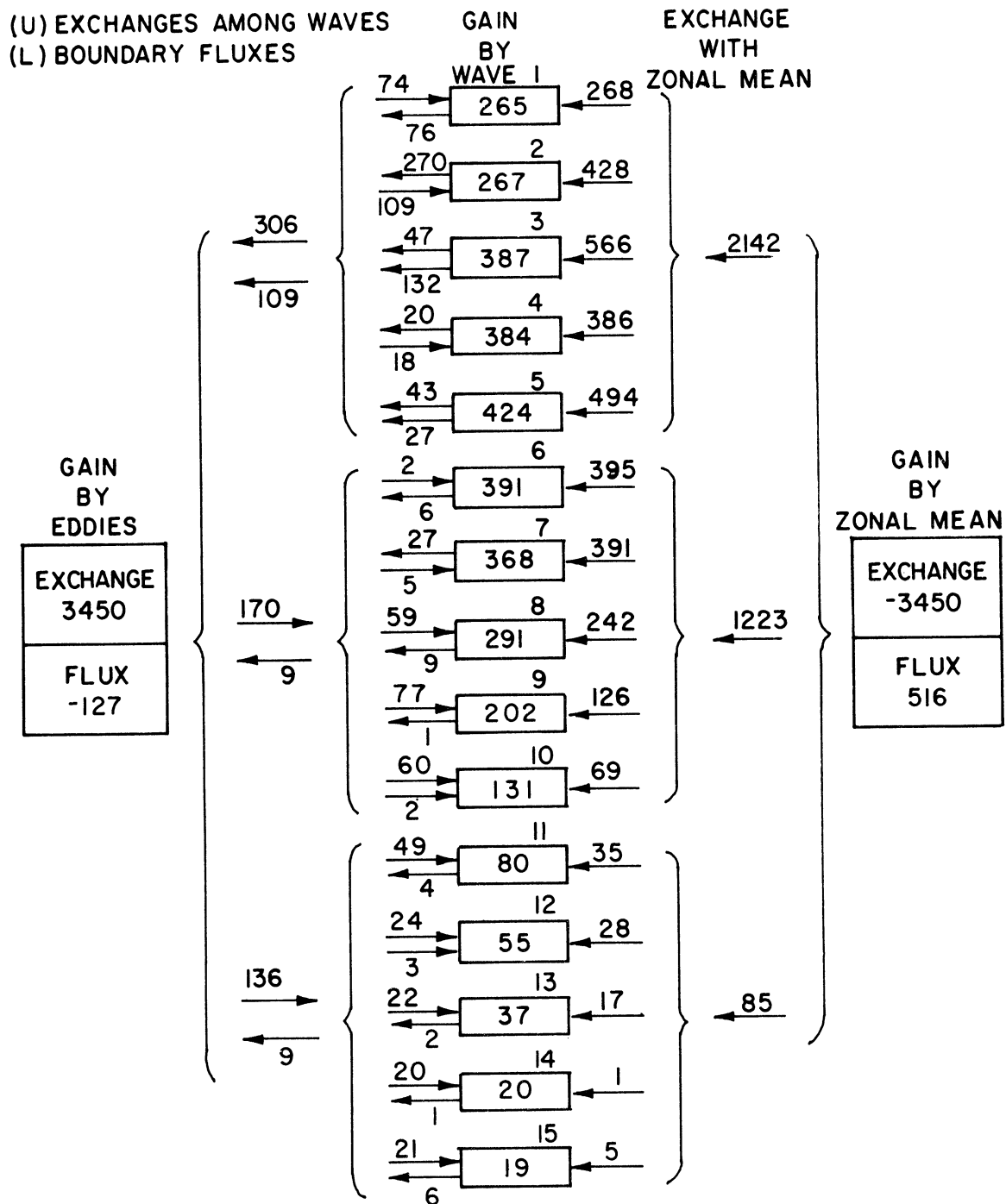


Fig. 3. Annual averages of exchanges and influxes of available potential energy ($\text{erg cm}^{-2} \text{sec}^{-1}$) in the total atmosphere (10~100 cb).

column of boxes in each figure represents the wave components and the set of an arrow and a numeral to the right of each box refers to the direction and the magnitude in units of $\text{ergs cm}^{-2} \text{ sec}^{-1}$ of the flow of energy in the conversion between each component and the zonal mean, $C(K_Z, K_N)$ or $C(E_Z, E_N)$. Similarly, the upper set of an arrow and a numeral to the left of each box gives the direction and magnitude of the energy conversion due to wave interaction, $\sum_m C(K_m, K_N)$ or $\sum_m C(E_m, E_N)$, while the lower set presents those of the net flux, $F(K_N)$ or $F(E_N)$. The numeral in each box is the net gain of the wave component through the three processes. Immediately outside the array stand three sets of arrow and numeral on each side that represent the conversions and fluxes of three wave groups, referred to as the long-, medium-, and short-wave groups, respectively, and on the rim are the total gains of the zonal mean to the right and that of the eddies to the left.

The amounts of conversion between the eddies and the zonal mean, $564 \text{ ergs cm}^{-2} \text{ sec}^{-1}$ ($10^{-6} \text{ kJm}^{-2} \text{ sec}^{-1}$) from the eddies to the zonal mean for kinetic energy and $3450 \text{ ergs cm}^{-2} \text{ sec}^{-1}$ from the zonal mean to the eddies for available potential energy, are both on the large side of the values quoted by Oort (1964) in his review on studies of atmospheric energetics. In both conversions it is seen that the long-wave group contributes the largest part whereas the short-wave group plays a rather insignificant role.

In the conversion arising from wave interaction it is noted that, while kinetic energy flows out of the medium-wave group into both long-

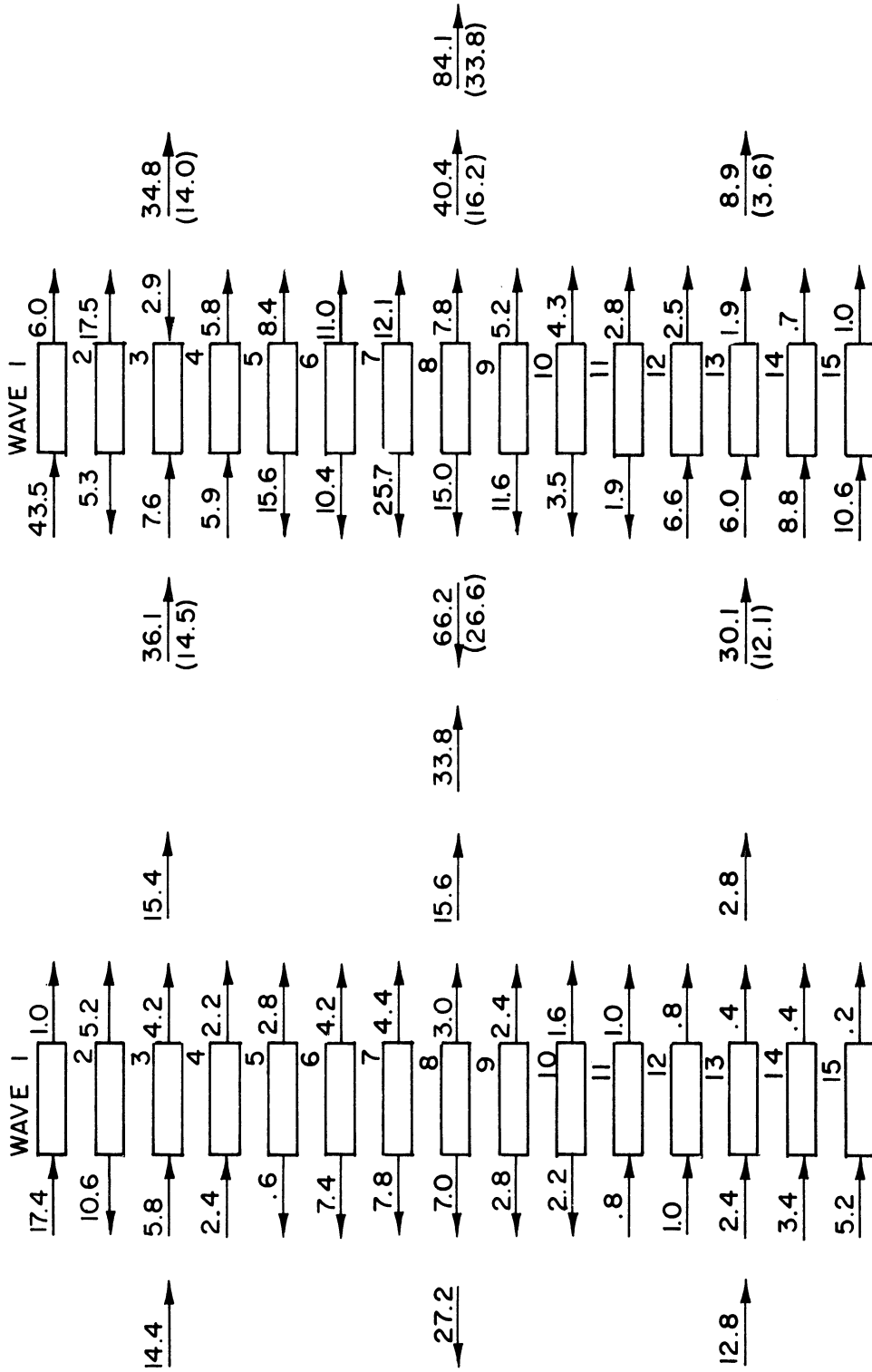
and short-wave groups with a nearly equal partitioning, the available potential energy is transferred from the long-wave group to the others with a larger amount to the closer group.

The net effect of the two exchange processes then places the medium-wave group and the zonal mean as the source of kinetic energy and available potential energy, respectively.

The amounts of the boundary influxes created by wave interaction are, in terms of both group and sum, smaller than those due to exchanges, although by no means unimportant, and much smaller than those of the influxes of the energies of the zonal mean.

The awareness of the fact that the results stated above are based on observations from a single year leads to a search for means of testing their credibility. The result is summarized in Fig. 4, where a figure--with a change in the unit--from a study of Saltzman and Teweles (1964) on the kinetic-energy exchanges at the 50-cb level over the 9-year period of 1955-1964 is reproduced with the corresponding set from the present study to its right side.

Since the total conversion of kinetic energy between the zonal mean and the eddies is perhaps the best established of all, the set of group values in the latter is aligned to the former by multiplying the latter by the ratio of the two values of total conversion between the zonal mean and the eddies and entered in the parentheses under the original figures. The comparison shows a surprisingly good agreement in all group values. The high level of exchanges obtained in the present study--about two and



SALTZMAN AND TEWELES (1964)

PRESENT STUDY

Fig. 4. A comparison between the results obtained by Saltzman and Teweles (1964) and those of the present study on the kinetic energy exchanges at 500 mb (unit: $\text{erg cm}^{-2} \text{ sec}^{-1}$).

a half times that of the 9-year averages obtained by Saltzman and Teweles— may be due to the fact that the year 1963 was an active year with regard to weather and circulation, as described in the preceding section.

The vertical compositions of the annual averages of exchanges and influxes of the wave groups are shown respectively in Fig. 5(A)-(C) for kinetic energy and in Fig. 6(A)-(C) for available potential energy while those of the zonal mean are presented in Fig. 7. In Fig. 5(A) which depicts the vertical cross section of $C(K_Z, K_E)$ it is quite obvious that the short-wave group contributes far less than the others at all levels and that the medium- and short-wave groups exhibit very similar variations with height. It is also observed that the contribution of the long-wave group toward the total conversion increases with height, while those of the shorter wave groups have maxima at a level slightly below the jet stream level. The total conversion from the eddies to the zonal flow increases with height to the level of the jet stream and then decrease above it. This reminds one of a similar variation with height of the kinetic energy itself as reported by Wiin-Nielsen (1967). The variations with height of the annual averages of K_Z and K_E are entered in Fig. 7(A) to show the similarity of the profiles.

In the exchange due to wave interaction, as shown in Fig. 5(B), it is seen that energy is transferred from the medium- and short-wave groups into the long-wave group at the bottom and from the medium- into both long- and short-wave groups in the bulk of troposphere before the long-wave group starts to lose its energy to shorter wave groups in the

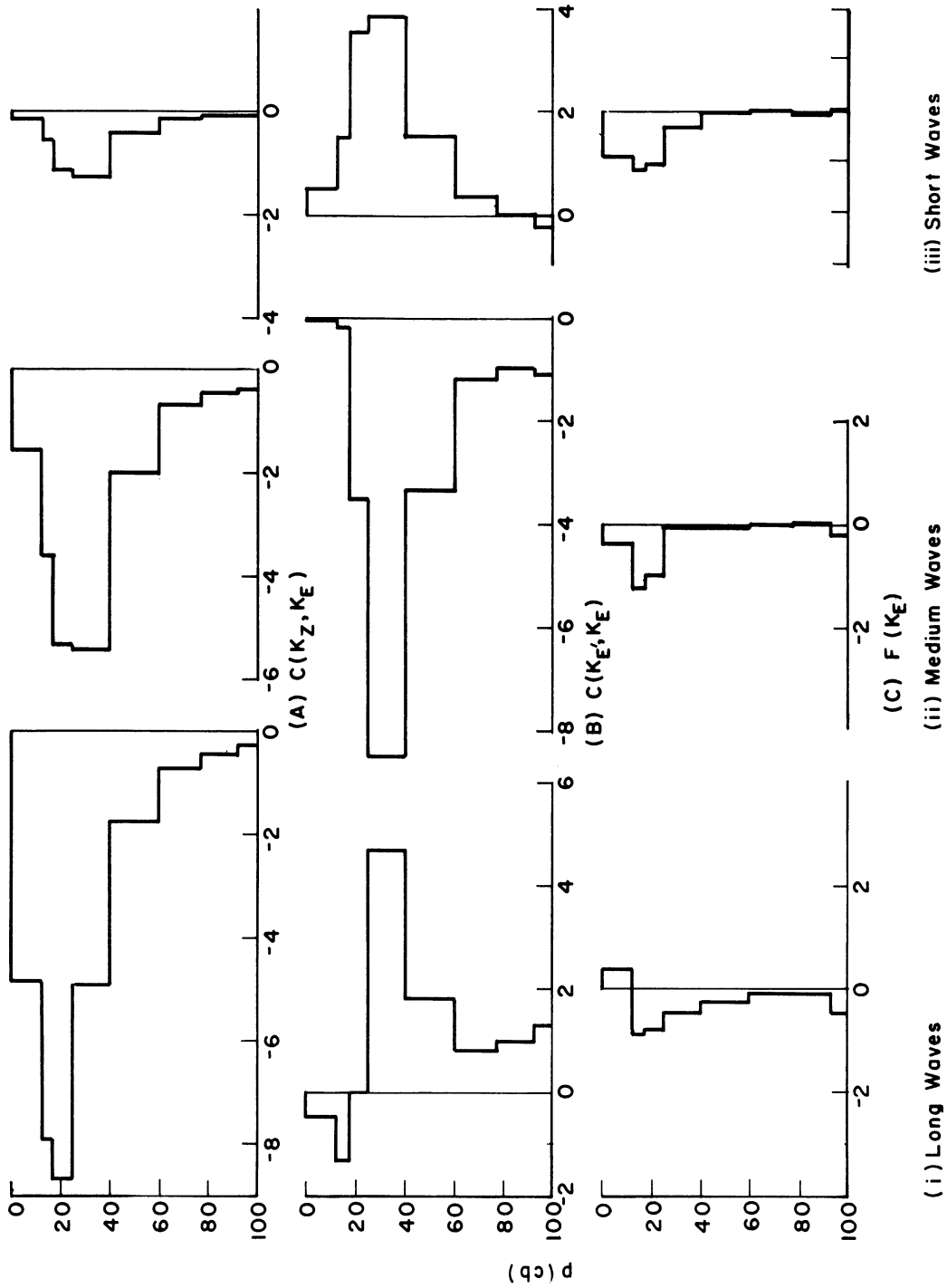


Fig. 5. Vertical variations of exchanges and influxes of eddy kinetic energy ($\text{erg cm}^{-2} \text{sec}^{-1} \text{cb}^{-1}$).

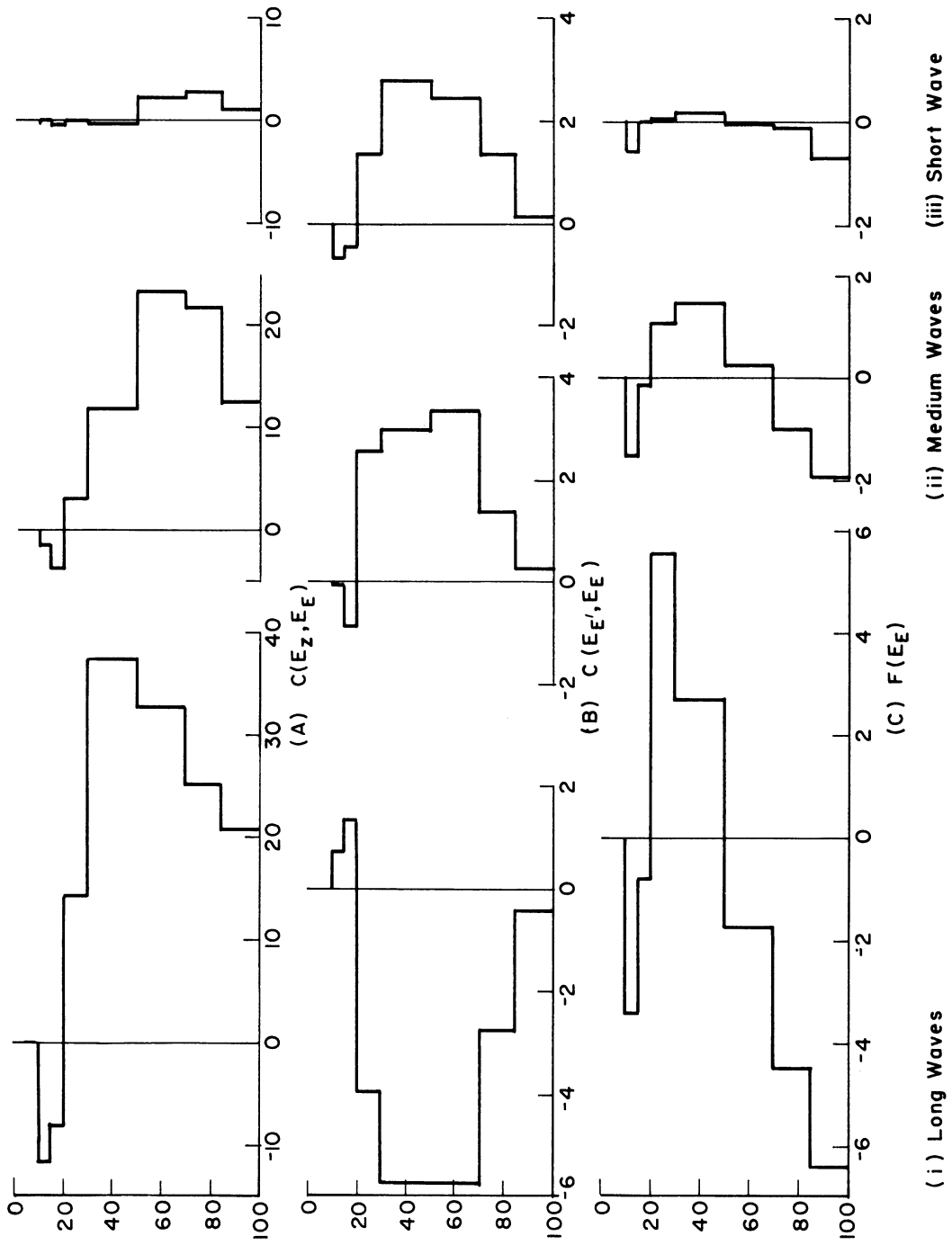


Fig. 6. Vertical variations of exchanges and influxes of eddy available potential energy ($\text{erg cm}^{-2} \text{sec}^{-1} \text{cb}^{-1}$).

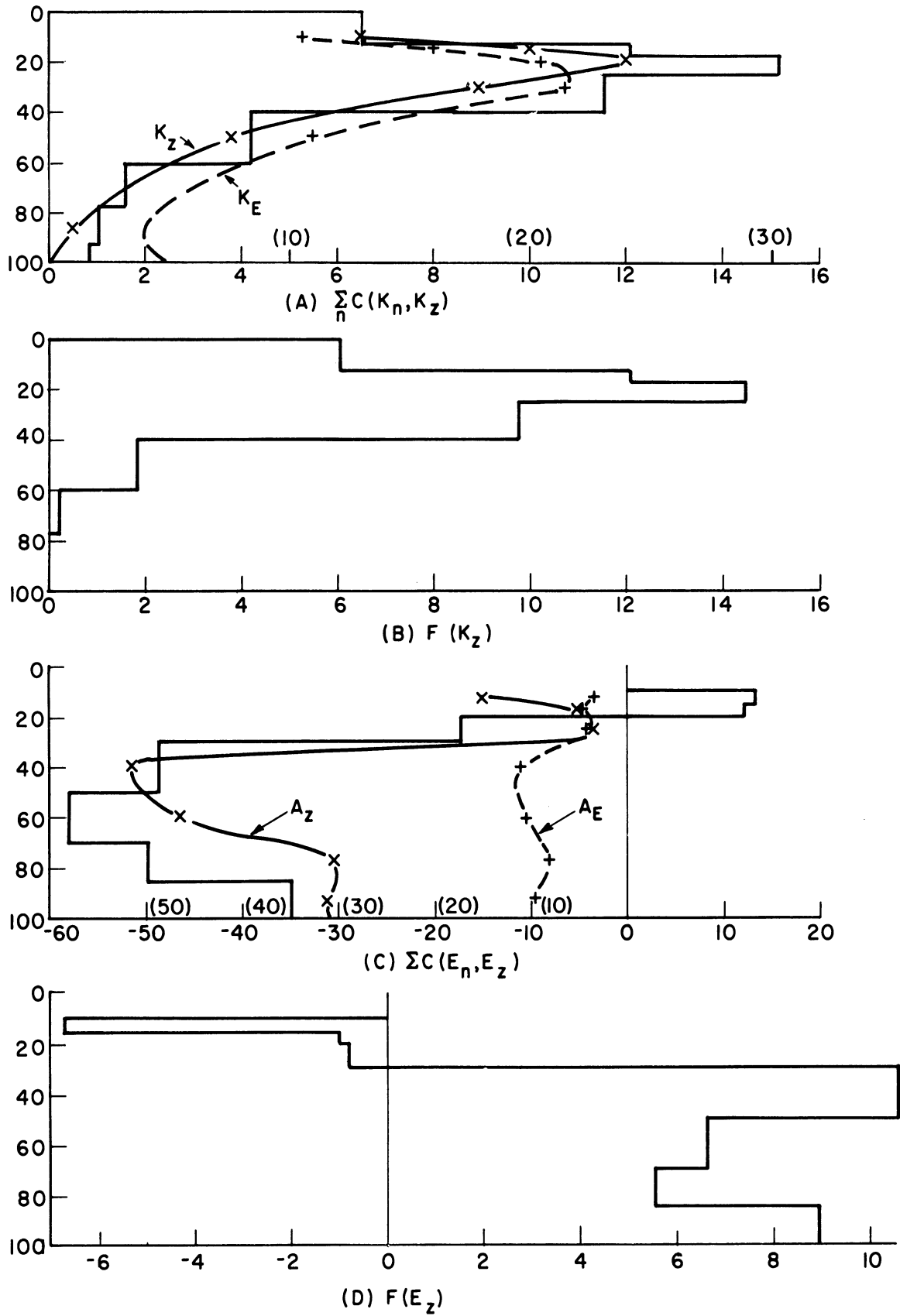


Fig. 7. Vertical variations of exchanges and influxes of kinetic and available potential energies of the zonal mean ($\text{erg cm}^{-2} \text{sec}^{-1} \text{cb}^{-1}$).

lower stratosphere. The magnitude of the exchange has a maximum at the 30-cb level which is attended by a sharp decrease on both sides.

A comparison of Fig. 5(A) and 5(B) reveals that in all the wave groups the exchange due to wave interaction contributes a greater amount than the exchange with the zonal flow in the troposphere, while the latter supercedes the former in the lower stratosphere.

Figure 5(C), which shows the vertical variation of $F(K_E)$, reveals, firstly, that the influx plays a less significant role than the exchange processes in the net change of kinetic energy in the individual wave groups and, secondly, that the eddy energy flows out of the area at all levels.

In available potential energy the energy is transferred from the zonal mean to the eddies in the troposphere and from the eddies to the zonal flow in the stratosphere (Fig. 6(A)). Here, the preponderance of the long-wave group at all levels is very striking. It is also observed that the level of the maximum intensity lowers as the wave becomes shorter in wave-length. The total conversion from the zonal mean to the eddies shows a maximum at the middle of the troposphere. As in kinetic energy, such a vertical variation seems to be very similar to that of the amount of available potential energy itself, and the results of Wiin-Nielsen (1967) are again entered in Fig. 7(C) for a comparison.

In Fig. 6(B), the vertical variation of the exchange due to wave interaction, it is seen that energy is given up by the long-wave group to the shorter-wave groups with a larger part to the medium- than to the

short-wave group throughout the troposphere, while the reverse transfer takes place in the lower stratosphere. It may be recalled that a similar reversal of transfer at the boundary between the troposphere and stratosphere was noted earlier in the exchange among waves of kinetic energy. The amplitude of the exchange has its maximum in the mid-troposphere as does that of transfer from the zonal mean. By comparing the two exchanges it is noted that the transfer from the zonal mean is in general greater than the transfer among waves for available potential energy, in contrast with what was observed earlier for kinetic energy.

The vertical variation of $F(E_E)$, which is shown in Fig. 6(C), shows a remarkable contrast between upper and lower troposphere, and indicates that the small magnitude of the outflux for the entire atmosphere is really made up of two large opposing contributions, in contrast to that for kinetic energy. It is also noted here that the long-wave group has a far larger influx than the others at all levels.

The role of the boundary flux in maintaining the zonal flow is quite significant, as can be readily observed in Fig. 7(B). Its effect is almost as large as that of the conversion from the eddies within the region except in the lower troposphere where it is totally absent. Since, as in all the boundary fluxes computed in the present study, the boundary flux arises largely at the southern boundary this signifies the importance of the eddy transport of kinetic energy from the tropics in sustaining the zonal flow in the extratropical region.

The boundary flux of the zonal available potential energy presented in Fig. 7(C), on the other hand, shows that while in the troposphere the import from the tropics replenishes only approximately 20% of the amount of conversion to the eddies, the export in the lower stratosphere accounts for about one half of the conversion from the eddies.

It may also be noted that while in kinetic energy the eddy boundary flux counters the zonal boundary flux by outflowing throughout the atmosphere, such a counteraction is seen only in the lower troposphere in the boundary fluxes of available potential energy.

3.3 ANNUAL VARIATIONS

The series of figures from Fig. 8 to Fig. 13 presents the annual variations of exchanges and influxes of the two forms of energy in terms of wave group, in which the A series is of the entire atmosphere expressed in the unit of $\text{ergs cm}^{-2} \text{ sec}^{-1}$, while the B series is of the three layers, namely, the lower stratosphere, the upper and the lower troposphere, expressed in the unit of $\text{ergs cm}^{-2} \text{ sec}^{-1} \text{ cb}^{-1}$.

In what follows, salient features in the amounts and variations of the individual quantities as they appear in these figures will be described.

(i) Exchange between the zonal mean and the eddies.--In the kinetic-energy exchange (Fig. 8(A) and 8(B)) it is observed first of all that the exchange is directed from the eddies to the zonal mean throughout the year except in the months of February and March. The great depar-

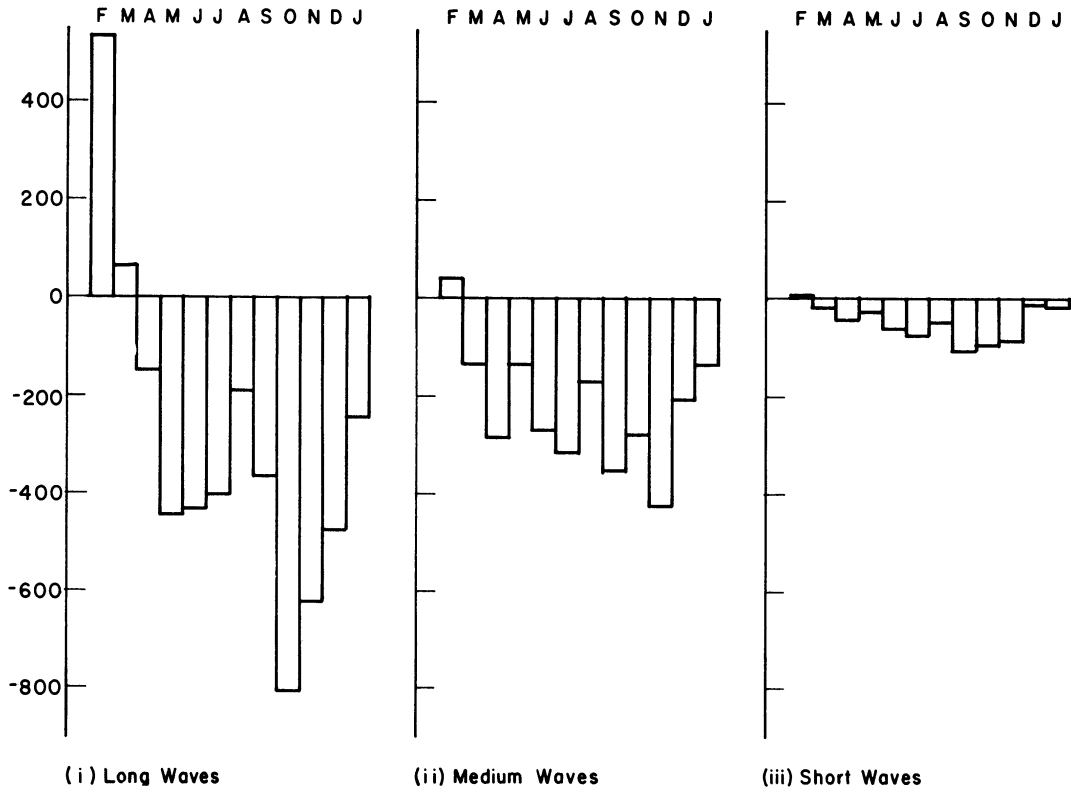


Fig. 8(A). $C(K_Z, K_E)$ ($\text{erg cm}^{-2} \text{sec}^{-1}$) in the total atmosphere (0~100 cb).

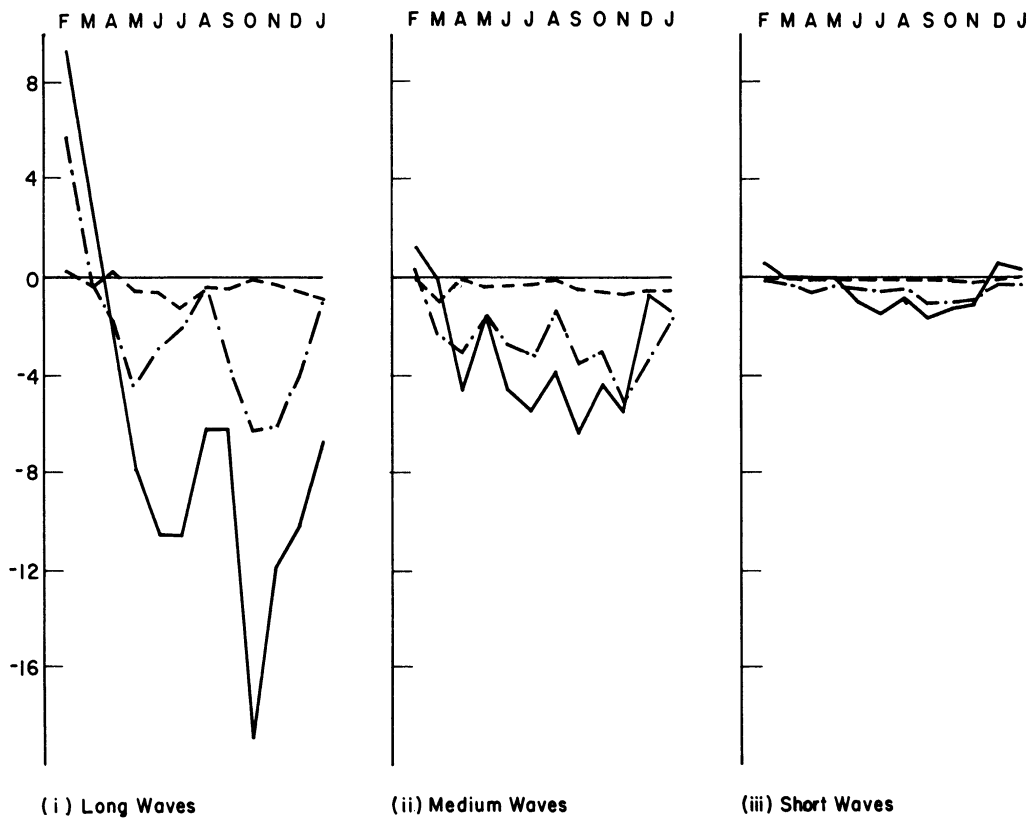


Fig. 8(B). $C(K_Z, K_E)$ ($\text{erg cm}^{-2} \text{sec}^{-1}$) in the individual layers. The lower stratosphere (solid), the upper troposphere (dash-dots), and the lower troposphere (dots).

ture in February is believed to be a reflection of the abnormal circulation observed in the mid-winter of 1962-63, as seen in the zonal indices (Appendix D), on which comments have been made in various works, e.g., Murakami and Tomatsu (1964) and Wiin-Nielsen (1964).

The amount and variation of the exchange are largest in the long-wave group and decrease toward the short-wave group throughout the year. It is quite apparent from Fig. 8(B) that this is primarily due to the large amount and variation observed in the lower stratosphere and the smallest contribution by the short-wave group in all the layers. On the other hand, the contribution from the exchange in the lower troposphere is consistently small in all the wave groups.

The exchange in available potential energy, as shown in Fig. 9(A) and 9(B), is directed from the zonal mean to the eddies throughout the year except the summer months of June and July. The largest magnitude and variation are found, as in the kinetic-energy exchange, in the long-wave group. The vertical distributions show that the exchange in the troposphere predominates and is opposed by a much smaller contribution from that in the lower stratosphere in all three wave groups, in contrast to what has been noted in the kinetic-energy exchange. The exchange in the troposphere is smallest in the summer for all three wave groups.

It is thus seen in both forms of energy that the exchanges between the zonal mean and the eddies in the individual months are in a qualitative agreement with those represented by the annual averages except in

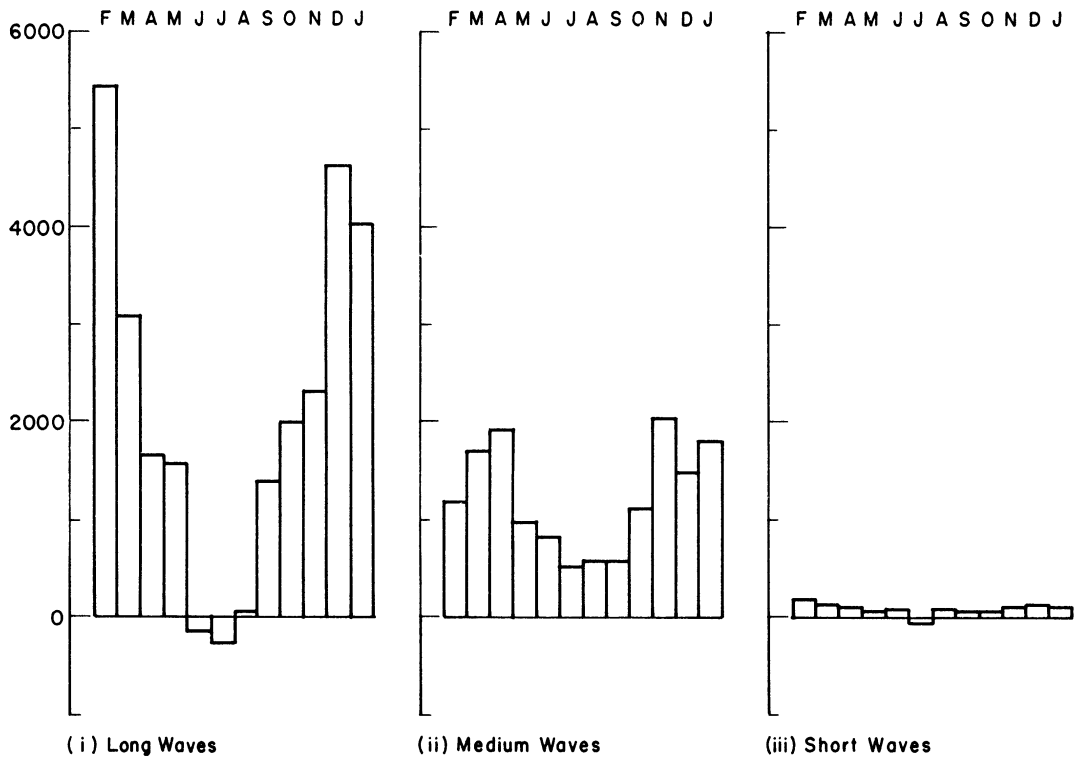


Fig. 9(A). $C(E_Z, E_E)$ ($\text{erg cm}^{-2} \text{sec}^{-1}$) in the total atmosphere ($10 \sim 100 \text{ cb}$).

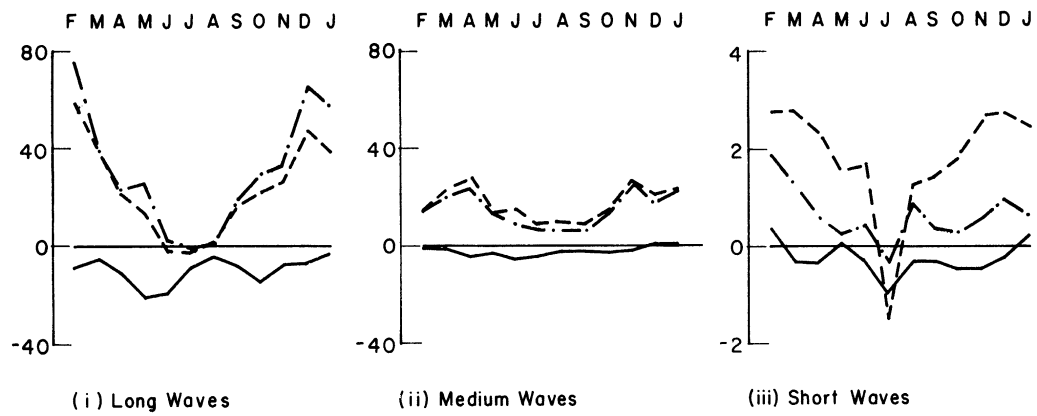


Fig. 9(B). $C(E_Z, E_E)$ ($\text{erg cm}^{-2} \text{sec}^{-1} \text{cb}^{-1}$) in the individual layers. The symbols are the same as those in Fig. 8(B).

the extreme seasons, although there are considerably large fluctuations in their magnitudes.

(ii) Exchange among waves in the eddies.—The variations by months of the exchanges due to wave interaction, as shown in Fig. 10(A) and (B) for kinetic energy and Fig. 11(A) and (B) for available potential energy, present more complicated patterns than those of the exchanges between the zonal mean and the eddies.

The relatively simple pattern exhibited by the variations in the exchanges of available potential energy is perhaps the only feature which is readily discernible in these figures. It shows that the long-wave group loses energy to the other wave groups during most of the year and the loss is greater in winter. It receives energy from the others during the summer months, but the amounts of gain in summer are small in comparison with the amounts of loss in winter. Thus, the long-wave group is seen in this exchange to play a similar role as the zonal mean does in the exchange of the same form of energy between the zonal mean and the eddies.

It may also be noted that large amounts and wide fluctuations of the exchange are generally found in the lower stratosphere and the upper troposphere in kinetic energy, but are largely confined to the troposphere in available potential energy.

In an effort to seek a qualitative picture which may describe these variations in a simpler manner the directions of energy flows due to the exchanges are defined in the individual layers and for the individual

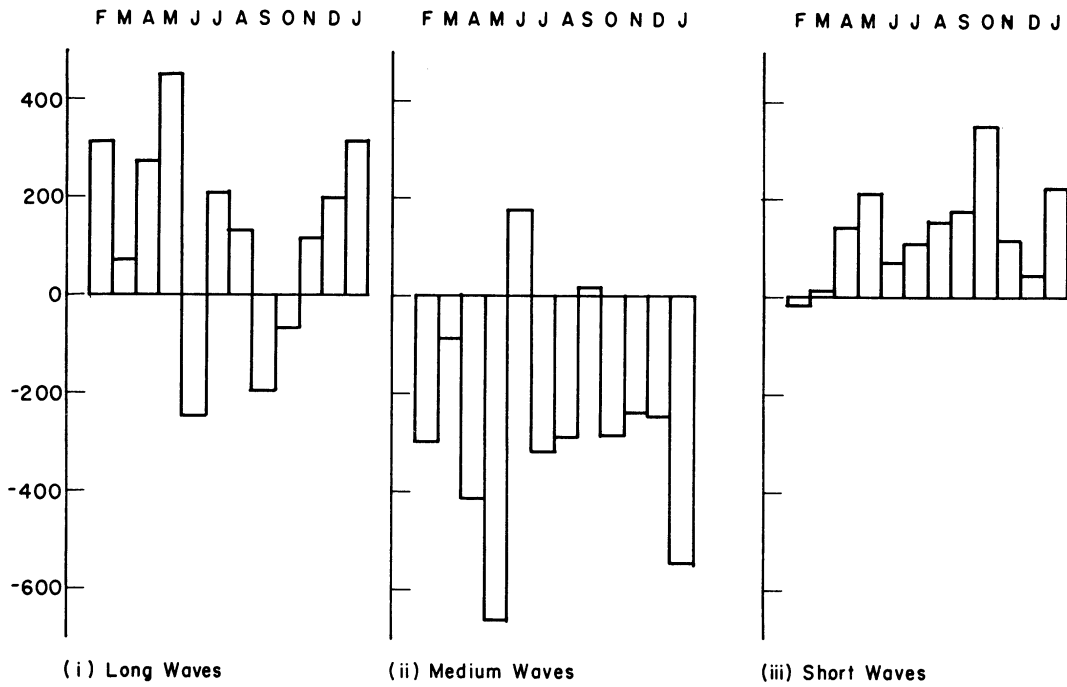


Fig. 10(A). $C(K_{E1}, K_{E2})$ ($\text{erg cm}^{-2} \text{sec}^{-1}$) in the total atmosphere (0~100 cb).

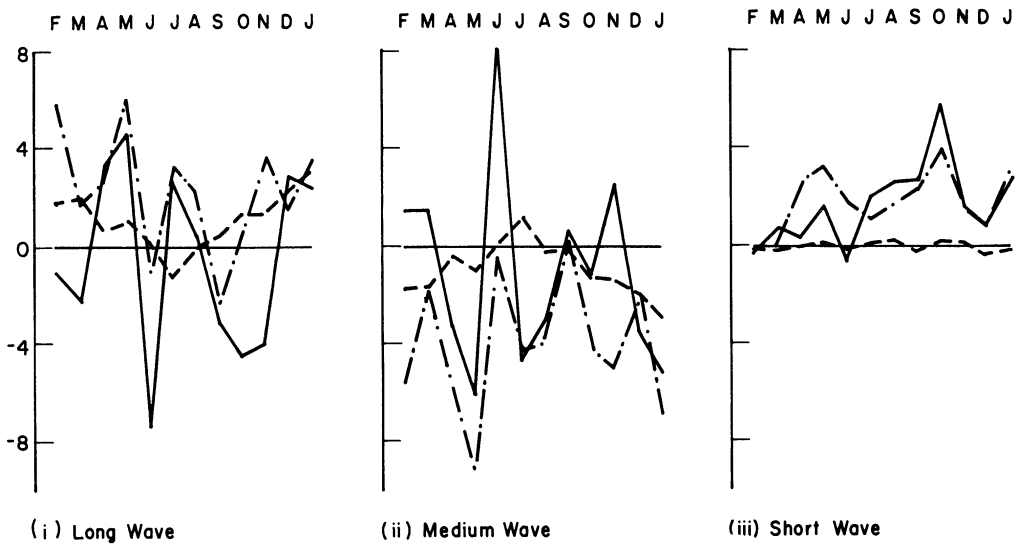


Fig. 10(B). $C(K_{E1}, K_{E2})$ ($\text{erg cm}^{-2} \text{sec}^{-1} \text{cb}^{-1}$) in the individual layers. The symbols are the same as those in Fig. 8(B).

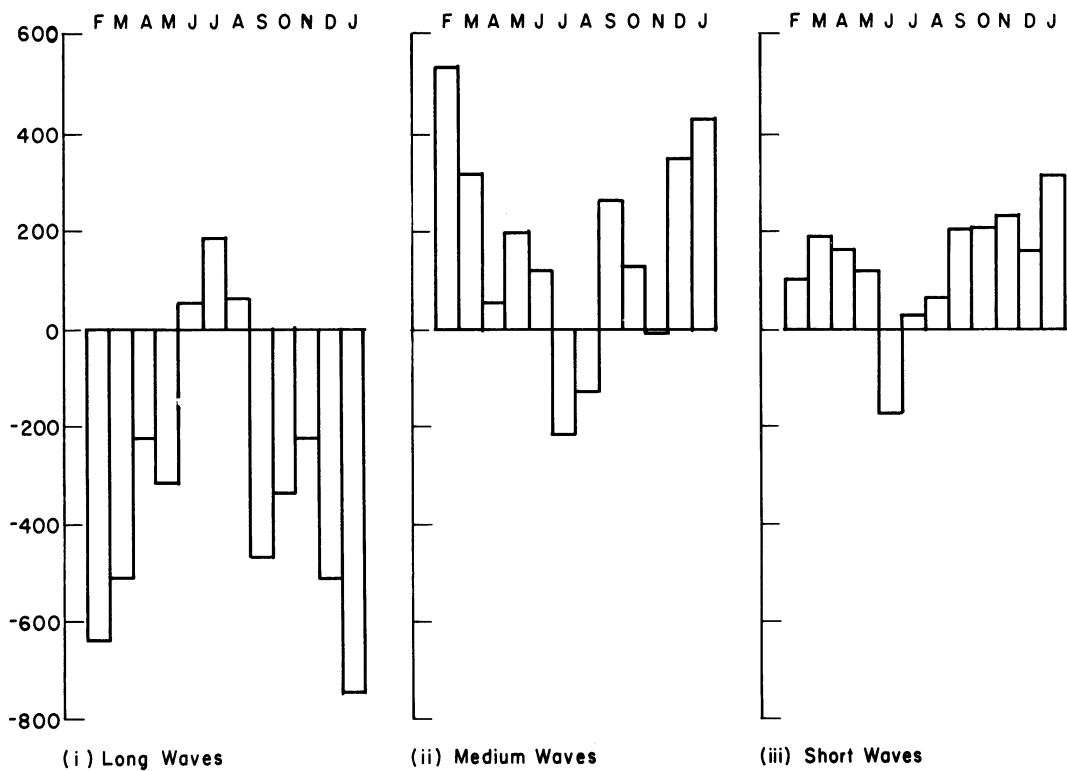


Fig. 11(A). $C(E_{E1}, E_E)$ ($\text{erg cm}^{-2} \text{sec}^{-1}$) in the total atmosphere (10~100 cb).

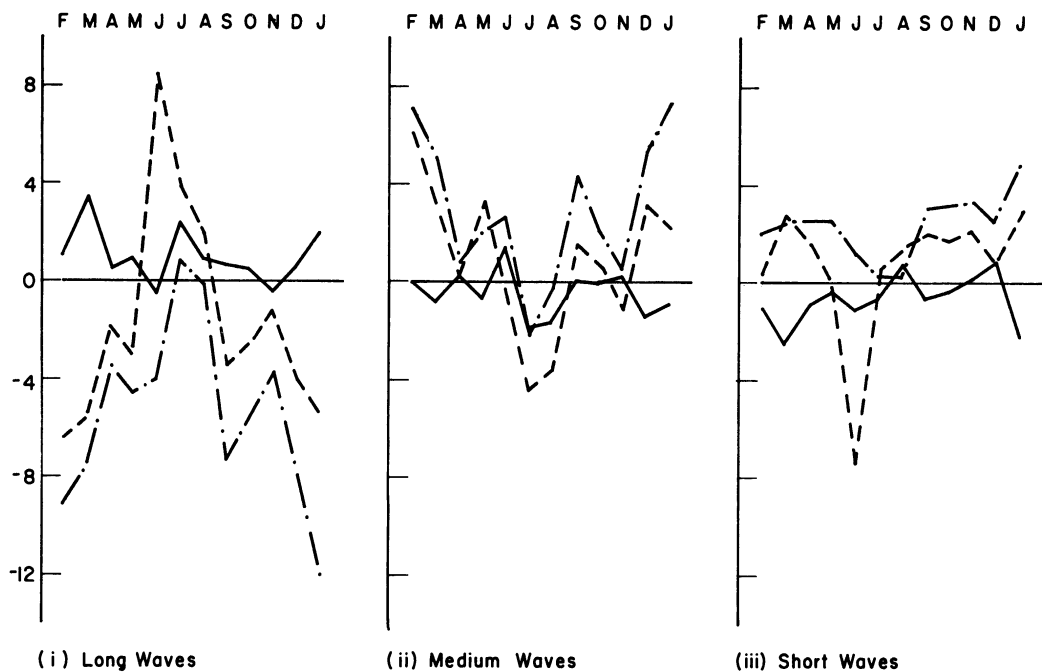


Fig. 11(B). $C(E_{E1}, E_E)$ ($\text{erg cm}^{-2} \text{sec}^{-1} \text{cb}^{-1}$) in the individual layers. The symbols are the same as those in Fig. 8(B).

months. The results are Tables 3 and 4, in which also shown are the resultants for the entire atmosphere. The variations with height and season of the characters of the exchanges seem to emerge rather clearly from these tables.

In Table 3, which shows the flows of kinetic energy, the exchange in the lower troposphere is predominantly from the medium- to long-wave group and the lack of participation by the short-wave group is very striking. If the up- and down-flow of energy are defined to be the flows which cause the net accumulation of energy in the longer and shorter wave groups, respectively, then this exchange in the lower troposphere is characterized by an up-flow. The similar up-flow is maintained in the upper troposphere during most of the period, but the increasing participation of the short-wave group on the receiving end of the exchange distinguishes it from that of the lower layer. There are also more cases of the down-flow observed here than in the lower layer. Finally, in the lower stratosphere, the two kinds of flow seem to alternate with each other.

The flows of available potential energy shown in Table 4, on the other hand, bring out clearly the contrast between the down-flow of the troposphere and the up-flow of the lower stratosphere. The up-flow in the troposphere is confined to the summer months and mainly to the lower layer.

(iii) Influxes of the energies of the eddies.—There is hardly an indication of any systematic change with the time of year in the varia-

TABLE 4

FLOW OF POTENTIAL ENERGY DUE TO THE INTERACTION AMONG WAVES

	Feb.	Mar.	Apr.	May	Jun.	Jul.	Aug.	Sep.	Oct.	Nov.	Dec.	Jan.
lower stratosphere	$\begin{matrix} L \leftarrow S \\ M \rightarrow \end{matrix}$	$\begin{matrix} L \leftarrow S \\ M \rightarrow \end{matrix}$	$\begin{matrix} L \leftarrow S \\ M \leftarrow S \end{matrix}$	$\begin{matrix} L \leftarrow S \\ M \rightarrow \end{matrix}$	$\begin{matrix} L \leftarrow S \\ M \leftarrow S \end{matrix}$	$\begin{matrix} L \leftarrow S \\ M \rightarrow \end{matrix}$	$\begin{matrix} L \leftarrow S \\ M \rightarrow S \end{matrix}$	$\begin{matrix} L \leftarrow S \\ M \rightarrow \end{matrix}$	$\begin{matrix} L \leftarrow S \\ M \rightarrow \end{matrix}$	$\begin{matrix} L \leftarrow S \\ M \rightarrow \end{matrix}$	$\begin{matrix} L \leftarrow S \\ M \rightarrow S \end{matrix}$	$\begin{matrix} L \leftarrow S \\ M \rightarrow \end{matrix}$
upper troposphere	$\begin{matrix} L \leftarrow S \\ M \rightarrow \end{matrix}$	$\begin{matrix} L \leftarrow S \\ M \rightarrow \end{matrix}$	$\begin{matrix} L \leftarrow S \\ M \rightarrow \end{matrix}$	$\begin{matrix} L \leftarrow S \\ M \rightarrow \end{matrix}$	$\begin{matrix} L \leftarrow S \\ M \rightarrow \end{matrix}$	$\begin{matrix} L \leftarrow S \\ M \rightarrow \end{matrix}$	$\begin{matrix} L \leftarrow S \\ M \rightarrow S \end{matrix}$	$\begin{matrix} L \leftarrow S \\ M \rightarrow \end{matrix}$	$\begin{matrix} L \leftarrow S \\ M \rightarrow \end{matrix}$	$\begin{matrix} L \leftarrow S \\ M \rightarrow \end{matrix}$	$\begin{matrix} L \leftarrow S \\ M \rightarrow S \end{matrix}$	$\begin{matrix} L \leftarrow S \\ M \rightarrow \end{matrix}$
lower troposphere	$\begin{matrix} L \leftarrow S \\ M \rightarrow \end{matrix}$	$\begin{matrix} L \leftarrow S \\ M \rightarrow \end{matrix}$	$\begin{matrix} L \leftarrow S \\ M \rightarrow \end{matrix}$	$\begin{matrix} L \leftarrow S \\ M \rightarrow \end{matrix}$	$\begin{matrix} L \leftarrow S \\ M \rightarrow \end{matrix}$	$\begin{matrix} L \leftarrow S \\ M \rightarrow S \end{matrix}$	$\begin{matrix} L \leftarrow S \\ M \rightarrow S \end{matrix}$	$\begin{matrix} L \leftarrow S \\ M \rightarrow \end{matrix}$	$\begin{matrix} L \leftarrow S \\ M \rightarrow \end{matrix}$	$\begin{matrix} L \leftarrow S \\ M \rightarrow S \end{matrix}$	$\begin{matrix} L \leftarrow S \\ M \rightarrow \end{matrix}$	$\begin{matrix} L \leftarrow S \\ M \rightarrow \end{matrix}$
total atmosphere	$\begin{matrix} L \leftarrow S \\ M \rightarrow \end{matrix}$	$\begin{matrix} L \leftarrow S \\ M \rightarrow \end{matrix}$	$\begin{matrix} L \leftarrow S \\ M \rightarrow \end{matrix}$	$\begin{matrix} L \leftarrow S \\ M \rightarrow \end{matrix}$	$\begin{matrix} L \leftarrow S \\ M \rightarrow S \end{matrix}$	$\begin{matrix} L \leftarrow S \\ M \rightarrow S \end{matrix}$	$\begin{matrix} L \leftarrow S \\ M \rightarrow S \end{matrix}$	$\begin{matrix} L \leftarrow S \\ M \rightarrow \end{matrix}$	$\begin{matrix} L \leftarrow S \\ M \rightarrow \end{matrix}$	$\begin{matrix} L \leftarrow S \\ M \rightarrow \end{matrix}$	$\begin{matrix} L \leftarrow S \\ M \rightarrow S \end{matrix}$	$\begin{matrix} L \leftarrow S \\ M \rightarrow \end{matrix}$

tions of the influxes of both kinetic and available potential energies of the eddies (Figs. 12(A), (B), and 13(A), (B)). Nor is there any detectable relation among the influxes in the individual layers. However, a couple of features may be noticed in the vertical compositions. In kinetic energy the magnitude of the flux in the lower stratosphere is generally so much greater than those in the other layers as to largely determine the variation by month of the total flux. This dominance of the flux in the lower stratosphere is most clearly exhibited by the short-wave group which has very small fluxes in the other layers throughout the year. In available potential energy, on the other hand, large fluxes are found in the troposphere. Extremely large fluxes in the months of June and July in the lower troposphere in all the wave groups tend to overshadow the rest.

(iv) Gains through exchanges with the eddies and influxes of the energies of the zonal mean.—The most remarkable feature in Figs. 14(A) and (B) that present the variations by month of exchanges and influxes of the energies of the zonal mean is that of $F(K_Z)$. It appears that the influx of the zonal kinetic energy from the tropics tends to complement the conversion from the eddies in the balance of the zonal kinetic energy during most months. No such simple regularity can be observed in the variation of the influx of the zonal available potential energy. The vertical compositions show in general that the relative contributions from the individual layers conform qualitatively to those given in Fig. 7 of the annual averages throughout the year except the summer months.

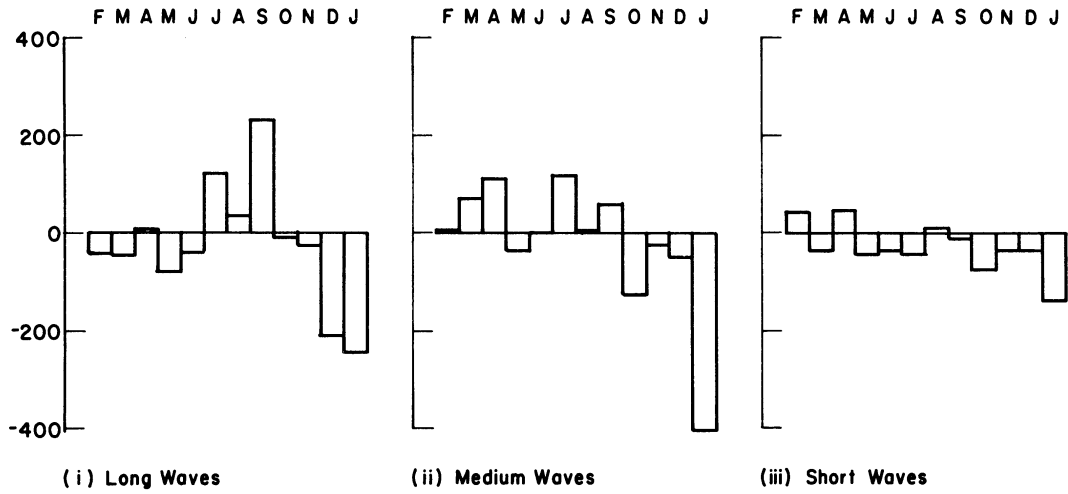


Fig. 12(A). $F(K_E)$ ($\text{erg cm}^{-2} \text{sec}^{-1}$) in the total atmosphere (0~100 cb).

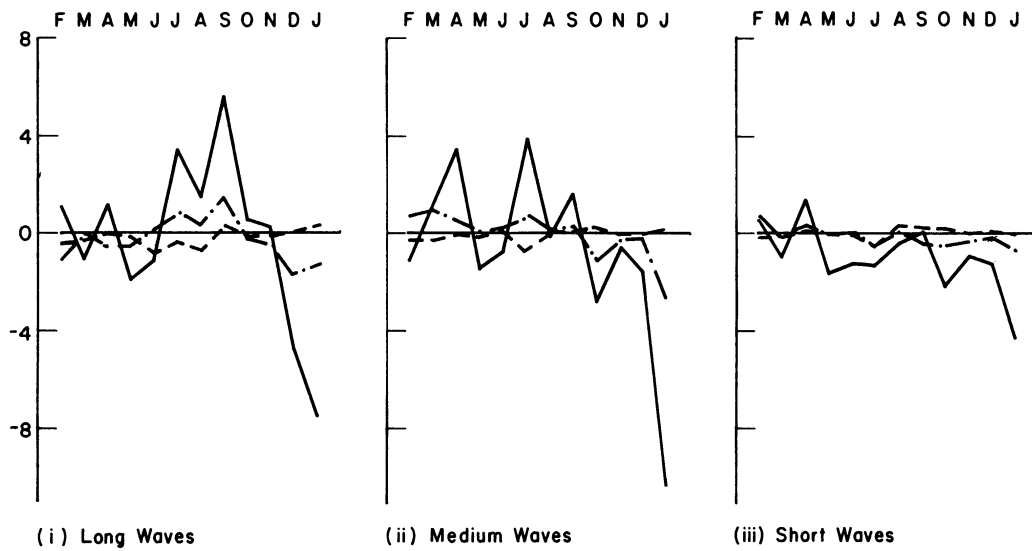


Fig. 12(B). $F(K_E)$ ($\text{erg cm}^{-2} \text{sec}^{-1} \text{cb}^{-1}$) in the individual layers. The symbols are the same as those in Fig. 8(B).

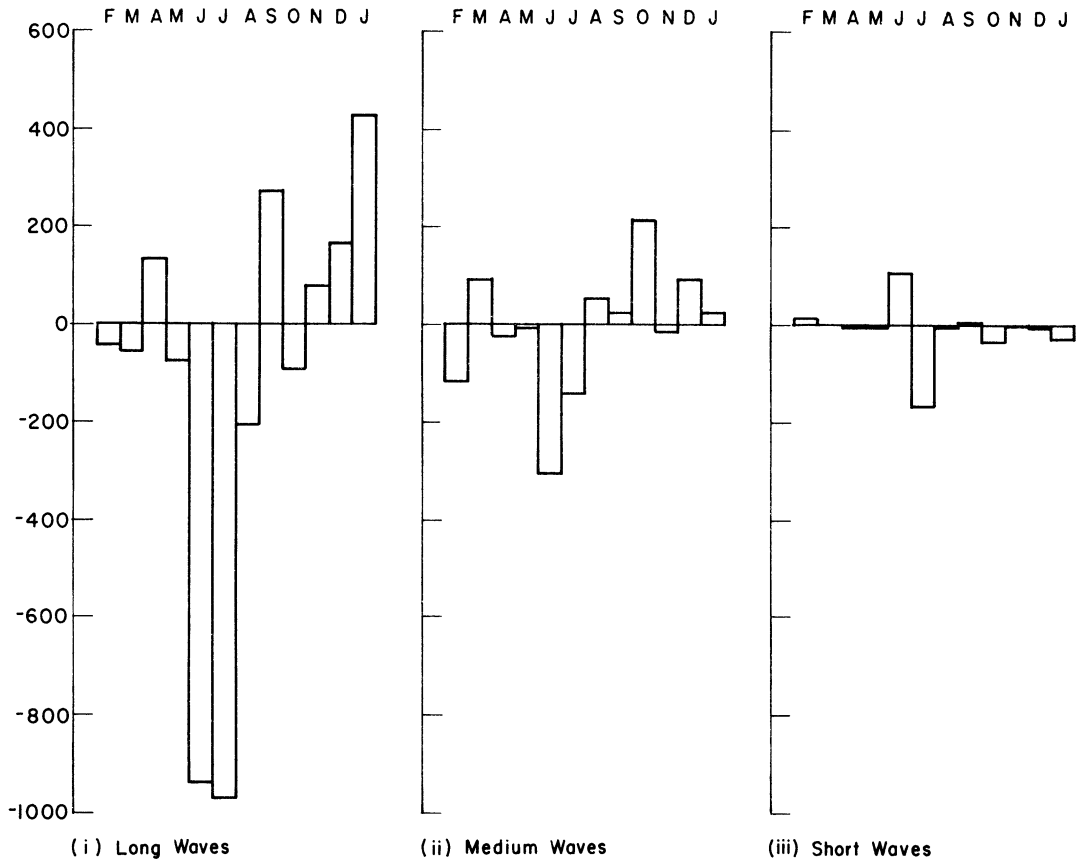


Fig. 13(A). $F(E_E)$ ($\text{erg cm}^{-2} \text{sec}^{-1}$) in the total atmosphere ($10 \sim 100 \text{ cb}$).

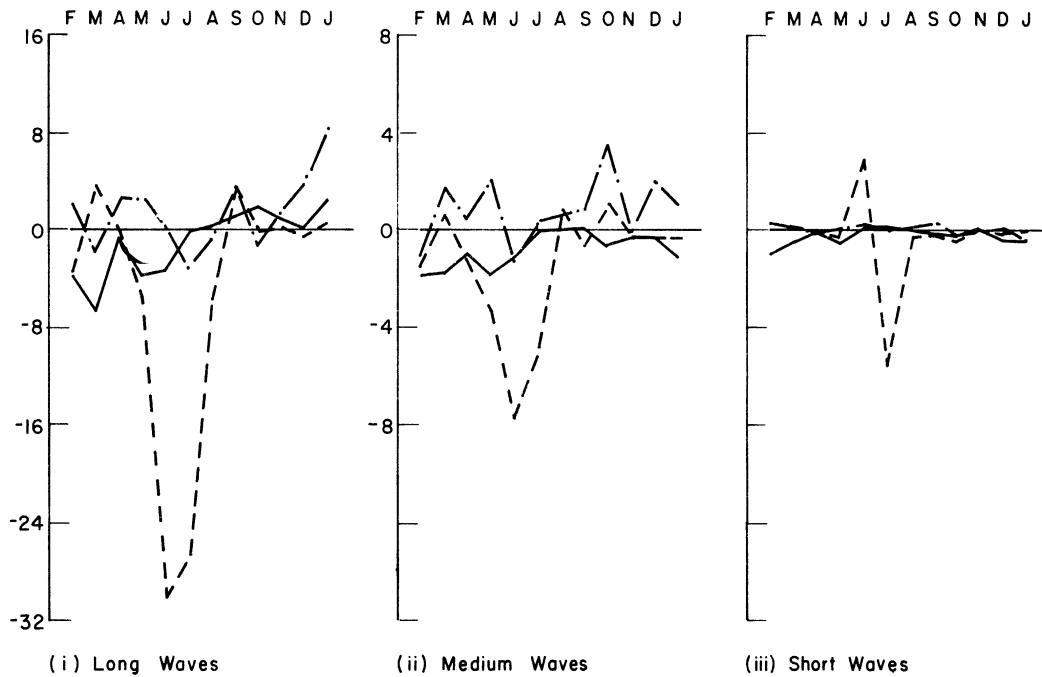


Fig. 13(B). $F(E_E)$ ($\text{erg cm}^{-2} \text{sec}^{-1} \text{cb}^{-1}$) in the individual layers. The symbols are the same as those in Fig. 8(B).

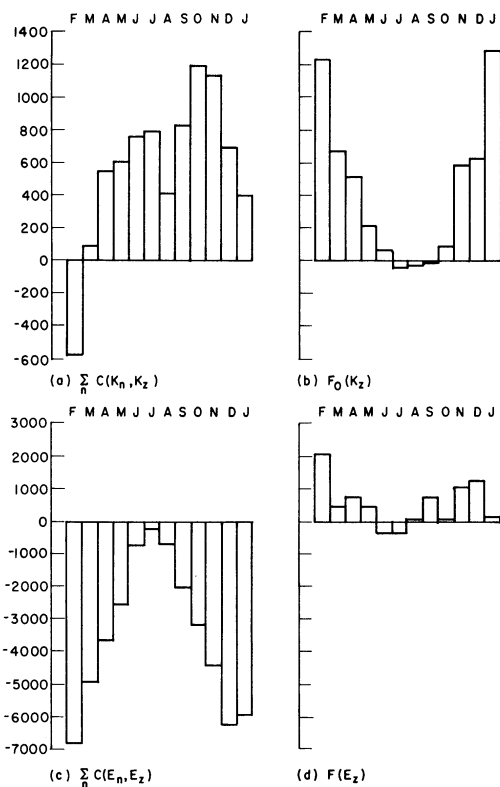


Fig. 14(A). Exchanges and influxes of energies of the zonal mean in the total atmosphere ($\text{erg cm}^{-2} \text{sec}^{-1}$).

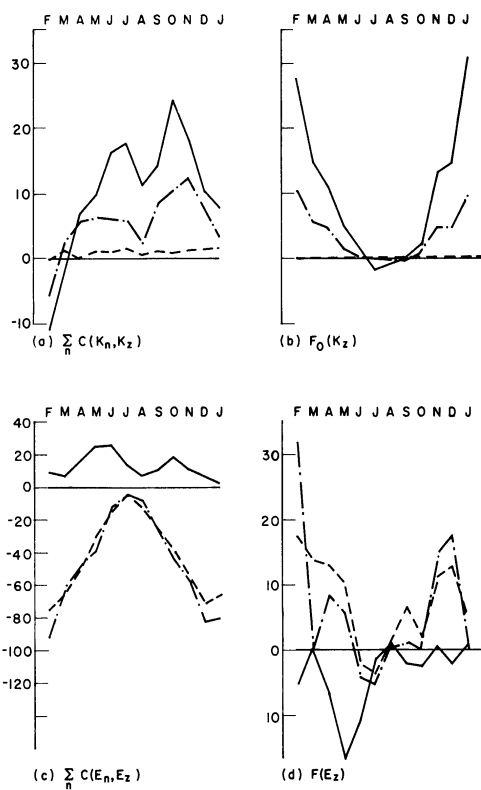


Fig. 14(B). Exchanges and influxes of energies of the zonal mean in the individual layers ($\text{erg cm}^{-2} \text{sec}^{-1} \text{cb}^{-1}$). The symbols are the same as those in Fig. 8(B).

3.4 DECOMPOSITION OF EXCHANGES AND INFLUXES IN THE TIME DOMAIN

Any integrable function of time $F(t)$ defined in a period $0 \leq t \leq \tau$ may be written as

$$F = [F] + \hat{F},$$

where

$$[F] = \frac{1}{\tau} \int_0^{\tau} F dt.$$

$[F]$ and \hat{F} will be called the standing and the moving part, respectively, of F in $0 \leq t \leq \tau$. The average over the period of a product of three such functions F , G , and H may then be written as

$$\begin{aligned} [F \cdot G \cdot H] &= [F] \cdot [G] \cdot [H] + \{ [F] \cdot [\hat{G} \cdot \hat{H}] + [G] \cdot [\hat{H} \cdot \hat{F}] + [H] \cdot [\hat{F} \cdot \hat{G}] \} + [\hat{F} \cdot \hat{G} \cdot \hat{H}] \\ &\equiv [F \cdot G \cdot H]_S + [F \cdot G \cdot H]_T \end{aligned}$$

in which

$$[F \cdot G \cdot H]_S = [F] \cdot [G] \cdot [H]$$

and

$$[F \cdot G \cdot H]_T = \{ [F] \cdot [\hat{G} \cdot \hat{H}] + [G] \cdot [\hat{H} \cdot \hat{F}] + [H] \cdot [\hat{F} \cdot \hat{G}] \} + [\hat{F} \cdot \hat{G} \cdot \hat{H}].$$

Thus, the average of a triple product over a period of time may be expressed as the sum of two parts; these will be called the stationary part and the transient part, designated by subscripts S and T , respectively. The stationary part of the time-average of a triple product is simply the triple product of the standing parts, while the transient

part is the sum of three terms, each of which is a product of the standing part of one function and the time-average of the product of the moving parts of the other two, and the time-average of the triple product of the moving parts. The transient part arises from the presence of the moving parts in the element functions and measures not only the effect of the interaction among the moving parts themselves but also the effect of the interactions between the moving parts and the standing parts, in contrast with the stationary part that measures solely the effect of the interaction of the standing parts.

This method of decomposition is first applied to each of the monthly averages of the exchanges and influxes in both forms of energy with the averaging period of a month in individual months to extract the part that is called the fast-transient part. The difference between the monthly average and the fast-transient part then defines the part which is stationary in the month. This part is further divided into two, one of which is called the slow-transient part and the other the stationary part, by subjecting it to the same method of decomposition with the averaging period of 12 months. Thus, the monthly average is expressed as the sum of three parts, among which the fast-transient part is the contribution from the interactions among the fast-moving waves and those between the fast-moving waves and the slow-moving waves as well as the standing waves. The slow-transient part is the contribution from the interactions among the slow-moving waves and those between the slow-moving waves and the standing waves. Lastly, the stationary part repre-

sents the exchanges or influx that would result if the flow were the annually-averaged flow.

The annual averages of such a decomposition of the exchanges and influxes in the entire atmosphere are presented in Table 5 for kinetic energy and in Table 6 for available potential energy. The contribution of each part to the total amount is also expressed as a percentage fraction and entered inside the parentheses next to the figure which is the specific value in $\text{ergs cm}^{-2} \text{ sec}^{-1}$.

In the exchanges between the waves and the zonal mean in both forms of energy it can be seen that the contribution from the fast-transient part increases toward the short-wave end. It may also be observed that the fast-transient part contributes more to the total in available potential energy than in kinetic energy. This can be largely explained, as will be shown later in the vertical compositions, by the fact that the major exchange in available potential energy takes place in the mid-troposphere, while that in kinetic energy occurs at the level of the jet stream.

The most remarkable fact in the exchanges among the wave groups is that the fast-transient part contributes so much more than the others as to make up practically the total amount in all the wave groups. It is also noted that while both the fast-transient and slow-transient parts have the same direction of flow of energy as the total, which is from the medium- to long- and short-wave groups with nearly equal proportions for kinetic energy, and from the long- to medium- and short-wave groups with a larger fraction into the medium-wave group in available potential en-

TABLE 5

COMPOSITIONS OF EXCHANGES AND INFLOXES OF KINETIC ENERGY IN THE TIME DOMAIN—
ANNUAL AVERAGES, TOTAL ATMOSPHERE (unit: ergs cm⁻² sec⁻¹)

Function	C(K _Z , K _E)			C(K _E , K _E)			F(K _E)		
	long	medium	short	long	medium	short	long	medium	short
Wave Group									
Total Amount	-295	-222	-47	132	-265	133	-24	-22	-28
Fast	-78 (26)	-168 (76)	-46 (98)	124 (94)	-245 (93)	121 (91)	-57 (238)	-38 (173)	-32 (114)
Slow	-147 (50)	-47 (21)	-3 (6)	23 (17)	-43 (16)	20 (15)	28 (-117)	14 (-64)	-1 (4)
Stationary	-70 (24)	-7 (3)	2 (-4)	-15 (-11)	23 (-9)	-8 (-6)	5 (-21)	2 (-9)	4 (-11)

TABLE 6

COMPOSITIONS OF EXCHANGES AND INFLOXES OF AVAILABLE POTENTIAL ENERGY IN THE
TIME DOMAIN—ANNUAL AVERAGES, TOTAL ATMOSPHERE (unit: ergs cm⁻² sec⁻¹)

Function	C(E _Z , E _E)			C(E _E , E _E)			F(E _E)		
	long	medium	short	long	medium	short	long	medium	short
Wave Group									
Total Amount	2142	1223	85	-306	170	136	-109	-9	-10
Fast	1019 (48)	1147 (94)	95 (112)	-307 (100)	167 (98)	140 (103)	-115 (105)	22 (-245)	-2 (20)
Slow	794 (37)	31 (2)	-3 (-4)	-19 (6)	13 (8)	6 (4)	10 (-9)	-16 (178)	-13 (130)
Stationary	329 (15)	45 (4)	-7 (-8)	20 (-6)	-10 (-7)	-10 (-7)	-4 (4)	-15 (167)	5 (-50)

ergy, respectively, the stationary part shows the reversal of direction in both forms of energy.

It is also interesting to observe that, while the significant portion of the exchange between the waves and the zonal flow by the slow-transient and stationary parts operate in the same direction, the two parts in the exchange among wave groups act in opposite directions.

There seems to be comparatively less information contained in the decomposition of the influxes than in that of the exchanges. While it shows that large amounts of influxes are generally attributable to the presence of the fast-moving waves, there is little indication of any systematic distribution. This may be due to the fact that the influxes are basically of a local nature, in contrast with the exchanges which are of a global nature.

Figures 15-20 present the annual variations of the individual parts of the exchanges and influxes in the individual wave groups. In the exchanges of both forms of energy between the waves and the zonal flow it may be seen that while the slow-transient part shows a larger variability than the fast-transient part in the long-wave group, the opposite is true in both the medium- and short-wave groups. In the long-wave group, moreover, the relative importance of the slow-transient part appears to increase toward the extreme seasons. On the other hand, the dominance of the fast-transient part is observed during most of the year except the summer months in both the medium- and short-wave groups.

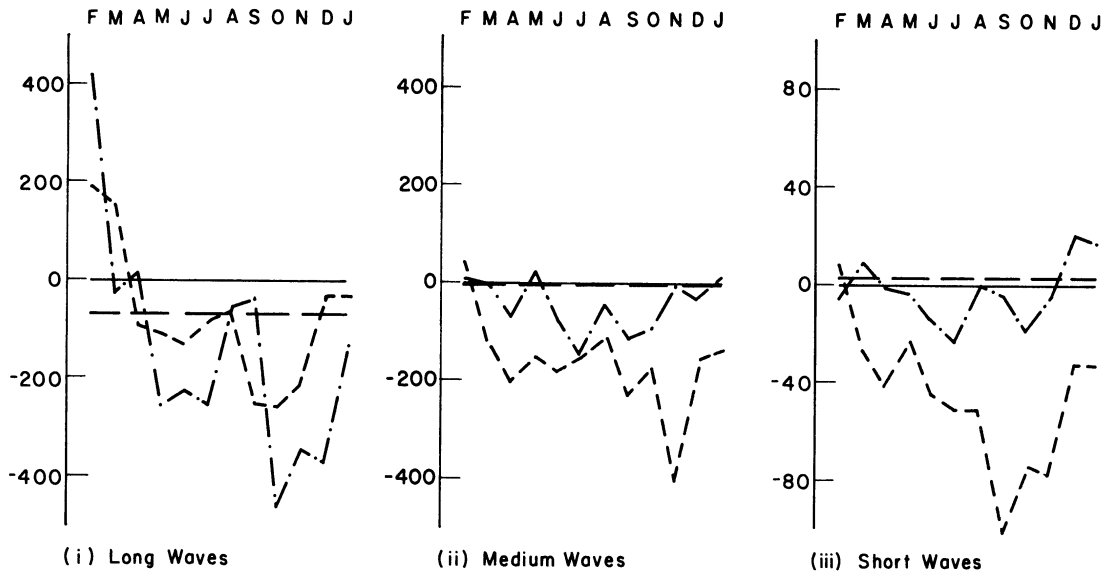


Fig. 15. Compositions of $C(K_Z, K_E)$ ($\text{erg cm}^{-2} \text{sec}^{-1}$) in the total atmosphere (0~100 cb). Fast-transient part (dotted line), slow-transient part (dash-dotted line), and stationary part (broken line).

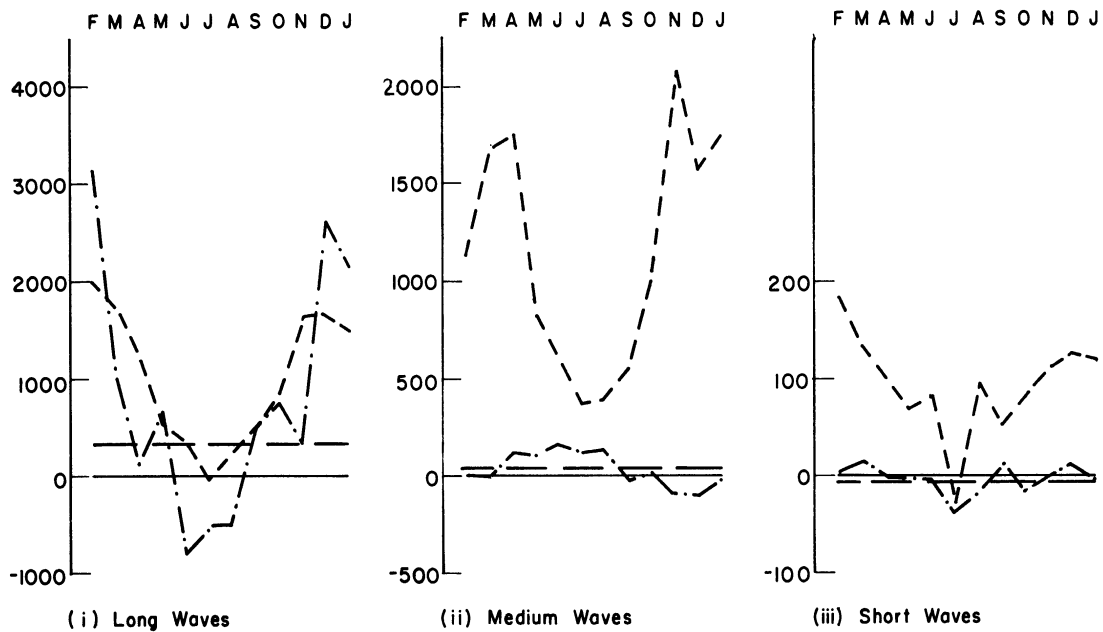


Fig. 16. Compositions of $C(E_Z, E_E)$ ($\text{erg cm}^{-2} \text{sec}^{-1}$) in the total atmosphere (10~100 cb). The symbols are the same as those in Fig. 15.

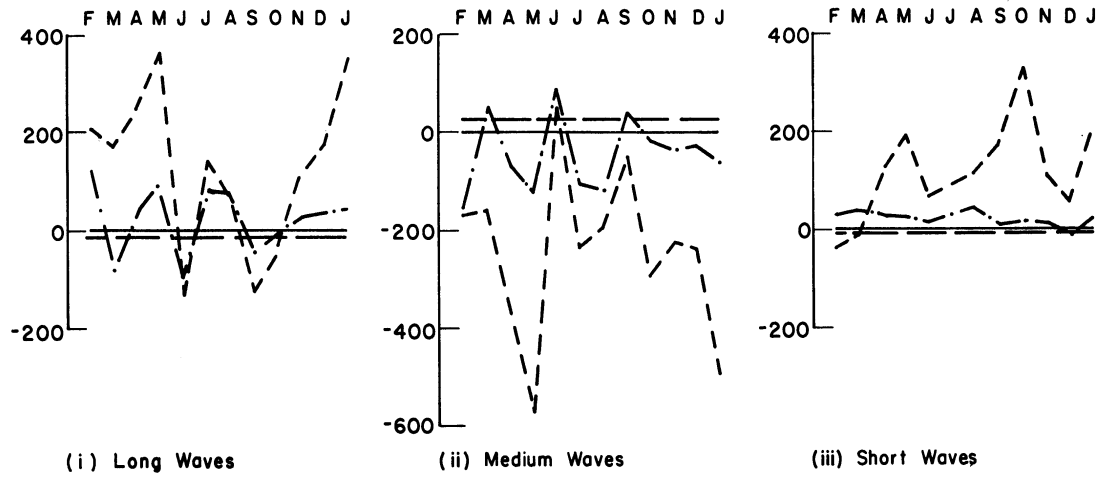


Fig. 17. Compositions of $C(K_{E1}, K_E)$ (erg cm⁻² sec⁻¹) in the total atmosphere (0~100 cb). The symbols are the same as those in Fig. 15.

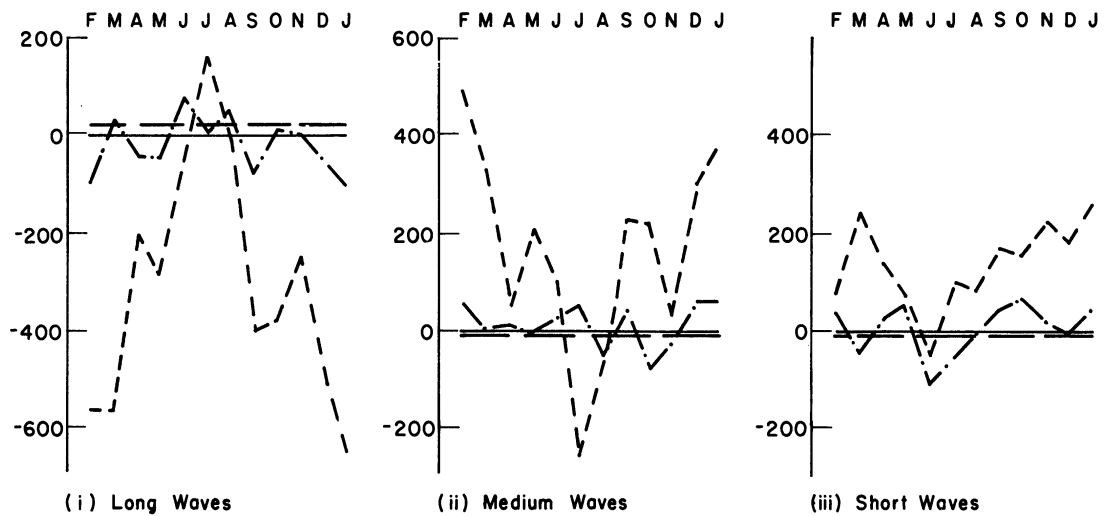


Fig. 18. Compositions of $C(E_{E1}, E_E)$ (erg cm⁻² sec⁻¹) in the total atmosphere (10~100 cb). The symbols are the same as those in Fig. 15.

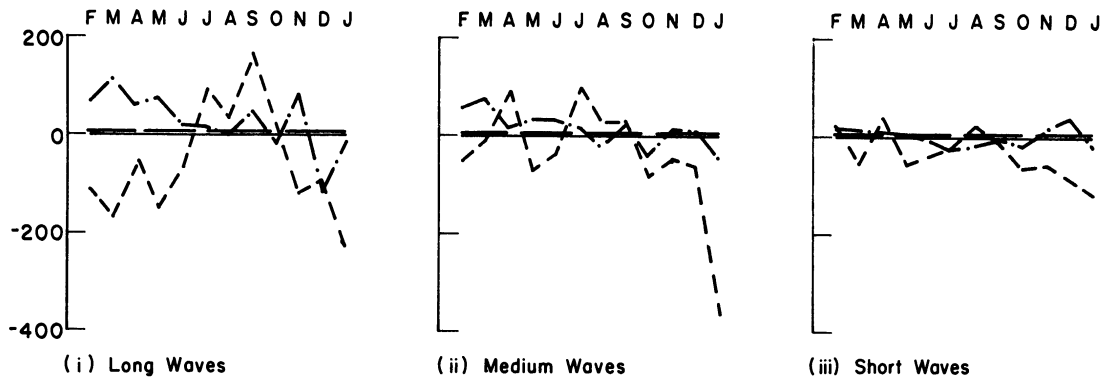


Fig. 19. Compositions of $F(K_E)$ ($\text{erg cm}^{-2} \text{sec}^{-1}$) in the total atmosphere (0~100 cb). The symbols are the same as those in Fig. 15.

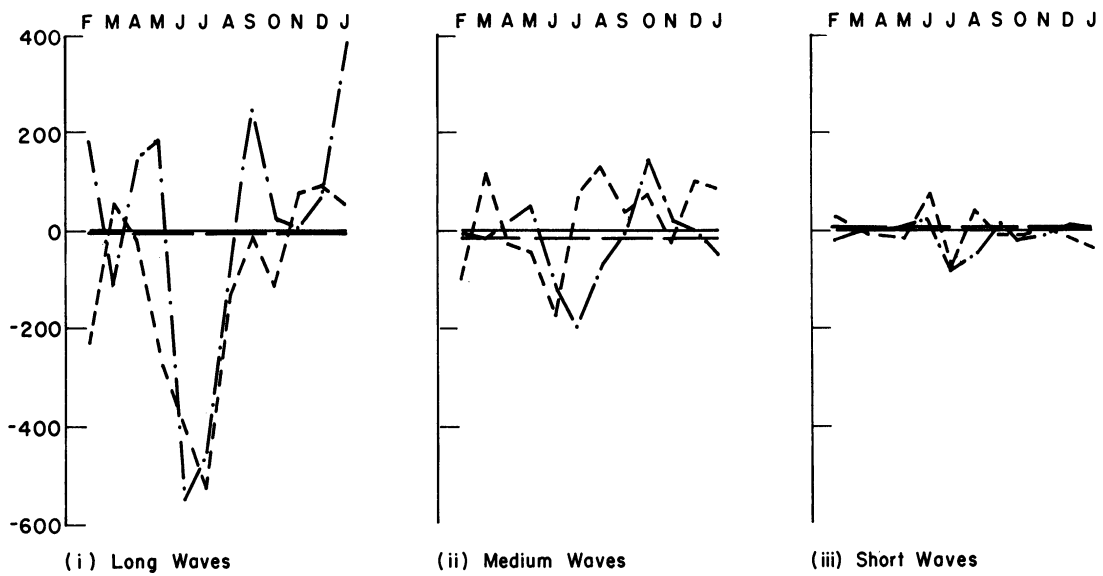


Fig. 20. Compositions of $F(K_E)$ ($\text{erg cm}^{-2} \text{sec}^{-1}$) in the total atmosphere (10~100 cb). The symbols are the same as those in Fig. 15.

In the exchanges among the wave groups the fast-transient part shows a far greater variation in addition to a generally greater magnitude than the slow-transient part in all the wave groups throughout most of the year, with the consequence that its annual variation determines to a large extent that of the total exchange. (Compare with Figs. 10(A) and 11(A).)

The ambiguity of the results of the decomposition of the influxes is again evident in their annual variations. Variabilities of the two transient parts are comparable in both forms of energy and in all three wave groups. It is also readily seen that the annual averages are small differences between large monthly value.

The same decomposition applied on the exchanges and influxes in the individual layers yields the annual averages that are summarized in Table 7 for kinetic energy and in Table 8 for available potential energy. Except for the unit, which is in $\text{ergs cm}^{-2} \text{ sec}^{-1} \text{ cb}^{-1}$, these have the same format as Tables 5 and 6. The variations in the vertical of the total amounts that appear in these tables have already been described in the second section of this chapter.

In the exchanges between the waves and the zonal flow of kinetic energy it may be stated that, with the exception of the short-wave group, the contribution from the fast-transient part decreases toward the lower stratosphere and toward the long-wave end. The conversion from the short-wave group is almost completely due to the presence of the fast-moving waves throughout the atmosphere.

TABLE 7

COMPOSITIONS OF EXCHANGES AND INFUXES OF KINETIC ENERGY IN THE TIME DOMAIN--
ANNUAL AVERAGES, INDIVIDUAL LAYERS (unit: ergs cm⁻² sec⁻¹ cb⁻¹)

Function	C(K _Z , K _E)			C(K _E , K _E)			F ₁ (K _E)		
	long	medium	short	long	medium	short	long	medium	short
(i) lower stratosphere (0 ~ 25 cb)									
Total	-6.59	-3.12	-0.53	-0.51	-1.11	1.62	-0.23	-0.72	-0.96
Fast	-.99(15)	-2.04(65)	-.54(102)	-.49(96)	-.79(71)	1.28(79)	-1.27(552)	-1.06(147)	-1.02(106)
Slow	-4.57(69)	-.90(29)	-.08(15)	.29(-57)	-.93(84)	.64(40)	.95(-413)	.30(-42)	-.08(8)
Stationary	-1.03(16)	-.18(6)	.09(-17)	-.31(61)	.61(-55)	-.30(-19)	.09(-39)	.04(-5)	.14(-15)
(ii) upper troposphere (25 ~ 77.5 cb)									
Total	-2.30	-2.55	-.59	2.30	-4.09	1.79	-.26	-.05	-.09
Fast	-.97(42)	-2.05(80)	-.58(98)	2.16(94)	-3.87(95)	1.71(95)	-.50(192)	-.25(500)	-.13(144)
Slow	-.56(24)	-.45(18)	-.01(2)	.27(12)	-.36(9)	.10(6)	.16(-61)	.17(-340)	.03(-33)
Stationary	-.77(34)	-.05(2)	-.00(0)	-.13(-6)	.14(-4)	-.01(-1)	.08(-34)	.03(-60)	.01(-11)
(iii) lower troposphere (77.5 ~ 100 cb)									
Total	-.41	-.46	-.10	1.07	-1.01	-.06	-.19	-.06	.01
Fast	-.13(32)	-.43(93)	-.12(120)	1.00(93)	-.99(98)	-.01(17)	.05(-26)	.06(-100)	.00(0)
Slow	-.12(29)	-.03(7)	.02(-20)	.08(8)	-.04(4)	-.04(67)	-.19(100)	-.10(167)	.00(0)
Stationary	-.16(39)	.00(0)	-.00(0)	-.01(-1)	.02(-2)	-.01(16)	-.05(-26)	-.02(33)	.01(100)

TABLE 8

COMPOSITIONS OF EXCHANGES AND INFLEXES OF AVAILABLE POTENTIAL ENERGY IN THE TIME DOMAIN—
ANNUAL AVERAGES, INDIVIDUAL LAYERS (unit: ergs cm⁻² sec⁻¹ cb⁻¹)

Function	C(E _Z , E _E)			C(E _E , E _E)			F(E _E)		
	long	medium	short	long	medium	short	long	medium	short
(i) lower stratosphere (10 ~ 20 cb)									
Total	-9.82	-2.52	-0.26	1.03	-0.47	-0.56	-2.07	-0.84	-0.29
Fast	-3.87 (39)	-1.91 (76)	-0.13 (50)	0.30 (29)	-0.35 (9)	-0.26 (46)	-0.71 (34)	-0.68 (81)	-0.15 (52)
Slow	-2.12 (22)	-0.37 (15)	-0.03 (12)	0.32 (31)	-0.16 (34)	-0.16 (29)	-0.80 (39)	-0.05 (6)	-0.11 (38)
Stationary	-3.83 (39)	-0.24 (9)	-0.10 (38)	0.41 (40)	-0.27 (57)	-0.14 (25)	-0.56 (27)	-0.11 (13)	-0.03 (10)
(ii) upper troposphere (20 ~ 70 cb)									
Total	30.88	14.63	0.66	-5.37	3.01	2.36	1.51	0.87	0.05
Fast	14.28 (46)	14.19 (97)	0.78 (118)	-5.12 (95)	3.06 (102)	2.07 (88)	-0.21 (-14)	0.63 (72)	0.05 (100)
Slow	9.91 (32)	0.27 (2)	-0.04 (-6)	-0.13 (2)	-0.12 (-4)	0.26 (11)	0.96 (64)	0.32 (37)	-0.08 (-160)
Stationary	6.69 (22)	0.17 (1)	-0.08 (-12)	-0.12 (2)	0.07 (2)	0.04 (1)	0.76 (50)	-0.08 (-9)	0.08 (160)
(iii) lower troposphere (70 ~ 100 cb)									
Total	23.21	17.22	1.82	-1.58	0.80	0.78	-5.45	-1.46	-0.30
Fast	11.47 (49)	15.21 (88)	1.90 (105)	-1.79 (113)	0.48 (60)	1.31 (168)	-3.24 (59)	-0.10 (6)	-0.10 (33)
Slow	10.05 (46)	0.71 (4)	-0.03 (-2)	-0.51 (32)	0.67 (84)	-0.17 (-22)	-1.01 (19)	-1.03 (71)	-0.24 (80)
Stationary	1.09 (5)	1.29 (8)	-0.05 (-3)	0.72 (-45)	-0.35 (-44)	-0.36 (-46)	-1.20 (22)	-0.33 (23)	0.04 (-13)

Nearly all of the exchanges of kinetic energy among the wave groups in the troposphere are due to the presence of the fast-transient parts. The relative significance of the other parts increases sharply in the lower stratosphere.

Here again, as mentioned earlier for the exchanges in the entire atmosphere, it may be observed that while the slow-transient and stationary parts tend to work in the same direction in the conversion from the waves into the zonal flow, they act more in the opposite directions and thus tend to cancel each other in the exchanges among the wave groups.

In the exchanges between the waves and the zonal mean of available potential energy the statement made previously with regard to those of kinetic energy in the long- and medium-wave groups holds true, although there is less difference between the troposphere and the lower stratosphere. In the short-wave group the fast-transient part still dominates the exchange in the troposphere, but its contribution drops to about 50% of the total in the lower stratosphere. The concerted action by the slow-transient and stationary parts may also be readily recognized.

On the other hand, in the exchanges among the wave groups the sudden drop in the fractional contribution of the fast-transient part in the lower stratosphere is remarkable. This is due more to the fact that the slow-transient and stationary parts work together than to the amounts of the exchange contributed by the fast-transient parts. The only distinct change in the energy flow between the slow-transient and stationary parts occurs in the lower troposphere where the amounts involved are relatively large compared with those in the other layers.

Finally, there seems to be very little reward for the effort made in distinguishing the individual layers as far as the decomposition of the influxes of the eddy energies is concerned.

The results of decomposition of exchanges and influxes involving the energies of the zonal flow are summarized in Fig. 21 and Table 9. The effect of summing the contributions from all three wave groups is seen in the similar variations with season of the fast- and slow-transient parts in both exchanges. The simple variations in both transient parts of the influx of the zonal kinetic energy are in great contrast with those of the influxes in the individual wave groups. The main feature which distinguishes Table 9 from Tables 7 and 8 is the lesser contrast among the different layers of the relative contributions from the individual parts.

3.5 DECOMPOSITION OF EXCHANGES AMONG WAVES INTO ELEMENTARY INTERACTIONS

A study which is presented in this section was prompted by the concern over the validity of the method that has been employed to satisfy the constraints on the exchanges among waves,

$$\sum_{n=1}^N \sum_{m=1}^N C(K_m, K_n) = \sum_{n=1}^N \sum_{m=1}^N C(E_m, E_n) = 0$$

in which N is the total number of the wave components in the system (Section 2.6).

To recapitulate, the method is based on the assumptions that the deviation from zero of the sum of all the exchanges due to the wave in-

TABLE 9

COMPOSITIONS OF EXCHANGES AND INFLUXES OF ENERGIES OF THE ZONAL MEAN IN
 THE TIME DOMAIN—ANNUAL AVERAGES, INDIVIDUAL LAYERS
 (ergs cm⁻² sec⁻¹ cb⁻¹) AND TOTAL ATMOSPHERE (ergs cm⁻² sec⁻¹)

	$\frac{\Sigma C(K_m, K_z)}{h}$	$F(K_z)$	$\frac{\Sigma C(E_z, E_n)}{h}$	$F(E_z)$
(i) lower stratosphere				
Total	10.24	9.81	-12.60	-3.89
Fast	3.57 (35)	4.93 (50)	-5.91 (47)	1.09 (-28)
Slow	5.55 (54)	4.96 (51)	-2.52 (20)	0.31 (-8)
Stationary	1.12 (11)	-0.08 (-1)	-4.17 (33)	-5.29 (136)
(ii) upper troposphere				
Total	5.43	3.54	46.16	6.74
Fast	3.59 (66)	2.06 (58)	29.24 (63)	0.88 (13)
Slow	1.02 (19)	1.31 (37)	10.24 (22)	-2.86 (-42)
Stationary	0.82 (15)	0.17 (5)	6.78 (15)	8.71 (129)
(iii) lower troposphere				
Total	0.98	0.03	42.25	7.26
Fast	0.68 (69)	-0.02 (-67)	28.58 (68)	3.28 (45)
Slow	0.14 (15)	-0.09 (-300)	11.33 (27)	-0.77 (-10)
Stationary	0.16 (16)	0.14 (467)	2.34 (5)	4.74 (65)
Total Atmosphere				
Total	563	432	3450	516
Fast	293 (52)	231 (53)	2260 (65)	156 (30)
Slow	196 (35)	191 (44)	822 (24)	-165 (-32)
Stationary	74 (13)	10 (2)	368 (11)	525 (102)

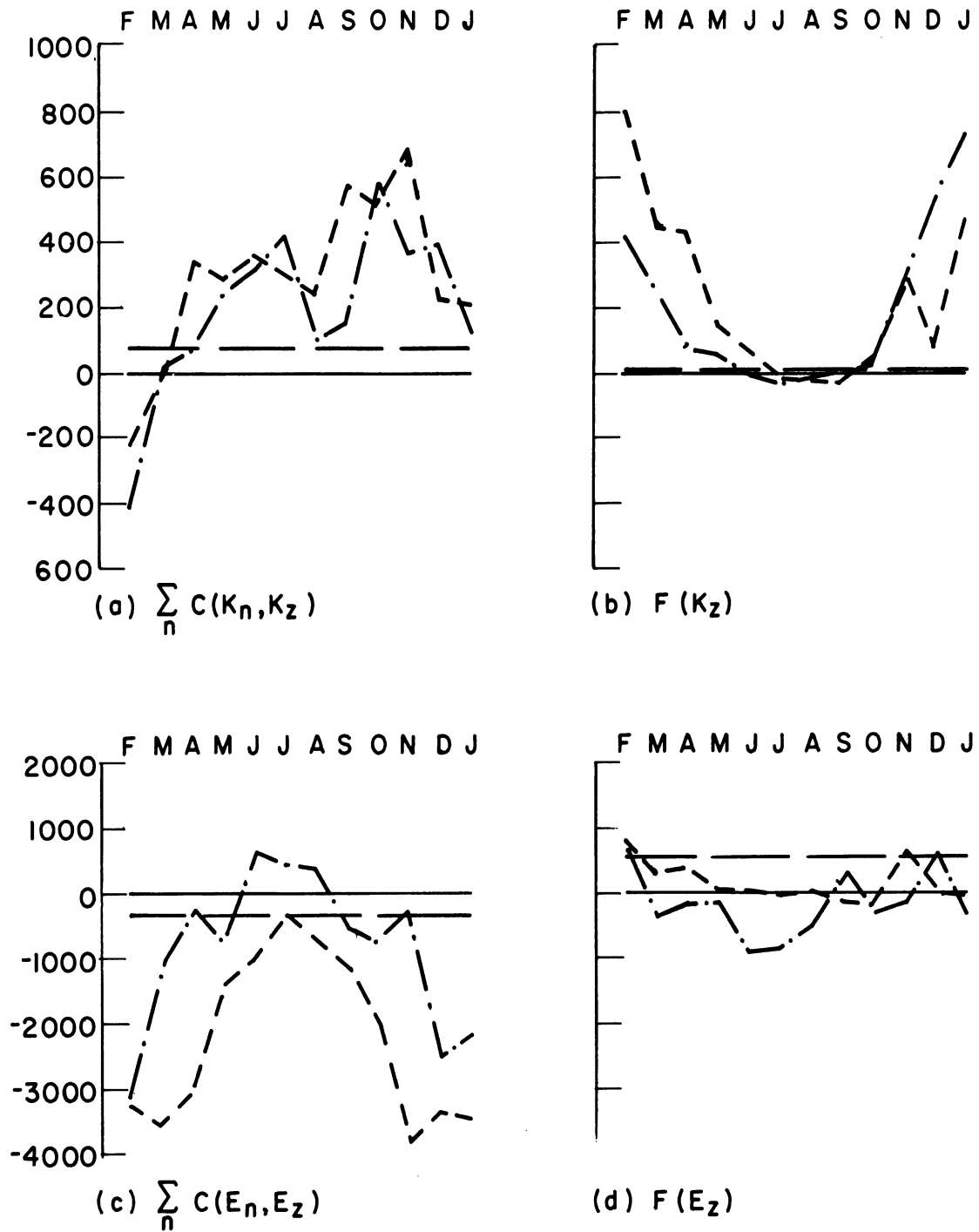


Fig. 21. Compositions of exchanges and influxes of energies of the zonal mean ($\text{erg cm}^{-2} \text{sec}^{-1}$) in the total atmosphere. The symbols are the same as those in Fig. 15.

interaction as computed from Eq. (2.48) of Chapter 2 by means of the finite-difference scheme is an error due to approximations and truncations in the computation and that the error is uniformly distributed over all scales of motion. The corrected value of the kinetic energy exchange of the component with wave number n , denoted by $\sum_{m=1}^N C(K_m, K_n)$, is therefore defined to be

$$\sum_{m=1}^N C(K_m, K_n) = \left[\sum_{m=1}^N C(K_m, K_n) \right]' - \frac{\sum_{n=1}^N \left[\sum_{m=1}^N C(K_m, K_n) \right]'}{N}$$

in which $\left[\sum_{m=1}^N C(K_m, K_n) \right]'$ denotes the value computed from Eq. (2.48) of Chapter 2, and the corrected value of the available potential energy exchange is similarly defined.

A question naturally arises from such a definition as to whether the values of the exchanges so determined would satisfy the property of the exchange. A means of answering this question was devised on the basis of the following argument.

Consider a system, S_N , which contains N wave components with wave number $n = 1 \dots N$. Consider also a system, S_{N-1} , which contains only the first $(N-1)$ wave components of S_N . Then, by definition of the exchange due to the wave interaction, for any pair of integers L and M such that $1 \leq L \leq N-1$, $1 \leq M \leq N-1$, and $L+M = N$ it holds that

$$\sum_{m=1}^N C(K_m, K_L) - \sum_{m=1}^{N-1} C(K_m, K_L) = G(K_M * K_N, K_L)$$

and

$$\sum_{\substack{m=1 \\ S_N}}^N C(K_m, K_M) - \sum_{\substack{m=1 \\ S_{N-1}}}^{N-1} C(K_m, K_M) = G(K_N * K_L, K_M)$$

in which $G(K_M * K_N, K_L)$ denotes the gain of kinetic energy in the wave component L due to the interaction of the three components L, M, and N. From

$$G(K_M * K_N, K_L) + G(K_N * K_L, K_M) + G(K_L * K_M, K_N) = 0$$

it follows that

$$\sum_{\substack{m=1 \\ S_N}}^N C(K_m, K_N) = \sum_{\substack{L=1 \\ L+M=N}}^{N-1} G(K_L * K_M, K_N) = - \sum_{\substack{m=1 \\ S_N}}^{N-1} [G(K_{N-m} * K_N, K_m)] .$$

By evaluating each term in the last member of the equation above as the difference of the exchanges of the particular wave component between two systems S_N and S_{N-1} , it may be easily checked whether the exchanges evaluated according to the present method would satisfy the equation and therefore conform to the basic property.

The values of $\sum_{m=1}^N C(K_m, K_N)$ for each of $n = 1 \dots N$, and $N = 2 \dots 15$ were computed and the values of the terms $G(K_{N-m} * K_N, K_m)$, $m = 1 \dots N-1$, were evaluated therefrom on each of 58 available sets of observations taken at 00Z or 12Z in the month of March, 1963. The results show that the last equation is satisfied within a limit of small error for all the exchanges on every occasion and at every level. It has therefore been concluded that the method employed is justified to the extent that it does not violate the basic property of the exchange.

A by-product of this analysis is the decomposition of the kinetic-energy exchanges into elementary interactions in which energy gain in any particular component due to the interaction of any particular triad (or pair) of the Fourier components is obtained.

The averages of such decomposition for the total atmosphere on the 58 sets of observations in March, 1963 are summarized in Table 10. An entry under (M,N) in row L gives the amount of energy gain in component L due to the interaction of components L, M, and N, while entry Σ at the end of each row gives the total gain of the component. It was prepared with a hope that such a decomposition might reveal statistically some systematic patterns among contributions of different elementary interactions to the gain of individual components. However, aside from showing that extremely large exchanges, say, of magnitude $200 \text{ erg cm}^{-2} \text{ sec}^{-1}$, are exclusively confined in those elementary interactions involving the long waves of wave number ranging from 0 to 4, the venture did not lead to any positive clue upon which further investigations might have been encouraged. The failure may have been partly due to the narrowness of the spectral band analyzed and partly to the smallness of the sample considered.

3.6 A FLOW DIAGRAM OF ATMOSPHERIC ENERGY

An attempt will be made to construct a flow diagram of atmospheric energy representing the average over the area north of 20°N and for the period of a year from February, 1963 to January, 1964 by

TABLE 10

DECOMPOSITION OF KINETIC-ENERGY EXCHANGES INTO ELEMENTARY INTERACTIONS
 AVERAGES OF 56 SETS OF OBSERVATIONS IN MARCH, 1965 FOR THE TOTAL ATMOSPHERE (unit: $\text{erg cm}^{-2} \text{sec}^{-1}$)

0	(1,1)	(2,2)	(3,3)	(4,4)	(5,5)	(6,6)	(7,7)	(8,8)	(9,9)	(10,10)	(11,11)	(12,12)	(13,13)	(14,14)	(15,15)	Σ
	11.5	251.5	-255.7	-95.7	-25.5	13.8	55.4	21.2	23.1	2.2	-10.9	14.5	1.7	3.0	-1.1	9.0
1	(1,0)	(2,1)	(3,2)	(4,3)	(5,4)	(6,5)	(7,6)	(8,7)	(9,8)	(10,9)	(11,10)	(12,11)	(13,12)	(14,13)	(15,14)	Σ
	-11.5	60.8	253.5	-90.7	-12.2	-49.4	5.0	42.8	-56.9	-8.4	-22.7	6.2	48.7	-3.6	-0.5	161.1
2	(1,1)	(2,0)	(3,1)	(4,2)	(5,3)	(6,4)	(7,5)	(8,6)	(9,7)	(10,8)	(11,9)	(12,10)	(13,11)	(14,12)	(15,13)	Σ
	-60.8	-251.5	-227.4	-164.5	6.7	22.3	-60.7	57.4	92.2	35.8	16.5	-5.3	-63.2	-9.8	-3.9	-616.2
3	(2,1)	(3,0)	(4,1)	(5,2)	(6,3)	(7,4)	(8,5)	(9,6)	(10,7)	(11,8)	(12,9)	(13,10)	(14,11)	(15,12)	(16,13)	Σ
	-26.1	255.7	113.0	28.1	-47.9	17.9	9.0	-49.2	-26.6	5.5	22.3	41.2	-6.9	-2.9	333.1	
4	(2,2)	(3,1)	(4,0)	(5,1)	(6,2)	(7,3)	(8,4)	(9,5)	(10,6)	(11,7)	(12,8)	(13,9)	(14,10)	(15,11)	(16,12)	Σ
	164.5	-22.3	95.7	74.7	2.8	-65.7	-24.4	-16.3	48.4	27.4	-49.6	12.4	6.4	13.4	267.4	
5	(3,2)	(4,1)	(5,0)	(6,1)	(7,2)	(8,3)	(9,4)	(10,5)	(11,6)	(12,7)	(13,8)	(14,9)	(15,10)	(16,11)	(17,12)	Σ
	-34.8	-62.5	25.5	124.9	69.8	21.0	21.9	5.8	-10.0	23.9	-15.7	-11.4	6.6	165.0		
6	(3,3)	(4,2)	(5,1)	(6,0)	(7,1)	(8,2)	(9,3)	(10,4)	(11,5)	(12,6)	(13,7)	(14,8)	(15,9)	(16,10)	(17,11)	Σ
	47.9	-25.1	-75.5	-13.8	34.9	10.4	12.0	-54.2	-7.0	-10.7	-58.1	-13.2	-12.6	-165.0		
7	(4,3)	(5,2)	(6,1)	(7,0)	(8,1)	(9,2)	(10,3)	(11,4)	(12,5)	(13,6)	(14,7)	(15,8)	(16,9)	(17,10)	(18,11)	Σ
	47.8	-9.1	-39.9	-55.4	16.7	-5.0	-1.1	-7.6	-35.3	-1.7	-5.6	-5.4	-101.6			
8	(4,4)	(5,3)	(6,2)	(7,1)	(8,0)	(9,1)	(10,2)	(11,3)	(12,4)	(13,5)	(14,6)	(15,7)	(16,8)	(17,9)	(18,10)	Σ
	24.4	-30.0	-67.8	-59.5	-21.2	21.7	-19.0	-7.4	48.9	33.1	-2.8	-5.3	-84.9			
9	(5,4)	(6,3)	(7,2)	(8,1)	(9,0)	(10,1)	(11,2)	(12,3)	(13,4)	(14,5)	(15,6)	(16,7)	(17,8)	(18,9)	(19,10)	Σ
	-5.6	37.2	-87.2	35.2	-23.1	82.8	-41.9	-40.1	14.6	-0.9	2.1	-26.9				
10	(5,5)	(6,4)	(7,3)	(8,2)	(9,1)	(10,0)	(11,1)	(12,2)	(13,3)	(14,4)	(15,5)	(16,6)	(17,7)	(18,8)	(19,9)	Σ
	-5.8	5.8	27.7	-16.8	-74.4	-2.2	39.7	40.3	7.9	-14.9	-11.3	-4.0				
11	(6,5)	(7,4)	(8,3)	(9,2)	(10,1)	(11,0)	(12,1)	(13,2)	(14,3)	(15,4)	(16,5)	(17,6)	(18,7)	(19,8)	(20,9)	Σ
	17.0	-19.8	1.9	25.4	-17.0	10.9	12.6	-26.4	17.9	-22.7	-0.2					
12	(6,6)	(7,5)	(8,4)	(9,3)	(10,2)	(11,1)	(12,0)	(13,1)	(14,2)	(15,3)	(16,4)	(17,5)	(18,6)	(19,7)	(20,8)	Σ
	10.7	11.4	0.7	17.8	-35.0	-18.8	-14.5	0.0	-24.4	-1.6	-53.7					
13	(7,6)	(8,5)	(9,4)	(10,3)	(11,2)	(12,1)	(13,0)	(14,1)	(15,2)	(16,3)	(17,4)	(18,5)	(19,6)	(20,7)	(21,8)	Σ
	59.8	-17.4	-27.0	-49.1	89.6	48.7	-1.7	2.0	21.7	29.2						
14	(7,7)	(8,6)	(9,5)	(10,4)	(11,3)	(12,2)	(13,1)	(14,0)	(15,1)	(16,2)	(17,3)	(18,4)	(19,5)	(20,6)	(21,7)	Σ
	5.6	16.0	12.3	8.5	-11.0	34.2	1.6	-3.0	4.0	68.2						
15	(8,7)	(9,6)	(10,5)	(11,4)	(12,3)	(13,2)	(14,1)	(15,0)	(16,1)	(17,2)	(18,3)	(19,4)	(20,5)	(21,6)	(22,7)	Σ
	10.7	10.5	4.7	9.3	4.5	-17.8	-3.5	1.1	19.5							

partitioning the atmospheric energy into four compartments consisting of E_Z , K_Z , E_E , and K_E . The main ingredients used for the task are the results obtained in this study and the results obtained by Wiin-Nielsen (1967) on amounts of the energies for the same period.

The balance equations for E_Z , K_Z , E_E , and K_E are given respectively by

$$\frac{dE_Z}{dt} = G(E_Z) - C(E_Z, E_E) - C(E_Z, K_Z) + F(E_Z) ,$$

$$\frac{dK_Z}{dt} = C(E_Z, K_Z) + C(K_E, K_Z) + F(K_Z) + D(K_Z) ,$$

$$\frac{dE_E}{dt} = G(E_E) + C(E_Z, E_E) - C(E_E, K_E) + F(E_E) ,$$

and

$$\frac{dK_E}{dt} = C(E_E, K_E) - C(K_E, K_Z) + F(K_E) + D(K_E) .$$

In these equations $C(A, B)$ and $F(A)$ denote, as before, the conversion from A to B and the influx of A, respectively, while $G(A)$ and $D(B)$ denote the generation of A and dissipation of B, respectively. All the conversions except $C(E_Z, K_Z)$ and $C(E_E, K_E)$, and all the fluxes that will be justifiably taken to represent the fluxes through the southern boundary, have been computed in the present study. The rates of change of the energies are estimated from the inter-diurnal changes of the energies, the values of which are taken from the work of Wiin-Nielsen. Thus, the values of $G(E_Z) - C(E_Z, K_Z)$, $C(E_Z, K_Z) + D(K_Z)$, $G(E_E) - C(E_E, K_E)$ and $C(E_E, K_E) + D(K_E)$ are evaluated from the above equations, and from them, in turn the values of $G(E_Z) + D(K_Z)$ and $G(E_Z) + D(K_E)$. The monthly aver-

ages of these quantities are presented in Table 11. These values show, in general, variations from winter to summer which are similar to those obtained by others but, perhaps, with larger amplitudes, particularly in the quantities involving available potential energies (see, for example, Oort (1964) Table 3).

Finally, the values of $C(E_Z, K_Z)$ and $C(E_E, K_E)$ estimated by Oort (loc. cit., Fig. 1) are introduced to estimate those of $G(E_Z)$, $D(K_Z)$, $G(E_E)$, and $D(K_E)$ individually and thereby to complete the flow diagrams. The result is represented in Fig. 22, which is modeled after the one by Oort (loc. cit.) and in which each of the values obtained through the use of Oort's values is placed inside a bracket. It shows good agreement with the one due to Oort in both direction and magnitude for each quantity.

TABLE 11

MONTHLY AVERAGES OF QUANTITIES EVALUATED FROM ENERGY BALANCE
(unit: ergs cm⁻² sec⁻¹)

	$G(E_Z)$	$-D(K_Z)$	$G(E_Z)$	$G(E_E)$	$-D(K_E)$	$G(E_E)$
	$-C(E_Z, K_Z)$	$-C(E_Z, K_Z)$	$+D(K_Z)$	$-C(E_E, K_E)$	$-C(E_E, K_E)$	$+D(K_E)$
Feb. 63	5086	659	4427	-6766	669	-7435
Mar. "	4408	924	3484	-5074	10	-5084
Apr. "	2473	1128	1345	-3839	-273	-3566
May "	1951	902	1049	-2436	-720	-1716
Jun. "	902	901	1	358	-779	1137
Jul. "	476	750	-274	1027	-572	1599
Aug. "	949	301	648	-568	-361	-207
Sep. "	1450	749	701	-2232	-611	-1621
Oct. "	3499	1166	2333	-3195	-1458	-1737
Nov. "	3227	1598	1629	-4423	-1344	-3079
Dec. "	5251	1229	4022	-6510	-932	-5578
Jan. 64	5552	1638	3914	-6226	-1275	-4951
Annual Average	2934	996	1938	-3323	-638	-2685

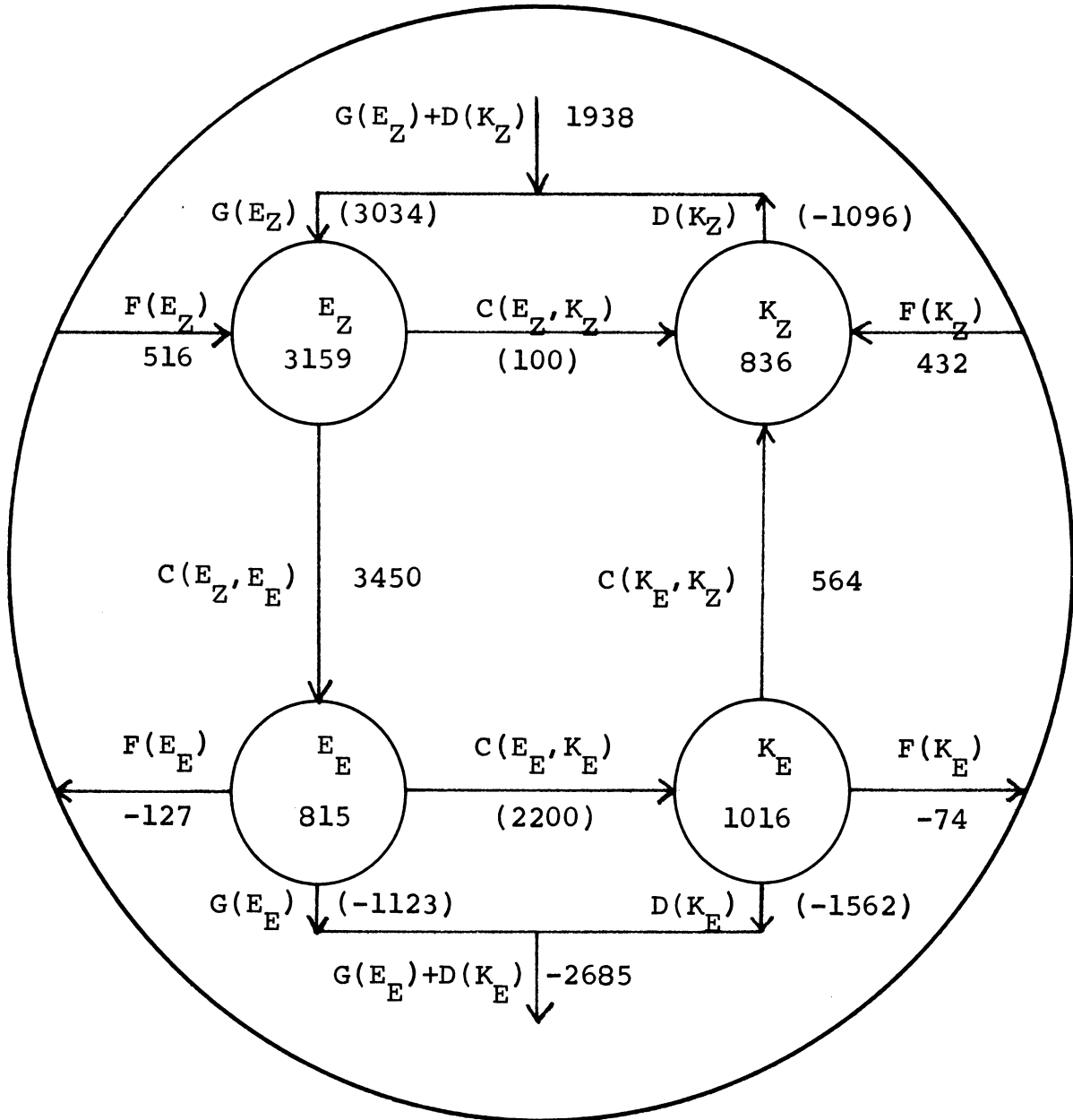


Fig. 22. Flow diagram of the atmospheric energy, averaged over a year from February, 1963 to January, 1964 for the region north of 20°N . Energy values are taken from Wiin-Nielsen (1967) and in the unit of 10^6 erg cm^{-2} . The values of $C(E_Z, K_Z)$ and $C(E_E, K_E)$ are taken from Oort (1964). Values of conversions and fluxes are in the unit of $\text{erg cm}^{-2} \text{ sec}^{-1}$. Quantities estimated are inside parentheses.

4. AN ANALYTICAL STUDY OF NONLINEAR EFFECTS
IN WEAK BAROCLINIC INSTABILITY

4.1 MODEL

We shall consider the so-called two-level quasi-geostrophic baroclinic model on a finite β -plane with a constant static stability (Fig. 23). In the (x,y,p) coordinate system the atmosphere occupies horizontally a rectangular region $0 \leq x \leq L$, $0 \leq y \leq W$ and extends vertically from $p = 100$ cb to $p = 0$ cb. At the bottom and the top of the atmosphere the vertical velocity $\omega = dp/dt$ is identically zero. The dynamics of the atmospheric flow in this parallelepiped is such that the quasi-nondivergent vorticity equation governs the flow at each of the levels $p = 25$ and 75 cb, while the thermodynamic equation is valid at $p = 50$ cb, where the horizontal flow is the average of those at 25 and 75 cb.

The effect of frictional dissipation is accounted for by horizontal eddy diffusivities; K_v for kinetic energy and K_T for thermal energy, respectively. A crude approximation to diabatic heating is also made by incorporating Newtonian heating in the model (see below in the derivation of the thermodynamic equation).

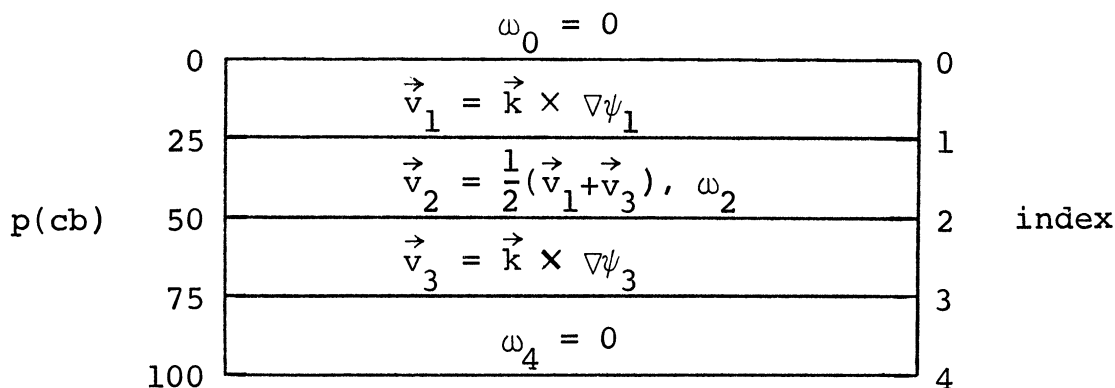


Fig. 23. A two-level quasi-geostrophic baroclinic model.

The quasi-nondivergent vorticity equation is given by

$$\frac{\partial \zeta}{\partial t} + \vec{v} \cdot \nabla (\zeta + \beta y) = f_0 \frac{\partial \omega}{\partial p} + K_V \nabla^2 \zeta \quad (4.1)$$

where $\zeta = \nabla^2 \psi$ is the vertical component of vorticity and f_0 a standard value of the Coriolis parameter. We shall assume that the rate of heating dQ/dt is given by the sum of the lateral diffusion and diabatic heating as

$$\frac{dQ}{dt} = \left(\frac{dQ}{dt} \right)_{\text{diffusion}} + \left(\frac{dQ}{dt} \right)_{\text{diabatic}}$$

in which

$$\left(\frac{dQ}{dt} \right)_{\text{diffusion}} = c_p K_T \nabla^2 T = c_p K_T \frac{p}{R} \nabla^2 \alpha$$

$$\left(\frac{dQ}{dt} \right)_{\text{diabatic}} = -c_p H T' = -c_p H \frac{p}{R} \alpha'$$

where T is temperature, α specific volume and the prime denotes deviation from the equilibrium state. The thermodynamic equation then becomes

$$\frac{d\alpha}{dt} + \vec{v} \cdot \nabla \alpha - \sigma \omega = \frac{R}{c_p p} \frac{dQ}{dt} = K_T \nabla^2 \alpha - H \alpha' \quad (4.2)$$

where σ is the static stability and assumed constant.

Applying Eq. (4.1) at levels 1 ($p = 25$ cb) and 3 ($p = 75$ cb) we obtain

$$\frac{\partial}{\partial t} (\nabla^2 \psi_1) + \vec{v}_1 \cdot \nabla (\nabla^2 \psi_1 + \beta y) = \frac{f_0}{\Delta p} \omega_2 + K_V \nabla^4 \psi_3 \quad (4.3)$$

$$\frac{\partial}{\partial t} (\nabla^2 \psi_3) + \vec{v}_3 \cdot \nabla (\nabla^2 \psi_3 + \beta y) = -\frac{f_0}{\Delta p} \omega_2 + K_V \nabla^4 \psi_3 \quad (4.4)$$

Applying Eq. (4.2) at level 2 ($p = 50$ cb) and making use of the hydrostatic and thermal-wind relations we obtain

$$\frac{\partial}{\partial t} (\psi_2 - \psi_3) + \vec{v}_2 \cdot \nabla (\psi_1 - \psi_3) - \frac{\sigma \Delta p}{f_0} \omega_2 = K_T \nabla^2 (\psi_1 - \psi_3) - H(\psi_1^i - \psi_3^i). \quad (4.5)$$

In these equations differentiations with respect to pressure have been replaced by the centered finite differences.

Introducing new dependent variables ψ_M and ψ_S defined by

$$\psi_M = \frac{1}{2} (\psi_1 + \psi_3), \quad \psi_S = \frac{1}{2} (\psi_1 - \psi_3)$$

so that

$$\psi_1 = \psi_M + \psi_S, \quad \psi_3 = \psi_M - \psi_S$$

we then obtain by adding Eqs. (4.3) and (4.4)

$$\frac{\partial}{\partial t} (\nabla^2 \psi_M) + \vec{v}_M \cdot \nabla (\nabla^2 \psi_M + \beta y) + \vec{v}_S \cdot \nabla (\nabla^2 \psi_S) = K_V \nabla^2 (\nabla^2 \psi_M)$$

and by subtracting Eq. (4.4) from (4.3)

$$\frac{\partial}{\partial t} (\nabla^2 \psi_S) + \vec{v}_M \cdot \nabla (\nabla^2 \psi_S) + \vec{v}_S \cdot \nabla (\nabla^2 \psi_M + \beta y) = \frac{f_0}{\Delta p} \omega_2 + K_V \nabla^2 (\nabla^2 \psi_S)$$

Eq. (4.5), on the other hand, can be written as

$$\frac{\partial}{\partial t} (\psi_S) + \vec{v}_M \cdot \nabla (\psi_S) = \frac{\sigma \Delta p}{2f_0} \omega_2 - H\psi_S^i + K_T \nabla^2 \psi_S$$

in which $\vec{v}_M = \vec{k} \times \nabla \psi_M$ and $\vec{v}_S = \vec{k} \times \nabla \psi_S$. Eliminating ω_2 from the last two equations we obtain

$$\begin{aligned} \frac{\partial}{\partial t} (\nabla^2 \psi_S) + \vec{v}_M \cdot \nabla (\nabla^2 \psi_S) + \vec{v}_S \cdot \nabla (\nabla^2 \psi_M + \beta y) \\ = q^2 \left\{ \frac{\partial \psi_S}{\partial t} + \vec{v}_M \cdot \nabla \psi_S + H \psi_S' - K_T \nabla^2 \psi_S \right\} + K_V \nabla^2 (\nabla^2 \psi_S) \end{aligned}$$

where

$$q^2 = \frac{2f_0^2}{\sigma(\Delta p)^2} = \text{constant.}$$

Consequently, the system of dynamic equations governing the two stream functions ψ_M and ψ_S is seen to consist of

$$\frac{\partial}{\partial t} (\nabla^2 \psi_M) + \vec{v}_M \cdot \nabla (\nabla^2 \psi_M + \beta y) + \vec{v}_S \cdot \nabla (\nabla^2 \psi_S) = K_V \nabla^2 (\nabla^2 \psi_M) \quad (4.6)$$

and

$$\begin{aligned} \frac{\partial}{\partial t} (\nabla^2 \psi_S) + \vec{v}_M \cdot \nabla (\nabla^2 \psi_S) + \vec{v}_S \cdot \nabla (\nabla^2 \psi_M + \beta y) \\ = q^2 \left\{ \frac{\partial \psi_S}{\partial t} + \vec{v}_M \cdot \nabla \psi_S + H \psi_S' - K_T \nabla^2 \psi_S \right\} + K_V \nabla^2 (\nabla^2 \psi_S). \quad (4.7) \end{aligned}$$

The boundary conditions on ψ_M and ψ_S are the condition that the normal velocities at the southern and northern walls should vanish for all x and t and the condition that the values of ψ_M and ψ_S at the end $x = 0$ are the same as those at the other end $x = L$ for same y and t .

These may be stated as

$$\left. \frac{\partial \psi_M}{\partial x} \right|_{y=0,W} = \left. \frac{\partial \psi_S}{\partial x} \right|_{y=0,W} = 0$$

$$\psi_M(0, y, t) = \psi_M(L, y, t), \quad \psi_S(0, y, t) = \psi_S(L, y, t). \quad (4.8)$$

4.2 LINEARIZED THEORY

Let the equilibrium flow be defined by

$$\psi_{M0} = -U_M y, \quad \psi_{S0} = -U_S y \quad (4.9)$$

and consider travelling disturbances of the form

$$\begin{aligned} \Psi_M(x, y, t) &= A_M e^{i\alpha_x(x-ct)} \sin(\alpha_y y) \\ \Psi_S(x, y, t) &= A_S e^{i\alpha_x(x-ct)} \sin(\alpha_y y) \end{aligned} \quad (4.10)$$

where

$$\alpha_x = \frac{2m\pi}{L}, \quad \alpha_y = \frac{n\pi}{W}$$

with integral m, n .

The linear perturbation equations for Ψ_M and Ψ_S are then found to

be

$$\frac{\partial}{\partial t} (\nabla^2 \Psi_M) + U_M \frac{\partial}{\partial x} (\nabla^2 \Psi_M) + U_S \frac{\partial}{\partial x} (\nabla^2 \Psi_S) + \beta \frac{\partial \Psi_M}{\partial x} - K_V \nabla^2 (\nabla^2 \Psi_M) = 0 \quad (4.11)$$

$$\begin{aligned} \frac{\partial}{\partial t} (\nabla^2 \Psi_S) + U_M \frac{\partial}{\partial x} (\nabla^2 \Psi_S) + U_S \frac{\partial}{\partial x} (\nabla^2 \Psi_M) + \beta \frac{\partial \Psi_S}{\partial x} - K_V \nabla^2 (\nabla^2 \Psi_S) \\ - q^2 \left\{ \frac{\partial \Psi_S}{\partial t} + U_M \frac{\partial \Psi_S}{\partial x} - U_S \frac{\partial \Psi_M}{\partial x} + H \Psi_S - K_T \nabla^2 \Psi_S \right\} = 0. \end{aligned} \quad (4.12)$$

Substituting (4.10) into these equations we obtain

$$\left(c - U_M + \frac{\beta}{\alpha_S^2} + i \frac{\alpha_S^2 K_V}{\alpha_x} \right) A_M - U_S A_S = 0$$

$$-\left(1 - \frac{q^2}{\alpha_S^2}\right) U_S A_M + \left[\left(1 + \frac{q^2}{\alpha_S^2}\right) (c - U_M) + \frac{\beta}{\alpha_S^2} + i \left[\frac{\alpha_S^2 K_V}{\alpha_X} + \frac{q^2}{\alpha_S^2} \frac{H + K_T \alpha_S^2}{\alpha_X} \right] \right] A_S = 0$$

where $\alpha_S^2 = \alpha_X^2 + \alpha_Y^2$.

Denoting

$$v_R = \frac{\beta}{\alpha_S^2}, \quad v_F = \frac{K_V \alpha_S^2}{\alpha_X}, \quad v_H = \frac{H + K_T \alpha_S^2}{\alpha_X}, \quad \rho^2 = \frac{q^2}{\alpha_S^2} \quad (4.13)$$

and calling

$$\lambda = c - U_M \quad (4.14)$$

we may rewrite the above equations as

$$(\lambda + v_R + i v_F) A_M - U_S A_S = 0 \quad (4.15)$$

$$-(1 - \rho^2) U_S A_M + [(1 + \rho^2) \lambda + v_R + i(v_F + \rho^2 v_H)] A_S = 0 \quad (4.16)$$

from which follows the characteristic equation of the eigenvalue problem

$$(1 + \rho^2) \lambda^2 + \{(2 + \rho^2)(v_R + i v_F) + i \rho^2 v_H\} \lambda + \{v_R^2 - v_F^2 - \rho^2 v_F v_H - (1 - \rho^2) U_S^2 + i(2 v_R v_F + \rho^2 v_R v_H)\} = 0 \quad (4.17)$$

which is quadratic in λ and has complex coefficients. Therefore, there exist, in general, two distinct eigenvalues λ_1 and λ_2 . If we designate

$$C_{21} = (1 + \rho^2), \quad C_{22} = 0$$

$$C_{11} = (2 + \rho^2) v_R, \quad C_{12} = (2 + \rho^2) v_F + \rho^2 v_H$$

$$C_{01} = v_R^2 - v_F^2 - \rho^2 v_F v_H - (1 - \rho^2) U_S^2, \quad C_{02} = 2 v_R v_F + \rho^2 v_R v_H \quad (4.18)$$

and put

$$\lambda = \lambda_r + i\lambda_i \quad (4.19)$$

in Eq. (4.17) and separate its real and imaginary components, we obtain two coupled nonlinear equations in λ_r and λ_i :

$$\begin{aligned} C_{21}(\lambda_r^2 - \lambda_i^2) + C_{11}\lambda_r - C_{12}\lambda_i + C_{01} &= F_1(\lambda_r, \lambda_i) = 0 \\ 2C_{21}\lambda_r\lambda_i + C_{12}\lambda_r + C_{11}\lambda_i + C_{02} &= F_2(\lambda_r, \lambda_i) = 0 . \end{aligned} \quad (4.20)$$

The system (4.20) can be solved numerically by the Newton-Raphson's iterative method.

Since λ is related to c by

$$\lambda = \lambda_r + i\lambda_i = (c_r - U_M) + ic_i$$

it follows that the wave disturbances of the form defined in Eq. (4.10) travel with phase velocity $c_r = \lambda_r + U_M$ while their amplitudes vary exponentially with time according to $\exp(\alpha_X \lambda_i t)$. It therefore follows that whenever $\lambda_i > 0$ the equilibrium flow is unstable.

The ratio of the amplitudes A_M, A_S corresponding to an eigenvalue $\lambda = \lambda_r + i\lambda_i$ can be obtained from Eq. (4.15) as

$$\begin{aligned} \text{Re} \left(\frac{A_S}{A_M} \right) &= C_{S1} = \frac{\lambda_r + v_R}{U_S} \\ \text{Im} \left(\frac{A_S}{A_M} \right) &= C_{S2} = \frac{\lambda_i + v_F}{U_S} \end{aligned} \quad (4.21)$$

4.3 CURVE OF CRITICAL STABILITY

With the notations introduced in (4.18) the characteristic equation (4.17) may be written as

$$C_{21}\lambda^2 + (C_{11}+iC_{12})\lambda + (C_{01}+iC_{02}) = 0 \quad (4.22)$$

so that the eigenvalues λ_1 and λ_2 are given by

$$(\lambda_1, \lambda_2) = -\frac{(C_{11}+iC_{12})}{2C_{21}} \pm \frac{\{(C_{11}+iC_{12})^2 - 4C_{21}(C_{01}+iC_{02})\}^{1/2}}{2C_{21}} \quad (4.23)$$

where it may be noted that C_{21} , C_{12} are positive.

If the imaginary component of either λ_1 or λ_2 is positive the equilibrium flow is unstable. To determine the curve of critical stability that separates the region of instability from that of stability we therefore seek the condition that gives rise to a positive imaginary component in the eigenvalues.

In (4.23) let

$$(C_{11}^2 - C_{12}^2 - 4C_{21}C_{01}) + i(2C_{11}C_{12} - 4C_{21}C_{02}) = D_r + iD_i \quad (4.24)$$

and put

$$(D_r + iD_i)^{1/2} = e_r + ie_i \quad .$$

Then

$$D_r = e_r^2 - e_i^2$$

$$D_i = 2e_re_i \quad .$$

Eliminating e_r from these equations we obtain

$$e_i^4 + D_r e_i^2 - \frac{D_i^2}{4} = 0$$

so that

$$e_i^2 = -\frac{D_r}{2} + \left(\frac{D_r^2 + D_i^2}{4} \right)^{1/2}.$$

A reference to (4.23) then shows that an imaginary component of the eigenvalues may become positive only when $e_i > 0$ and $e_i^2 > C_{12}^2$. The latter condition is equivalent to

$$\frac{D_r^2 + D_i^2}{4} > C_{12}^4 + C_{12}^2 D_r + \frac{D_r^2}{4}.$$

Substituting the expressions for D_r and D_i from (4.24) the last inequality becomes

$$C_{21}C_{02}^2 - C_{11}C_{12}C_{02} + C_{12}^2C_{01} > 0.$$

With (4.18) this becomes

$$\begin{aligned} (1+\rho^2)(2v_F+\rho^2v_H)^2v_R^2 - (2+\rho^2)(2v_F+\rho^2v_H)\{(2+\rho^2)v_F+\rho^2v_H\}v_R^2 \\ + \{v_R^2-v_F^2-\rho^2v_Fv_H-(1-\rho^2)U_S^2\}\{(2+\rho^2)v_F+\rho^2v_H\}^2 > 0. \end{aligned}$$

Upon rearrangement this may in turn be reduced to

$$\cdot \{(2+\rho^2)v_F+\rho^2v_H\}^2 \left\{ (1-\rho^2)U_S^2 + \frac{\rho^4(v_F^2+\rho^2v_Fv_H)}{\{(2+\rho^2)v_F+\rho^2v_H\}^2} v_R^2 + (v_F^2+\rho^2v_Fv_H) \right\} > 0.$$

which shows that, since $\{(2+\rho^2)v_F+\rho^2v_H\}^2 \geq 0$, $\rho^4(v_F^2+\rho^2v_Fv_H)v_R^2 \geq 0$, and

$(v_F^2+\rho^2v_Fv_H) \geq 0$, no real value of U_S fulfills the inequality in the region

$1-\rho^2 > 0$ or $\alpha_S^2 > q^2$. Therefore $\alpha_S^2 = q^2$ may be called the short-wave cut-off in the sense that the equilibrium flow with any value of U_S is stable with respect to wave disturbances characterized by $\alpha_S^2 > q^2$. On the other hand, in the region $1-\rho^2 < 0$, or $\alpha_S^2 < q^2$ (the long-wave side of the cut-off), if the value of U_S is such that

$$U_S^2 > U_{SC}^2$$

where U_{SC} is the critical wind shear defined by

$$U_{SC}^2 = \frac{v_F(v_F + \rho^2 v_H)}{(\rho^2 - 1)} \left[1 + \frac{\rho^4}{\{(2 + \rho^2)v_F + \rho^2 v_H\}^2} v_R^2 \right], \quad (4.25)$$

at least one of the imaginary components of eigenvalues becomes positive and, therefore, the equilibrium flow is unstable. When $U_S = U_{SC}$ one of the imaginary components is zero while the other is negative, as may be readily seen in the foregoing analysis. Thus, (4.25) defines the curves of critical stability that separate the regions of stability and instability.

4.4 SYSTEM OF NONLINEAR EQUATIONS

In investigating the nonlinear effects on stability of the equilibrium flow $\psi_{M0} = -U_M y$, $\psi_{S0} = -U_S y$ we return to Eqs. (4.6) and (4.7) and, by collecting all the terms linear in perturbation quantities on the left-hand side and the nonlinear terms on the right-hand side, rewrite them as follows:

$$\begin{aligned}
& \frac{\partial}{\partial t} (\nabla^2 \Psi_M) + U_M \frac{\partial}{\partial x} (\nabla^2 \Psi_M) + U_S \frac{\partial}{\partial x} (\nabla^2 \Psi_S) + \beta \frac{\partial \Psi_M}{\partial x} - K_V \nabla^2 (\nabla^2 \Psi_M) \\
& = - \{J(\Psi_M, \nabla^2 \Psi_M) + J(\Psi_S, \nabla^2 \Psi_S)\}
\end{aligned} \tag{4.26}$$

$$\begin{aligned}
& \frac{\partial}{\partial t} (\nabla^2 \Psi_S) + U_M \frac{\partial}{\partial x} (\nabla^2 \Psi_S) + U_S \frac{\partial}{\partial x} (\nabla^2 \Psi_M) + \beta \frac{\partial \Psi_S}{\partial x} - K_V \nabla^2 (\nabla^2 \Psi_S) \\
& - q^2 \left\{ \frac{\partial \Psi_S}{\partial t} + U_M \frac{\partial \Psi_S}{\partial x} - U_S \frac{\partial \Psi_M}{\partial x} + H \Psi_S - K_T \nabla^2 \Psi_S \right\} \\
& = - \{J(\Psi_M, \nabla^2 \Psi_S) + J(\Psi_S, \nabla^2 \Psi_M)\} + q^2 J(\Psi_M, \Psi_S)
\end{aligned} \tag{4.27}$$

in which $J(f,g)$ is the Jacobian symbol,

$$J(f,g) = \frac{\partial f}{\partial x} \frac{\partial g}{\partial y} - \frac{\partial f}{\partial y} \frac{\partial g}{\partial x} \tag{4.28}$$

and, as before

$$\begin{aligned}
\Psi_M(x,y,t) &= \psi_M(x,y,t) - \psi_{M0}(y) \\
\Psi_S(x,y,t) &= \psi_S(x,y,t) - \psi_{S0}(y)
\end{aligned} \tag{4.29}$$

are the perturbation stream functions.

We now put

$$\begin{aligned}
\Psi_M &= \Psi_{M0} + (\Psi_{M1} + \tilde{\Psi}_{M1}) + (\Psi_{M2} + \tilde{\Psi}_{M2}) + \dots \\
\Psi_S &= \Psi_{S0} + (\Psi_{S1} + \tilde{\Psi}_{S1}) + (\Psi_{S2} + \tilde{\Psi}_{S2}) + \dots
\end{aligned} \tag{4.30}$$

where

$$\begin{aligned}
\Psi_{M0} &= \phi'_{M0}(y,t), & \Psi_{S0} &= \phi'_{S0}(y,t) \\
\Psi_{M1} &= \phi'_{M1}(y,t)e^{i\alpha_x(x-c_r t)}, & \Psi_{S1} &= \phi'_{S1}(y,t)e^{i\alpha_x(x-c_r t)} \\
\Psi_{M2} &= \phi'_{M2}(y,t)e^{i2\alpha_x(x-c_r t)}, & \Psi_{S2} &= \phi'_{S2}(y,t)e^{i2\alpha_x(x-c_r t)} \quad (4.31)
\end{aligned}$$

and $\tilde{\Psi}$ denotes the complex conjugate of Ψ . Ψ_{M1} and Ψ_{S1} are the fundamental disturbances that would have amplitudes of the form $\exp(\alpha_x c_i t)$ and phase velocity c_r , where c_i and c_r have the values obtained by the linearized theory, if there were no nonlinear interactions. The effect of the nonlinear interactions of the fundamental disturbances would appear as modification on the zonally-averaged flow, which is represented by Ψ_{M0} and Ψ_{S0} , on the one hand, and as generation of the first harmonics Ψ_{M2} and Ψ_{S2} on the other. Generation of higher harmonics would then take place as the result of interactions among the disturbances.

Upon substitution of (4.30) and (4.31) into Eqs. (4.26) and (4.27) we obtain a system of equations for the amplitudes of individual harmonic components. With primes denoting the differentiation with respect to y , the equations take the forms:

(i) The fundamental disturbances

$$\begin{aligned}
& - \left\{ \phi'_{M0} + (c_r - U_M) + \frac{i}{\alpha_x} \frac{\partial}{\partial t} \right\} (\phi''_{M1} - \alpha_x^2 \phi'_{M1}) + (\phi'''_{M0} + \beta) \phi'_{M1} + \frac{i}{\alpha_x} K_V (\alpha_x \phi'_{M1} - 2\alpha_x^2 \phi''_{M1} + \phi'''_{M1}) \\
& - (\phi'_{S0} - U_S) (\phi''_{S1} - \alpha_x^2 \phi'_{S1}) + \phi'''_{S0} \phi'_{S1} \\
& = - \{ -\tilde{\phi}'_{M1} [\phi'''_{M2} - 4\alpha_x^2 \phi'_{M2}] - 2\tilde{\phi}'_{M1} [\phi''_{M2} - 4\alpha_x^2 \phi'_{M2}] \} \\
& - \{ -\tilde{\phi}'_{S1} [\phi'''_{S2} - 4\alpha_x^2 \phi'_{S2}] - 2\tilde{\phi}'_{S1} [\phi''_{S2} - 4\alpha_x^2 \phi'_{S2}] \} \\
& - \{ 2\phi'_{M2} [\tilde{\phi}'''_{M1} - \alpha_x^2 \tilde{\phi}'_{M1}] + \phi'_{M2} [\tilde{\phi}''_{M1} - \alpha_x^2 \tilde{\phi}'_{M1}] \} \\
& - \{ 2\phi'_{S2} [\tilde{\phi}'''_{S1} - \alpha_x^2 \tilde{\phi}'_{S1}] + \phi'_{S2} [\tilde{\phi}''_{S1} - \alpha_x^2 \tilde{\phi}'_{S1}] \} + o(\tilde{\phi}'_{M2} \phi'_{M3}) \quad (4.32)
\end{aligned}$$

$$\begin{aligned}
& - \left[\phi'_{M0} + (c_r - U_M) + \frac{i}{\alpha_x} \frac{\partial}{\partial t} + \frac{i}{\alpha_x} q^2 K_T \right] (\phi''_{S1} - \alpha_x^2 \phi_{S1}) + \left[(\phi'''_{M0} + \beta) + q^2 \left[\phi'_{M0} \right. \right. \\
& \quad \left. \left. + (c_r - U_M) + \frac{i}{\alpha_x} \frac{\partial}{\partial t} + \frac{i}{\alpha_x} H \right] \right] \phi_{S1} + \frac{i}{\alpha_x} K_V (\alpha_x^4 \phi_{S1} - 2\alpha_x^2 \phi''_{S1} + \phi_{S1}) \\
& - (\phi'_{S0} - U_S)(\phi''_{M1} - \alpha_x^2 \phi_{M1}) + (\phi'''_{S0} - q^2 \phi'_{S0} + q^2 U_S) \phi_{M1} \\
& = - \{ -\tilde{\phi}'_{M1} [\phi'''_{S2} - 4\alpha_x^2 \phi'_{S2}] - 2\tilde{\phi}'_{M1} [\phi''_{S2} - 4\alpha_x^2 \phi_{S2}] \} \\
& - \{ -\tilde{\phi}'_{S1} [\phi'''_{M2} - 4\alpha_x^2 \phi'_{M2}] - 2\tilde{\phi}'_{S1} [\phi''_{M2} - 4\alpha_x^2 \phi_{M2}] \} \\
& - \{ 2\phi_{M2} [\tilde{\phi}''_{S1} - \alpha_x^2 \tilde{\phi}'_{S1}] + \phi'_{M2} [\tilde{\phi}''_{S1} - \alpha_x^2 \tilde{\phi}'_{S1}] \} \\
& - \{ 2\phi_{S2} [\tilde{\phi}'''_{M1} - \alpha_x^2 \tilde{\phi}'_{M1}] + \phi'_{S2} [\tilde{\phi}''_{M1} - \alpha_x^2 \tilde{\phi}'_{M1}] \} \\
& + q^2 \{ -\tilde{\phi}'_{M1} \phi'_{S2} + \tilde{\phi}'_{S1} \phi'_{M2} + 2\phi_{M2} \tilde{\phi}'_{S1} - 2\phi_{S2} \tilde{\phi}'_{M1} \} + o(\tilde{\phi}'_{M2} \phi_{M3}) . \quad (4.33)
\end{aligned}$$

(ii) The first harmonics

$$\begin{aligned}
& - \left\{ \phi'_{M0} + (c_r - U_M) + \frac{i}{2\alpha_x} \frac{\partial}{\partial t} \right\} (\phi''_{M2} - 4\alpha_x^2 \phi_{M2}) + (\phi'''_{M0} + \beta) \phi_{M2} \\
& \quad + \frac{i}{2\alpha_x} K_V \{ 16\alpha_x^4 \phi_{M2} - 8\alpha_x^2 \phi''_{M2} + \phi_{M2} \} \\
& - (\phi'_{S0} - U_S)(\phi''_{S2} - 4\alpha_x^2 \phi_{S2}) + \phi'''_{S0} \phi_{S2} \\
& = - \frac{1}{2} \{ \phi_{M1} \phi'''_{M1} - \phi'_{M1} \phi''_{M1} + \phi_{S1} \phi'''_{S1} - \phi'_{S1} \phi''_{S1} \} + o(\phi_{M1} \phi_{M3}) \quad (4.34)
\end{aligned}$$

$$\begin{aligned}
& - \left\{ \phi'_{M0} + (c_r - U_M) + \frac{i}{2\alpha_x} \frac{\partial}{\partial t} + \frac{i}{2\alpha_x} q^2 K_T \right\} (\phi''_{S2} - 4\alpha_x^2 \phi_{S2}) + \left[(\phi'''_{M0} + \beta) + q^2 \left\{ \phi'_{M0} \right. \right. \\
& \quad \left. \left. + (c_r - U_M) + \frac{i}{2\alpha_x} \frac{\partial}{\partial t} + \frac{i}{2\alpha_x} H \right\} \right] \phi_{S2} + \frac{i}{2\alpha_x} K_V \{ 16\alpha_x^4 \phi_{S2} - 8\alpha_x^2 \phi''_{S2} + \phi_{S2}^{iv} \} \\
& - (\phi'_{S0} - U_S) (\phi''_{M2} - 4\alpha_x^2 \phi_{M2}) + (\phi'''_{S0} - q^2 \phi'_{S0} + q^2 U_S) \phi_{M2} \\
& = - \frac{1}{2} \{ \phi_{M1} \phi_{S1}''' - \phi_{M1}' \phi_{S1}'' + \phi_{S1} \phi_{M1}''' - \phi_{S1}' \phi_{M1}'' \} \\
& \quad + \frac{q^2}{2} \{ \phi_{M1} \phi_{S1}' - \phi_{M1}' \phi_{S1} \} + O(\tilde{\phi}_{M1} \phi_{S3}) \quad . \quad (4.35)
\end{aligned}$$

(iii) The zonally-averaged flows

$$\begin{aligned}
\frac{i}{\alpha_x} K_V \phi_{M0}^{iv} - \frac{i}{\alpha_x} \frac{\partial}{\partial t} (\phi''_{M0}) & = - [\phi_{M1} \tilde{\phi}'_{M1} - \tilde{\phi}'_{M1} \phi_{M1} + \phi_{S1} \tilde{\phi}'_{S1} - \tilde{\phi}'_{S1} \phi_{S1}]'' \\
& - 2[\phi_{M2} \tilde{\phi}'_{M2} - \tilde{\phi}'_{M2} \phi_{M2} + \phi_{S2} \tilde{\phi}'_{S2} - \tilde{\phi}'_{S2} \phi_{S2}]'' \\
& + O(\phi_{M3} \tilde{\phi}_{M3}) \quad (4.36)
\end{aligned}$$

$$\begin{aligned}
\frac{i}{\alpha_x} K_V \phi_{S0}^{iv} - \frac{i}{\alpha_x} q^2 (K_T \phi_{S0}'' - H \phi_{S0}) - \frac{i}{\alpha_x} \frac{\partial}{\partial t} (\phi''_{S0} - q^2 \phi_{S0}) \\
& = - [\phi_{M1} \tilde{\phi}'_{S1} - \tilde{\phi}'_{M1} \phi_{S1} + \phi_{S1} \tilde{\phi}'_{M1} - \tilde{\phi}'_{S1} \phi_{M1}]'' \\
& \quad + q^2 [\phi_{M1} \tilde{\phi}'_{S1} - \tilde{\phi}'_{M1} \phi_{S1}]' \\
& \quad - 2[\phi_{M2} \tilde{\phi}'_{S2} - \tilde{\phi}'_{M2} \phi_{S2} + \phi_{S2} \tilde{\phi}'_{M2} - \tilde{\phi}'_{S2} \phi_{M2}]'' \\
& \quad + 2q^2 [\phi_{M2} \tilde{\phi}'_{S2} - \tilde{\phi}'_{M2} \phi_{S2}]' + O(\phi_{M3} \tilde{\phi}_{S3}) \quad (4.37)
\end{aligned}$$

The equations for the amplitude functions of other harmonics can be similarly obtained.

4.5 SIMPLIFICATION OF THE NONLINEAR PROBLEM OF STABILITY IN THE LIMIT OF $c_i \rightarrow 0$

In the following we shall consider the problem of superimposing a fundamental disturbance of mode (m,n) which corresponds to one of the two eigenvalues determined in the linearized theory on an equilibrium flow which is weakly unstable (or stable), i.e., $|c_i| \ll 1$, with respect to the fundamental disturbance but otherwise stable (or more stable) with respect to all harmonics of the fundamental disturbance. We shall assume that the amplitudes of the fundamental disturbance are never of greater order of magnitude than $c_i^{1/2}$ and that $\partial/\partial t$ is at most of order c_i .

It has been found in the linearized theory that the fundamental disturbance is defined by a set of amplitudes of the form

$$\begin{aligned}\phi_{ML} &= A_M Y_1(y) \exp(\alpha_X c_i t) \\ \phi_{SL} &= C_S A_M Y_1(y) \exp(\alpha_X c_i t)\end{aligned}\tag{4.38}$$

in which $Y_1(y) = \sin(\alpha_Y Y)$ and $C_S = C_{S1} + i C_{S2}$, where C_{S1} and C_{S2} have been defined in (4.21). It can then be shown that

$$\phi_{ML} \phi_{ML}^{(2)} - \phi_{ML}^i \phi_{ML}'' = 0, \quad \phi_{SL} \phi_{SL}^{(2)} - \phi_{SL}^i \phi_{SL}'' = 0$$

$$\phi_{ML} \phi_{SL}^{(2)} - \phi_{ML}^i \phi_{SL}'' = 0, \quad \phi_{SL} \phi_{ML}^{(2)} - \phi_{SL}^i \phi_{ML}'' = 0$$

and

$$\phi_{ML} \phi_{SL}^i - \phi_{ML}^i \phi_{SL} = 0.$$

We may therefore conclude that, to the order of c_1 , the nonlinear effect of the fundamental disturbance in generating the first harmonics is null. Thus, to the first order of approximation, the system of the perturbations may be considered as consisting of the fundamental disturbance and the distortions in the zonally-averaged flows, of which the amplitude functions are determined by the following system of equations:

$$\frac{i}{\alpha_x} K_v \phi_{MO}^{iv} - \frac{i}{\alpha_x} \frac{\partial}{\partial t} (\phi_{MO}''') = - [\phi_{M1} \tilde{\phi}_{M1}' - \tilde{\phi}_{M1}' \phi_{M1}' + \phi_{S1} \tilde{\phi}_{S1}' - \tilde{\phi}_{S1}' \phi_{S1}']'' \quad (4.39)$$

$$\begin{aligned} \frac{i}{\alpha_x} K_v \phi_{SO}^{iv} - \frac{i}{\alpha_x} q^2 (K_T \phi_{SO}'' - H \phi_{SO}') - \frac{i}{\alpha_x} \frac{\partial}{\partial t} (\phi_{SO}'' - q^2 \phi_{SO}') \\ = - [\phi_{M1} \tilde{\phi}_{S1}' - \tilde{\phi}_{M1}' \phi_{S1}' + \phi_{S1} \tilde{\phi}_{M1}' - \tilde{\phi}_{S1}' \phi_{M1}']'' + q^2 [\phi_{M1} \tilde{\phi}_{S1}' - \tilde{\phi}_{M1}' \phi_{S1}']' \end{aligned} \quad (4.40)$$

for the zonally-averaged flows and

$$\begin{aligned} - \left\{ \phi_{MO}' + (c_r - U_M) + \frac{i}{\alpha_x} \frac{\partial}{\partial t} \right\} (\phi_{M1}'' - \alpha_x^2 \phi_{M1}') + (\phi_{MO}'' + \beta) \phi_{M1} \\ + \frac{i}{\alpha_x} K_v (\alpha_x^4 \phi_{M1}' - 2\alpha_x^2 \phi_{M1}'' + \phi_{M1}^{iv}) \\ - (\phi_{SO}' - U_S) (\phi_{S1}'' - \alpha_x^2 \phi_{S1}') + \phi_{SO}''' \phi_{S1} = 0 \end{aligned} \quad (4.41)$$

$$\begin{aligned}
& - \left\{ \phi'_{MO} + (c_r - U_M) + \frac{i}{\alpha_x} q^2 K_T + \frac{i}{\alpha_x} \frac{\partial}{\partial t} \right\} (\phi''_{S1} - \alpha_x^2 \phi_{S1}) \\
& + \left[(\phi'''_{MO} + \beta) + q^2 \left\{ \phi'_{MO} + (c_r - U_M) + \frac{i}{\alpha_x} H + \frac{i}{\alpha_x} \frac{\partial}{\partial t} \right\} \right] \phi_{S1} \\
& + \frac{i}{\alpha_x} K_V (\alpha_x^4 \phi_{S1} - 2\alpha_x^2 \phi''_{S1} + \phi_{S1}^{iv}) \\
& - (\phi'_{SO} - U_S) (\phi''_{M1} - \alpha_x^2 \phi_{M1}) \\
& + (\phi'''_{SO} - q^2 \phi'_{SO} + q^2 U_S) \phi_{M1} = 0
\end{aligned} \tag{4.42}$$

for the fundamental disturbance.

We now put

$$\phi_{M1}(y, t) = A_M(t) Y_1(y) + A_{M1}(t) \eta_{M1}(t)$$

$$\phi_{S1}(y, t) = (C_S A_M(t) + B(t)) Y_1(y) + A_{S1}(t) \eta_{S1}(y) \tag{4.43}$$

$$\phi_{MO}(y, t) = A_{MO}(t) \eta_{MO}(y)$$

$$\phi_{SO}(y, t) = A_{SO}(t) \eta_{SO}(y)$$

where η_{M1} , η_{S1} , η_{MO} , η_{SO} are all of order unity, and A_M is of order $c^{1/2}$.

By substituting (4.43) into Eqs. (4.39) and (4.40), we then obtain, to

the order of c_i ,

$$K_V \eta_{MO}^{iv} A_{MO} - \eta_{MO}'' \frac{dA_{MO}}{dt} = 0$$

$$\frac{i}{\alpha_x} (K_V \eta_{SO}^{iv} - q^2 K_T \eta_{SO}'' + q^2 H \eta_{SO}) A_{SO} - \frac{i}{\alpha_x} (\eta_{SO}'' - q^2 \eta_{SO}) \frac{dA_{SO}}{dt}$$

$$= -i2\alpha_y q^2 C_{S2} |A_M|^2 \sin(2\alpha_y Y) .$$

These equations can be satisfied by

$$\eta_{MO} = \eta_{SO} = \sin(2\alpha_y y) = Y_2(y) \quad (4.44)$$

and A_{MO} , A_{SO} that satisfy the following equations:

$$\mu_M A_{MO} + \nu_M \frac{dA_{MO}}{dt} = 0 \quad (4.45)$$

with

$$\mu_M = (2\alpha_y)^4 K_V, \quad \nu_M = (2\alpha_y)^2$$

and

$$\mu_S A_{SO} + \nu_S \frac{dA_{SO}}{dt} = -\delta_S |A_M|^2 \quad (4.46)$$

with

$$\mu_S = \{(2\alpha_y)^4 K_V + (2\alpha_y)^2 q^2 K_T + q^2 H\},$$

$$\nu_S = (2\alpha_y)^2 + q^2,$$

$$\delta_S = 2\alpha_x \alpha_y q^2 C_{S2}.$$

Thus, to the first order of approximation, there is no distortion on the zonally-averaged vertical-mean flow. On the other hand, for the distortion on the zonally-averaged vertical shear flow we may distinguish the following two cases:

Case A: $\nu_S c_i \ll \mu_S$ for which

$$A_{SO} = -\frac{\delta_S}{\mu_S} |A_M|^2 \quad (4.47)$$

and

Case B: $v_S c_i \simeq \mu_S$ for which

$$A_{S0} = - \frac{\delta_S}{v_S} \int_{t_0}^t |A_M|^2 e^{-\frac{\mu_S}{v_S} (t-\tau)} d\tau. \quad (4.48)$$

Consequently, the distortions in the zonally-averaged flows are, to the order of c_i ,

$$\phi_{M0} = 0$$

$$\phi_{S0} = A_{S0}(t) Y_2(y) \quad (4.49)$$

where A_{S0} is given by either (4.47) or (4.48).

Next, when we substitute (4.43) and (4.49) into Eqs. (4.41) and (4.42), retain the terms of order not higher than $c_i^{3/2}$ while assuming that A_{S0} , A_{M1} , A_{S1} and B are of order $c_i^{3/2}$, and make use of the relations obtained in the linearized theory that read as

$$\begin{aligned} & \{ (c_r - U_M) + i c_i + V_R + i V_F \} A_M - U_S C_S A_S = 0 \\ & - \left(1 - \frac{q^2}{\alpha_S^2} \right) U_S A_M + \left[\left(1 + \frac{q^2}{\alpha_S^2} \right) (c_r - U_M + i c_i) + V_R + i \left(V_F + \frac{q^2}{\alpha_S^2} V_H \right) \right] \\ & C_S A_M = 0 \end{aligned}$$

we obtain

$$\begin{aligned} & \left(- i c_i A_M + \frac{i}{\alpha_x} \frac{dA_M}{dt} \right) \alpha_S^2 Y_1 - \left[\left(1 - \frac{(2\alpha_y)^2}{\alpha_S^2} \right) \alpha_y C_S A_{S0} A_M + U_S B \right] \alpha_S^2 Y_1 \\ & + \left[\left(1 - \frac{(2\alpha_y)^2}{\alpha_S^2} \right) \alpha_y C_S A_{S0} A_M \right] \alpha_S^2 Y_3 - (c_r - U_M) A_{M1} (\eta_{M1}'' - \alpha_x^2 \eta_{M1}') + B A_{M1} \eta_{M1} \\ & + \frac{i}{\alpha_x} K_V A_{M1} (\alpha_x^4 \eta_{M1}'' - 2\alpha_x^2 \eta_{M1}'' + \eta_{M1}^{iv}) + U_S A_{S1} (\eta_{S1}'' - \alpha_x^2 \eta_{S1}') = 0 \end{aligned}$$

$$\begin{aligned}
& \left(1 + \frac{q^2}{\alpha_S^2}\right) \left(-ic_i A_M + \frac{i}{\alpha_x} \frac{dA_M}{dt}\right) \alpha_S^2 C_S Y_1 - \left[1 - \frac{(2\alpha_y)^2 + q^2}{\alpha_S^2}\right] \alpha_y A_{SO} A_M \\
& - \left\{ \left(1 + \frac{q^2}{\alpha_S^2}\right) (c_r - U_M) + v_R + i \left(v_F + \frac{q^2}{\alpha_S^2} v_H\right) \right\} B \alpha_S^2 Y_1 \\
& + \left[1 - \frac{(2\alpha_y)^2 + q^2}{\alpha_S^2}\right] \alpha_y A_{SO} A_M \alpha_S^2 Y_3 \\
& - \left\{ (c_r - U_M) + \frac{i}{\alpha_x} q^2 K_T \right\} A_{S1} (\eta_{S1}'' - \alpha_x^2 \eta_{S1}) \\
& + \left[\beta + q^2 (c_r - U_M) + \frac{i}{\alpha_x} q^2 H \right] A_{S1} \eta_{S1} \\
& + \frac{i}{\alpha_x} K_v A_{S1} (\alpha_x^4 \eta_{S1} - 2\alpha_x^2 \eta_{S1}'' + \eta_{S1}^{iv}) + U_{S'ML} A_{ML} (\eta_{ML}'' - \alpha_x^2 \eta_{ML}) + q^2 U_{S'ML} A_{ML} \eta_{ML} = 0
\end{aligned}$$

in which $Y_3 = \sin(3\alpha_y)$. These equations can be satisfied if

$$\eta_{M1} = \eta_{S1} = \sin(3\alpha_y) = Y_3$$

and their coefficients satisfy the following equations:

$$\left(\frac{dA_M}{dt} - \alpha_x c_i A_M\right) + i\alpha_x \alpha_y \left(1 - \frac{(2\alpha_y)^2}{\alpha_S^2}\right) C_S A_{SO} A_M + i\alpha_x U_{S'B} = 0 \quad (4.50)$$

$$\begin{aligned}
& C_S \left(1 + \frac{q^2}{\alpha_S^2}\right) \left(\frac{dA_M}{dt} - \alpha_x c_i A_M\right) + i\alpha_x \alpha_y \left(1 - \frac{(2\alpha_y)^2 + q^2}{\alpha_S^2}\right) A_{SO} A_M \\
& - i\alpha_x \left\{ \left(1 + \frac{q^2}{\alpha_S^2}\right) (c_r - U_M) + v_R + i \left(v_F + \frac{q^2}{\alpha_S^2} v_H\right) \right\} B = 0 \quad (4.51)
\end{aligned}$$

for the coefficients of Y_1 and

$$\{(c_r - U_M) + v_{R1} + i v_{F1}\} A_{M1} - U_{S'A_{S1}} = -\alpha_y \frac{\alpha_S^2 - (2\alpha_y)^2}{\alpha_{S1}^2} C_S A_{SO} A_M \quad (4.52)$$

$$\begin{aligned}
& - \left(1 - \frac{q^2}{\alpha_{S1}^2}\right) U_{S1} A_{M1} + \left\{ \left(1 + \frac{q^2}{\alpha_{S1}^2}\right) (c_r - U_M) + v_{R1} + i \left(v_{F1} + \frac{q^2}{\alpha_{S1}^2} v_{H1} \right) \right\} A_{S1} \\
& = - \alpha_y \frac{\alpha_S^2 - (2\alpha_y)^2 - q^2}{\alpha_{S1}^2} A_{S0} A_M \quad (4.53)
\end{aligned}$$

for the coefficients of Y_3 , where

$$\begin{aligned}
\alpha_{S1}^2 &= \alpha_x^2 + (3\alpha_y)^2 \\
v_{R1} &= \frac{\beta}{\alpha_{S1}^2}, \quad v_{F1} = \frac{K_V \alpha_{S1}^2}{\alpha_x}, \quad v_{H1} = \frac{H + K_T \alpha_{S1}^2}{\alpha_x} \quad (4.54)
\end{aligned}$$

are the parameters associated with perturbations of mode $(m, 3n)$, the presence of which is the result of interactions between the fundamental disturbance and the distortion on the zonally-averaged vertical shear flow. We shall hereafter assume that the mode $(m, 3n)$ is stable or more stable than the fundamental disturbance.

By eliminating B from Eqs. (4.50) and (4.51), and by introducing the following notations:

$$\begin{aligned}
P &= \left(1 + \frac{q^2}{\alpha_S^2}\right) (c_r - U_M + C_{S1} U_S) + v_R \\
Q &= v_F + \frac{q^2}{\alpha_S^2} v_H + \left(1 + \frac{q^2}{\alpha_S^2}\right) C_{S2} U_S \\
V &= \left(1 - \frac{(2\alpha_y)^2}{\alpha_S^2}\right) C_{S1} \left\{ \left(1 + \frac{q^2}{\alpha_S^2}\right) (c_r - U_M) + v_R \right\} \\
&\quad - \left(1 - \frac{(2\alpha_y)^2}{\alpha_S^2}\right) C_{S2} \left(v_F + \frac{q^2}{\alpha_S^2} v_H \right) + \left(1 - \frac{(2\alpha_y)^2 + q^2}{\alpha_S^2} U_S \right) \quad (4.53)
\end{aligned}$$

$$\begin{aligned}
W &= \left(1 - \frac{(2\alpha_y)^2}{\alpha_S^2}\right) C_{S2} \left\{ \left(1 + \frac{q^2}{\alpha_S^2}\right) (c_r - U_M) + v_R \right\} \\
&+ \left(1 - \frac{(2\alpha_y)^2}{\alpha_S^2}\right) C_{S1} \left(v_F + \frac{q^2}{\alpha_S^2} v_H \right) \\
\kappa_r &= \alpha_y \operatorname{Re} \left(\frac{V+iW}{P+iQ} \right) = \alpha_y \frac{PV+QW}{P^2+Q^2} \\
\kappa_i &= \alpha_y \operatorname{Im} \left(\frac{V+iW}{P+iQ} \right) = \alpha_y \frac{PW-QV}{P^2+Q^2},
\end{aligned} \tag{4.54}$$

we obtain

$$\frac{dA_M}{dt} = \alpha_x c_i A_M - i\alpha_x (\kappa_r + i\kappa_i) A_{S0} A_M. \tag{4.55}$$

The complex conjugate of Eq. (4.55) is given by

$$\frac{d\tilde{A}_M}{dt} = \alpha_x c_i \tilde{A}_M + i\alpha_x (\kappa_r - i\kappa_i) A_{S0} \tilde{A}_M, \tag{4.56}$$

since A_{S0} is real. From Eqs. (4.55) and (4.56) we obtain the equation for the square of the amplitude A_M in the form

$$\frac{d|A_M|^2}{dt} = 2\alpha_x c_i |A_M|^2 + 2\alpha_x \kappa_i A_{S0} |A_M|^2. \tag{4.57}$$

In the following we shall consider Eq. (4.57) first for the case where $v_S c_i \ll \mu_S$ and then for the case where $v_S c_i \simeq \mu_S$.

Case A. $v_S c_i \ll \mu_S$: By substituting (4.47) into (4.57) we obtain

$$\frac{d|A_M|^2}{dt} = 2\alpha_x c_i |A_M|^2 - 2\alpha_x \kappa_i \frac{\delta_S}{\mu_S} |A_M|^4 \tag{4.58}$$

and its solution is given by

$$|A_M|^2 = \frac{c_i C \exp(2\alpha_x c_i t)}{1 + \kappa_i \frac{\delta_S}{\mu_S} C \exp(2\alpha_x c_i t)} \quad (4.59)$$

where C is any arbitrary real constant.

If $c_i > 0$, which implies that the fundamental disturbance tends to grow with time, the solution (4.59) has a meaningful equilibrium value ($|A_M|^2 > 0$) if $\epsilon_i = \kappa_i \frac{\delta_S}{\mu_S} > 0$; in this case the disturbance amplifies in the manner predicted by the linearized theory ($|A_M|^2 \sim \exp(2\alpha_x c_i t)$) at $t = -\infty$, and tends to the equilibrium value $|A_M|_{\infty}^2 = \frac{c_i}{\epsilon_i}$ as $t \rightarrow +\infty$. If $\epsilon_i < 0$, there exists no equilibrium amplitude; Eq. (4.58) shows that the rate of growth at any moment is greater than that predicted by the linearized theory. In either case, solution (4.59) gives a correct prediction only for such values of t that $|A_M|^2$ is bounded and of order c_i .

On the other hand, if $c_i < 0$, the solution (4.59) has a meaningful equilibrium value if $\epsilon_i < 0$; the disturbance takes on the equilibrium value $|A_M|_{-\infty}^2 = \frac{|c_i|}{|\epsilon_i|}$ at $t = -\infty$, but the equilibrium is unstable in the sense that, when the amplitude at any moment is less than this equilibrium value, the disturbance decays to zero as $t \rightarrow +\infty$, but if the amplitude at any moment is greater than the equilibrium value, it tends to grow with time, as can be readily seen from Eq. (4.58). If $\epsilon_i > 0$, the rate of decay at any moment is greater than that predicted by the linearized theory. Figure 24 shows schematically the time variations of $|A_M|^2$ as predicted by Eq. (4.58) for the cases each of which has an equilibrium value.

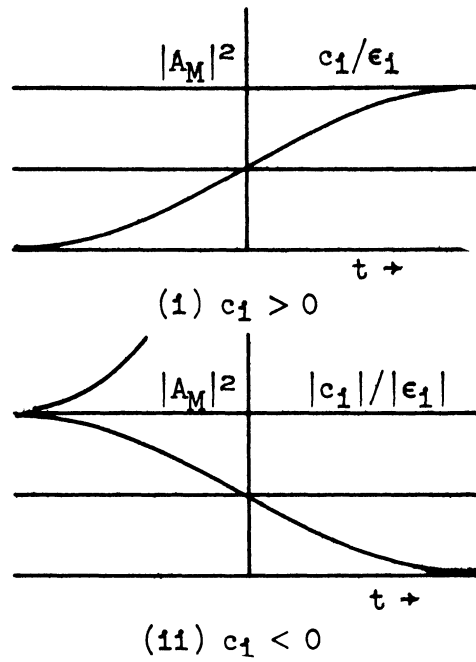


Fig. 24. Variation of $|A_M|^2$ with time.

To solve for A_M , we first multiply Eq. (4.55) by \tilde{A}_M^{-1} , Eq. (4.56) by $-A_M \tilde{A}_M^{-2}$ and add the results we obtain

$$\left(\frac{A_M}{\tilde{A}_M}\right)^{-1} \frac{d}{dt} \left(\frac{A_M}{\tilde{A}_M}\right) = i2\alpha_x \kappa_r \frac{\delta_S}{\mu_S} |A_M|^2$$

which, when integrated, yields

$$\frac{A_M}{\tilde{A}_M} = \exp \left\{ i2\alpha_x \epsilon_r \int_{t_0}^t |A_M|^2 dt \right\}$$

where $\epsilon_r = \frac{\delta_S}{\mu_S} \kappa_r$. This may be written in the form

$$A_M = |A_M| \exp \left\{ i\alpha_x \epsilon_r \int_{t_0}^t |A_M|^2 dt \right\} \quad (4.60)$$

by multiplying the last equation by $|A_M|^2$ and taking the square root.

Expression (4.60) may be readily interpreted from (4.59) in those cases where there exists an equilibrium value. Thus, if $c_1 > 0$ and

$\epsilon_i > 0$, it can be readily verified that

$$A_M^{-\infty} = \lim_{t \rightarrow -\infty} A_M = C^{1/2} c_i^{1/2} \exp(\alpha_x c_i t + i\theta) \quad (4.61)$$

where θ is a constant the value of which depends on t_0 but not on t , and

$$A_M^{+\infty} = \lim_{t \rightarrow +\infty} A_M = \left(\frac{c_i}{\epsilon_i} \right) \exp \left\{ i\alpha_x c_i \frac{\epsilon_r}{\epsilon_i} (t - t'_0) \right\} \quad (4.62)$$

where t'_0 is an arbitrary phase depending on t_0 . Formulas (4.61) and (4.62) show that, even if A_M is non-oscillatory at $t = -\infty$, it eventually develops a fluctuation as t progresses and attains the limiting form (4.62) as $t \rightarrow +\infty$.

The limiting forms of the fundamental disturbance are consequently given, to the order of $c_i^{1/2}$, by

$$\begin{aligned} \psi_{M+}^{-\infty} &= c_i^{1/2} (C^{1/2} e^{i\theta}) \sin(\alpha_y y) \exp[i\alpha_x (x - c_r t - i c_i t)] \\ \psi_{M+}^{+\infty} &= \left(\frac{c_i}{\epsilon_i} \right)^{1/2} \sin(\alpha_y y) \exp \left[i\alpha_x \left\{ x - \left(c_r - \frac{c_i \epsilon_r}{\epsilon_i} \right) (t - t''_0) \right\} \right] \end{aligned} \quad (4.63)$$

which shows that the phase velocity in the equilibrium state is given by

$$c_{re} = c_r - \frac{c_i \kappa_r}{\kappa_i}. \quad (4.64)$$

Similarly, if $c_i < 0$ and $\epsilon_i < 0$, the fundamental disturbance has the limiting forms

$$\begin{aligned} \psi_{M-}^{-\infty} &= \left(\frac{|c_i|}{|\epsilon_i|} \right)^{1/2} \sin(\alpha_y y) \exp \left[i\alpha_x \left\{ x - \left(c_r - \frac{|c_i| \epsilon_r}{|\epsilon_i|} \right) (t - t''_0) \right\} \right] \\ \psi_{M-}^{+\infty} &= c_i^{1/2} (C^{1/2} e^{i\theta}) \sin(\alpha_y y) - \exp[i\alpha_x (x - c_r t - i c_i t)] \end{aligned} \quad (4.65)$$

which has the limiting phase velocity

$$c_{re} = c_r - \frac{|c_i| \kappa_r}{\kappa_i} \quad (4.66)$$

Case B. $v_S c_i \approx \mu_S$: Here, the square of the amplitude $|A_M|^2$ is governed by an integro-differential equation of the form

$$\frac{d|A_M|^2}{dt} = 2\alpha_x c_i |A_M|^2 \left(1 - \frac{\kappa_i}{c_i} \frac{\delta_S}{\mu_S} \int_{t_0}^t |A_M|^2 \exp \left[-\frac{\mu_S}{v_S} (t-\tau) \right] dt \right) \quad (4.67)$$

which is obtained by substituting Eq. (4.48) into Eq. (4.57). Since Eq. (4.67) does not appear to be integrable in terms of known functions an attempt will be made to investigate qualitatively the characteristics of the solution in this section while the results of numerical integrations are presented in the next section.

Instead of dealing directly with Eq. (4.67) we may formulate a system of equations which is equivalent to Eq. (4.67) as follows:

$$\begin{aligned} \frac{d|A_M|^2}{dt} &= 2\alpha_x c_i |A_M|^2 \left(1 + \frac{\kappa_i}{c_i} A_{SO} \right) \\ \frac{dA_{SO}}{dt} &= -\frac{\delta_S}{v_S} |A_M|^2 - \frac{\mu_S}{v_S} A_{SO} \end{aligned} \quad (4.68)$$

and the initial conditions

$$\begin{aligned} |A_M|^2 &= Z_{10} > 0 \\ A_{SO} &= 0 \end{aligned} \quad \text{at } t = t_0 \quad (4.69)$$

The second equation in (4.68) has been obtained by differentiating Eq. (4.48) with respect to t . Equation (4.68) is a system of first-order

nonlinear ordinary differential equations with real coefficients for the real variables $|A_M|^2$ and A_{S0} .

For the sake of simplifying notations we shall transform (4.68) by introducing new variables Z_1, Z_2 defined by

$$Z_1 = |A_M|^2, \quad Z_2 = -\frac{v_S}{\delta_S} A_{S0} \quad (4.70)$$

and new coefficients defined by

$$a = 2\alpha_X c_i, \quad b = \frac{\delta_S}{v_S} \frac{\kappa_i}{c_i}, \quad c = \frac{\mu_S}{v_S} > 0 \quad (4.71)$$

into

$$\begin{aligned} \frac{dZ_1}{dt} &= aZ_1(1-bZ_2) \\ \frac{dZ_2}{dt} &= Z_1 - cZ_2 \end{aligned} \quad (4.72)$$

for which the initial conditions are

$$Z_1 = Z_{10} > 0, \quad Z_2 = 0 \quad \text{at } t = t_0. \quad (4.73)$$

It is immediately obvious from (4.72) and (4.73) that the cases in which $a > 0, b < 0$ or $a < 0, b < 0$ are of no practical interest since in the former the system grows indefinitely with time while in the latter the system decays to zero.

Case B1. $a > 0, b > 0$ or, equivalently $c_i > 0, \epsilon_i > 0$: Here, of the two singular points of the system, namely, one at the origin and the other at $(c/b, 1/b)$, only the latter is of interest. For, the origin

may be readily seen to be unstable even for the linear system obtained from (4.72) by deleting the nonlinear term.

To investigate the singular point at $(c/b, 1/b)$, we introduce the new coordinates X_1, X_2 defined by

$$X_1 = Z_1 - (c/b), \quad X_2 = Z_2 - (1/b)$$

and transform (4.72) into

$$\begin{aligned} \dot{X}_1 &= -acX_2 - abX_1X_2 \\ \dot{X}_2 &= X_1 - cX_2 \end{aligned} \quad (4.72')$$

in which the singular point in question is now located at the origin of the new coordinate system (X_1, X_2) . The coefficient matrix of the linear part of (4.72') has eigenvalues given by

$$\lambda_{1,2} = -\frac{c}{2} \left[1 \pm \left(1 - \frac{4a}{c} \right)^{1/2} \right]$$

and since $c > 0$, the origin is seen to be an attractor for the linear system and therefore an attractor also for the nonlinear system (4.72') (see e.g., Coddington and Levinson (1955), Chapt. 15). When $4a > c$, the origin is a spiral point for the linear system and since the nonlinear term $q(X_1, X_2) = -abX_1X_2$ is such that $q(X_1, X_2) \leq (ab/2)(X_1^2 + X_2^2)$, it is a proper spiral point for system (4.72'). Consequently, the solutions of the system tend asymptotically to the only equilibrium state $(c/b, 1/b)$. On the other hand, when $4a \leq c$, the origin is an improper node for the linear system and, therefore, there is a neighborhood around

the origin in which once the trajectory of the nonlinear system falls the system will tend to the origin. An investigation of the variations of the solutions of system (4.72) and the initial conditions (4.73), which is given below, shows that the initial trajectory of the nonlinear system has a spiral-like form and suggests that the system would tend to the equilibrium state for the range of initial values under consideration.

It is obvious from (4.72) that in the time interval where $Z_2 < 1/b$ \dot{Z}_1 remains positive and that, since Z_2 is initially zero, Z_2 is an increasing function of time in the initial lapse of time where $Z_1 > cZ_2$. Let T_1 be the critical time at which $Z_2 = 1/b$ for the first time, and let T_2 be the critical time at which $Z_1 = cZ_2$ for the first time. Our first assertion is that $T_2 \geq T_1$. For, suppose otherwise; then, $\dot{Z}_2 = 0$ at T_2 and since Z_2 has been increasing up to T_2 , T_2 must be either the time at which Z_2 is a maximum or the time at which Z_2 reaches a point of inflexion. But, according to our supposition, $(\ddot{Z}_2)_{T_2} = (\dot{Z}_1)_{T_2} > 0$. This is a contradiction.

Suppose $T_1 = T_2 = T_c$. Then,

$$(Z_1)_{T_c} = c/b, \quad (Z_2)_{T_c} = 1/b \quad (4.74)$$

and

$$(Z_1^{(n)})_{T_c} = 0, \quad (Z_2^{(n)})_{T_c} = 0 \text{ for all } n \geq 1. \quad (4.75)$$

Hence, the system reaches the equilibrium state defined by (4.74).

When $T_2 > T_1$,

$$(\dot{Z}_1)_{T_1} = 0, \quad (\ddot{Z}_1)_{T_1} < 0; \quad (\dot{Z}_2)_{T_1} > 0,$$

so that Z_1 reaches a maximum $(Z_1)_{T_1}$, the value of which is greater than the equilibrium value c/b , at T_1 and starts to decrease while Z_2 continues to increase with time. In the time interval $T_1 < t < T_2$, Z_1 decreases and Z_2 increases. It is also obvious that the equilibrium state cannot be realized in this time interval. And, eventually at T_2 where

$$0 < (Z_1)_{T_2} = c(Z_2)_{T_2} < (Z_1)_{T_1}, \quad (\dot{Z}_1)_{T_2} < 0; \quad (\dot{Z}_2)_{T_2} = 0, \quad (\ddot{Z}_2)_{T_2} < 0,$$

Z_2 attains a maximum, the value of which is less than $(Z_1)_{T_1}/c$. It may also be inferred from this observation that T_2 is bounded and, therefore, so is T_1 .

After T_2 , both Z_1 and Z_2 decrease. If we denote by T_3 the time at which $Z_2 = 1/b$ for the second time and by T_4 the time at which $Z_1 = cZ_2$ for the second time, our next assertion is that $T_3 \leq T_4$. For, suppose that $T_4 < T_3$. Then, at T_4 , $\dot{Z}_1 = aZ_1(1-bZ_2) > 0$, which contradicts our supposition.

If $T_3 = T_4 = T_c$, then the system attains at T_c the equilibrium state defined by (4.74). On the other hand, if $T_3 < T_4$,

$$(\dot{Z}_1)_{T_3} = 0, \quad (\ddot{Z}_1)_{T_3} > 0; \quad (\dot{Z}_2)_{T_3} < 0,$$

and Z_1 attains a minimum value, which is less than the equilibrium value, at T_3 while Z_2 is still decreasing. Z_2 reaches a minimum at T_4 where both Z_1 and Z_2 have the values less than the equilibrium values. And,

after T_4 , the system goes through cycles each of which is similar to the one described above, namely, $t_0 \rightarrow T_1 \rightarrow T_2 \rightarrow T_3 \rightarrow T_4$, unless either $T_1 = T_2$ or $T_3 = T_4$ is attained in its course of variation. Whenever $T_1 = T_2$ or $T_3 = T_4$ happens, the system attains the equilibrium state defined by (4.74).

Case B2. $a < 0$, $b > 0$ or equivalently $c_1 < 0$, $a_1 < 0$: In this case, the singularity at $(c/b, 1/b)$ is seen to be characterized by the eigenvalues

$$\lambda_{1,2} = -\frac{c}{2} \left[1 \pm \left(1 + \frac{4|a|}{c} \right)^{1/2} \right]$$

which show that it is a saddle point for the linear system. It is therefore unstable for both the linear and nonlinear systems. On the other hand, the singularity at the origin has eigenvalues

$$\lambda_1 = -|a| < 0, \quad \lambda_2 = -c < 0$$

for the linear system. Therefore, it is an improper node for the linear system and every trajectory of the nonlinear system near the origin tends to it. An investigation on the variations of the system (4.72) with time reveals, as is presented below, that (i) when the initial value $Z_{10} < c/b$, the system approaches the origin and (ii) when the initial value $Z_{10} > c/b$ and $b < 1$, the system grows without a bound.

(i) $Z_{10} \leq c/b$. Let T_1 be the critical time at which $Z_2 = 1/b$ and let T_2 be the critical time at which $Z_1 = cZ_2$. Suppose $T_2 \geq T_1$. Then, $(\dot{Z}_2)_{T_1} > 0$ and $(Z_1)_{T_1} \geq c(Z_2)_{T_1} - c/b$, the latter being contrary to our

supposition. Therefore, $T_2 < T_1$. Then, $(\dot{Z}_2)_{T_2} = 0$, $(\dot{Z}_1)_{T_2} = (\dot{Z}_1)_{T_2} < 0$, so that Z_2 attains a maximum which is less than $1/b$ at T_2 while Z_1 continues to decrease. It may furthermore be shown that both Z_1 and Z_2 decrease monotonically after T_2 . Suppose there were a $T_4 > T_2$ such that $(\dot{Z}_2)_{T_4} = 0$. Then, $(\ddot{Z}_2)_{T_4} = (\ddot{Z}_1)_{T_4} < 0$ by our supposition and Z_2 would have to be a maximum at T_4 , but that is impossible. Hence, there is no other critical time beyond which either Z_1 or Z_2 would reverse its decreasing trend. This shows that insofar as the initial value of Z_1 is less than the equilibrium value, the system decays asymptotically to zero as t tends to infinity.

(ii) $Z_{10} > c/b$, $b < 1$. Here, it is first claimed that $T_1 < T_2$.

Suppose the converse were true. Then, at T_2 it would be true that $Z_1 < c/b$ and $Z_2 < 1/b$. Now, since $\dot{Z}_1 = -|a|Z_1(1-bZ_2) > -|a|Z_1$, if $Z_{10} = k(c/b)$, $k > 1$,

$$Z_1 > k(c/b)\exp(-|a|t) \text{ for } 0 < t < T_2$$

T_2 must then be greater than T_A that satisfies

$$k(c/b)\exp(-|a|T_A) = c/b$$

or

$$T_A = (\ln k)/|a| ,$$

that is,

$$T_2 > (\ln k)/|a| .$$

On the other hand, since

$$Z_2 = \int_{t_0}^t Z_1 \exp(-c(t-\tau)) d\tau > k(c/b) \exp(-(|a|+c)t) \int_{t_0}^t \exp(c\tau) d\tau$$

T_2 must be less than T_B that satisfies

$$k(c/b) \exp(-(|a|+c)T_B) \int_0^{T_B} \exp(c\tau) d\tau = 1/b,$$

or

$$T_B < (\ln(kb))/|a| ,$$

that is,

$$T_2 < (\ln(kb))/|a| .$$

Consequently, it would be true that

$$(\ln k)/|a| < T_2 < (\ln(kb))/|a| ,$$

but no such T_2 exists if $b < 1$. Hence $T_1 < T_2$.

Now, if $T_1 < T_2$, $(\dot{Z}_1)_{T_1} = 0$, $(\dot{Z}_1)_{T_1} > 0$ by our supposition so that Z_1 must attain a minimum at T_1 , while Z_2 continues to increase. After T_1 , both Z_1 and Z_2 increase as long as \dot{Z}_2 remains positive. Suppose there were a $T_2 > T_1$ such that $(\dot{Z}_2)_{T_2} = 0$. Then, $(Z_1)_{T_2} > 0$, $(Z_2)_{T_2} > 0$ and Z_2 would have to attain a minimum at T_2 , but this is impossible. Thus, there is no other critical time beyond T_1 at which the increase of both Z_1 and Z_2 may be arrested and, hence, the system grows without a bound.

Even when $b > 1$, if T_1 precedes T_2 , it may be shown by the same argument as that employed in case (ii) that the system grows without a

bound as t tends to infinity. On the other hand, if T_2 precedes T_1 , it is possible with the argument employed in case (i) to show that the system decays to zero as time progresses. However, no argument which may establish the order of events has been found.

When $|A_M|^2$ and A_{SO} are obtained by solving (4.68) A_M can then be expressed in terms of them as

$$A_M = |A_M| \exp \left\{ -i\alpha_{\chi\kappa r} \int_{t_0}^t A_{SO} d\tau \right\} \quad (4.76)$$

by following a similar procedure as that with which Eq. (4.60) has been obtained.

Finally, in both Case A and Case B the second-order amplitude functions B , A_{M1} and A_{S1} may be determined from Eqs. (4.50) and (4.52) in terms of A_M and A_{SO} . They are given by

$$B = - \frac{\kappa - b_0 C_S}{a_{12}} A_{SO} A_M \quad (4.77)$$

$$A_{M1} = \frac{\begin{vmatrix} b_1 & a_{12} \\ b_2 & a_{22} \end{vmatrix}}{\begin{vmatrix} a_{11} & a_{12} \\ a_{21} & a_{22} \end{vmatrix}} A_{SO} S_M \quad (4.78)$$

$$A_{S1} = \frac{\begin{vmatrix} a_{11} & b_1 \\ a_{12} & b_2 \end{vmatrix}}{\begin{vmatrix} a_{11} & a_{12} \\ a_{21} & a_{22} \end{vmatrix}} A_{SO} A_M \quad (4.79)$$

where

$$\begin{aligned}
\kappa &= \kappa_r + i\kappa_i, & b_0 &= -\alpha_y \left(1 - \frac{(2\alpha_y)^2}{\alpha_S^2} \right), \\
a_{11} &= (c_r - U_M) + v_{R1} + iv_{F1}, & a_{12} &= -U_S, \\
a_{12} &= - \left(1 - \frac{q^2}{\alpha_{S1}^2} \right) U_S, & a_{22} &= \left(1 + \frac{q^2}{\alpha_{S1}^2} \right) (c_r - U_M) + v_{R1} + i \left(v_{F1} + \frac{q^2}{\alpha_{S1}^2} v_{H1} \right) \\
b_1 &= -\alpha_y \frac{\alpha_S^2 - (2\alpha_y)^2}{\alpha_{S1}^2} C_S, & b_2 &= -\alpha_y \frac{\alpha_S^2 - (2\alpha_y)^2 - q^2}{\alpha_{S1}^2} \quad (4.80)
\end{aligned}$$

It may be noted here that our premise requires that B , A_{M1} and A_{S1} should be at most of the order $c_i^{3/2}$.

4.6 NUMERICAL RESULTS

The model atmosphere on which the numerical calculations are made is characterized by the following set of fixed values of parameters:

$$\begin{aligned}
L &= 30 \times 10^3 \text{ km}, & W &= 5 \times 10^3 \text{ km} \\
q^2 &= 4 \times 10^{-12} \text{ m}^{-2}, & \beta &= 1.6 \times 10^{-11} \text{ m}^{-1} \text{ sec}^{-1}
\end{aligned}$$

It represents a middle-latitude belt which has a width one half the distance between the equator and pole and a static stability $\sigma = 2 \times 10^{-6} \text{ kg}^{-2} \text{ m}^4 \text{ sec}^2$, which is characteristic of the mid-troposphere. The value of the horizontal eddy diffusivity for heat K_T is assumed to be the same as that for kinetic energy K_v and chosen as $k \times 10^5 \text{ m}^2 \text{ sec}^{-1}$, with $k = 0.5, 1$ and 2 (Phillips (1956)). The value of the coefficient of diabatic heating H used in this study is $4 \times 10^{-7} \text{ sec}^{-1}$ (Wiin-Nielsen, et al. (1967)).

The nondimensionalization of the dynamic equations (4.6) and (4.7) is carried out with the set of characteristic values consisting of $L_0 = 1000$ km for length, $V_0 = 10$ m sec⁻¹ for speed, and $T_0 = L_0/V_0 = 10^5$ sec for time. It may be noted that, with such a choice of the characteristic motion, therefore, when we speak of such a relation as $|A_M|^2 \sim c_i$, for instance, it is understood that A_M is expressed in the unit of 10^7 m² sec⁻¹ and c_i in the unit of 10 m sec⁻¹.

The numerical values of various variables which pertain to the exposition presented in the preceding sections will be given in the following; first, for the case where eddy diffusion is the only dissipative mechanism and, second, for the case where diabatic heating joins eddy diffusion in the dissipative action.

Case A. Eddy diffusion only: Table 12A presents the values of critical wind shear in the unit of m sec⁻¹ for each mode of disturbance characterized by the longitudinal wave number m and the transversal wave number n . The value of critical wind shear in the adiabatic and frictionless model is entered in the row designated by * for the purpose of comparison. It is readily seen from this table that eddy diffusion acts to stabilize the wave disturbances and the stabilizing effect is greater with a larger value of diffusivity. This effect of horizontal eddy diffusion differs on two significant aspects from the corresponding effect of skin friction. In the latter the values of critical wind shear have been found to be smaller than those in the

TABLE 12

CRITICAL WIND SHEAR (m sec^{-1})

n,k	m									
	1	2	3	4	5	6	7	8	9	
A. Eddy Diffusion Only										
	*	18.35	14.17	10.34	7.59	5.78	4.66	4.07	4.17	12.59
	1/2	18.35	14.17	10.34	7.59	5.78	4.66	4.08	4.18	12.66
1	1	18.35	14.17	10.34	7.59	5.78	4.67	4.09	4.20	12.85
	2	18.35	14.17	10.34	7.59	5.80	4.69	4.14	4.32	13.61
	*	5.39	5.07	4.66	4.27	4.02	4.13	5.93		
	1/2	5.43	5.08	4.67	4.28	4.03	4.14	5.96		
2	1	5.52	5.12	4.69	4.30	4.06	4.19	6.08		
	2	5.90	5.25	4.78	4.39	4.18	4.38	6.52		
	*	5.08	5.93	12.59						
	1/2	6.30	6.38	13.17						
3	1	9.02	7.59	14.79						
	2	15.75	11.19	19.98						
B. Eddy Diffusion and Diabatic Heating										
	*	18.35	14.17	10.34	7.59	5.78	4.66	4.07	4.17	12.59
	1/2	8.33	7.24	6.08	5.10	4.34	3.82	3.57	3.83	11.99
1	1	10.93	9.32	7.60	6.14	5.04	4.28	3.89	4.10	12.73
	2	13.62	11.30	8.88	6.92	5.49	4.56	4.10	4.33	13.78
	*	5.39	5.07	4.66	4.27	4.02	4.13	5.93		
	1/2	4.35	4.07	3.85	3.66	3.58	3.80	5.62		
2	1	5.16	4.68	4.34	4.06	3.91	4.10	6.03		
	2	6.09	5.19	5.19	4.36	4.19	4.42	6.63		
	*	5.08	5.93	12.59						
	1/2	7.25	6.52	13.07						
3	1	10.61	8.28	15.58						
	2	17.69	12.24	21.41						

adiabatic and frictionless model, and, furthermore, independent of the intensity of friction (Wiin-Nielsen, et al. (1967)).

Before proceeding to consider the nonlinear effect on the wave disturbances it should be noticed that the results obtained toward the end of the last section do not hold for a class of wave disturbances whose higher harmonics are more unstable. It is readily recognized in Table 12A that modes (1,1), (1,2), (1,3), (2,1), (2,2), (3,1), (3,2), and (4,1), where the first number refers to the longitudinal and the second to the transversal wave number of the mode, belong to such a class and should, therefore, be excluded from further consideration.

The nature and importance of the first-order effect of the nonlinear interactions on the amplitude of the fundamental disturbance is represented by ϵ_1 which has been defined in the preceding section. A continuous function of wind shear, it is seen in the numerical results to vary much slower than c_1 in the vicinity of the critical stability. The values of ϵ_1 at the critical stability, $(\epsilon_1)_c$, are therefore selected to exhibit differences in the first-order nonlinear effect for different modes of disturbance and different values of eddy diffusivity K_V (Table 13A). The fact that $(\epsilon_1)_c$ is positive in all the cases considered indicates that the eddy heat transfer modifies the parallel shear flow in such a way as to reduce with time the energy transfer from the parallel flow into the fundamental disturbance. It is also observed in Table 13A that $(\epsilon_1)_c$ is inversely proportional to K_V in all modes of disturbance. This apparently reflects the fact that the amplitude of the modification

TABLE 13

VALUE OF $\epsilon_i (10^{-13} \text{ m}^{-3} \text{ sec})$ ON THE CRITICAL STABILITY

(m,n)	k		
	0.5	1	2
A. Eddy Diffusion Only			
(5,1)	26.94	13.47	6.73
(6,1)	30.24	15.12	7.56
(7,1)	28.81	14.40	7.20
(8,1)	23.20	11.60	5.80
(9,1)	14.14	7.07	3.53
(4,2)	12.91	6.46	3.23
(5,2)	17.76	8.88	4.44
(6,2)	21.50	10.75	5.37
(7,2)	23.53	11.77	5.88
(1,3)	4.06	2.03	1.02
(2,3)	8.17	4.08	2.04
(3,3)	12.27	6.13	3.07
B. Eddy Diffusion and Diabatic Heating			
(5,1)	1.3×10^{-2}	5.0×10^{-2}	.23
(6,1)	3.8×10^{-2}	.17	.81
(7,1)	.10	.50	1.74
(8,1)	.22	1.04	2.14
(9,1)	.35	1.23	1.55
(4,2)	.23	.73	1.51
(5,2)	.48	1.52	2.53
(6,2)	1.00	2.92	3.60
(7,2)	2.02	4.77	4.36
(1,3)	2.07	1.46	.86
(2,3)	3.52	2.88	1.73
(3,3)	4.73	4.31	2.62

on the parallel shear flow and its effect, in turn, on the fundamental disturbance is greater, the smaller the eddy diffusivity.

Figure 25 presents the variations of c_i , ϵ_i and the equilibrium amplitudes of the fundamental disturbance in the vicinity of the critical stability within the unstable regime for different values of eddy diffusivity. Each of the three modes, namely, (7,1), (5,2) and (2,3), selected for an exhibition of the general patterns has the smallest critical wind shear for a given transversal wave number, as may be confirmed from Table 12A. The values of μ_S/v_S for these modes are given in Table 14A.

TABLE 14

VALUE OF μ_S/v_S (10 msec^{-1})

(m,n)	k		
	0.5	1	2
A. Eddy Diffusion Only			
(7,1)	7.91×10^{-3}	1.58×10^{-2}	3.16×10^{-2}
(5,2)	3.16×10^{-2}	6.32×10^{-2}	1.26×10^{-1}
(2,3)	7.11×10^{-2}	1.42×10^{-1}	2.84×10^{-1}
B. Eddy Diffusion and Diabatic Heating			
(7,1)	3.66×10^{-2}	4.45×10^{-2}	6.03×10^{-2}
(5,2)	4.71×10^{-2}	7.87×10^{-2}	1.42×10^{-1}
(2,3)	7.99×10^{-2}	1.51×10^{-1}	2.93×10^{-1}

Case B. Eddy diffusion and diabatic heating: When the diabatic heating is included in the model the critical wind shear assumes the values for individual modes of disturbance as shown in Table 12B. The combined effect of the diabatic heating and the eddy diffusion, which

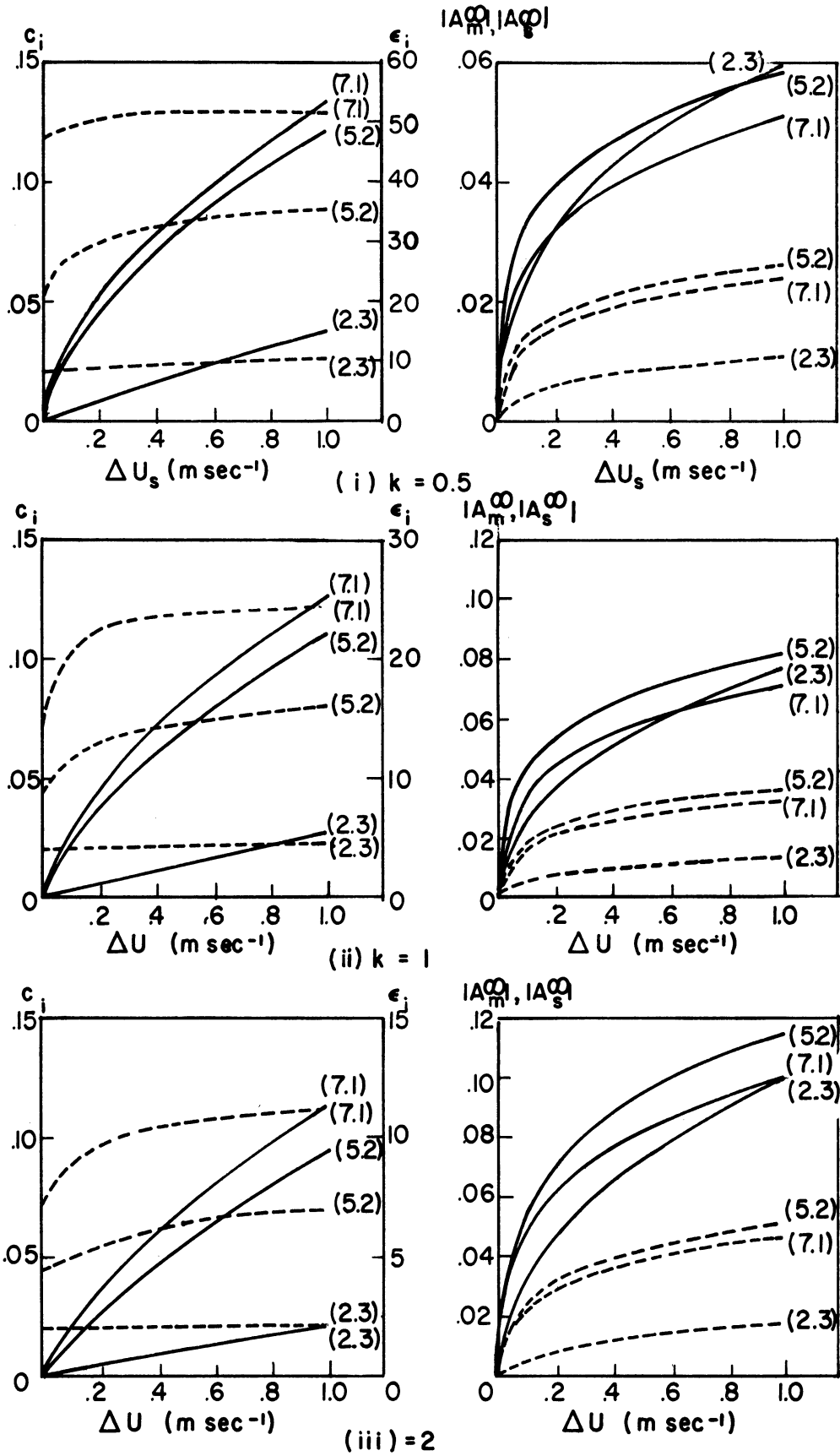


Fig. 25. Variations of c_i , ϵ_i , $|A_M^\infty|$, $|A_S^\infty|$ with $\Delta U_G = U_G - U_{SC}$. $K_V = k \times 10^5 \text{ m}^2 \text{ sec}^{-1}$, $H = 0$. c_i and $|A_M^\infty|$ are represented by solid curves and ϵ_i and $|A_S^\infty|$ by dashed curves.

is to destabilize long waves and stabilize short waves, can be recognized by comparing the corresponding values of critical wind shear between Table 12A and 12B. This is in conformity with the effect diabatic heating brings about when acting alone. The coupling between the eddy diffusion and the diabatic heating is seen in the larger values of critical wind shear for larger values of eddy diffusivity.

As is true in Case A, modes (1,1), (1,2), (1,3), (2,1), (2,2), (3,1), (3,2), and (4,1) are found to have larger values of critical wind shear than their higher harmonics and will therefore be excluded from further consideration.

The values of ϵ_i on the critical stability are presented in Table 13B. They are smaller than their counterparts in Case A and reflect the fact that a reduction in the amplitude of the modification on the parallel shear flow by the inclusion of the diabatic heating reduces the damping effect of the nonlinear term. Furthermore, their variations with eddy diffusivity show no regularity such as the one observed in Case A.

Variations of c_i , ϵ_i , and the equilibrium amplitudes of the fundamental disturbance in the vicinity of the critical stability are shown in Fig. 26 for three modes (7,1), (5,2) and (2,3), each of which is again found to have the smallest critical wind shear for a given transversal wave number. The modes (7,1) and (5,2) for the case of $K_V = .5 \times 10^5 \text{ m}^2 \text{ sec}^{-1}$ are found to yield too great values of the second-order amplitudes for the validity of the approximations and have therefore been omitted. The values of μ_S/ν_S for these modes are given in Table 14B.

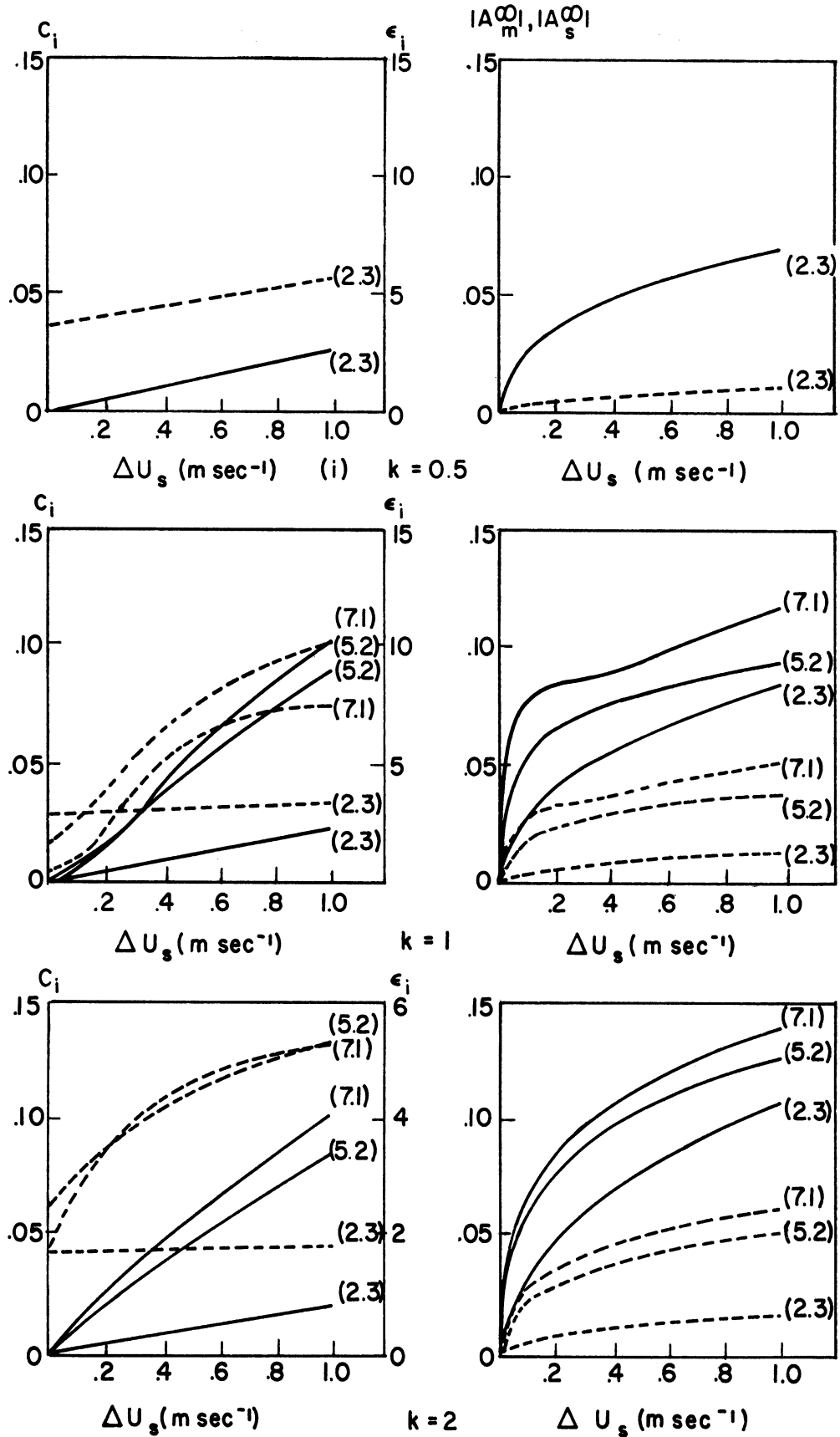


Fig. 26. Variations of c_i , ϵ_i , $|A_M^\infty|$, $|A_S^\infty|$ with $\Delta U_S = U_S - U_{SC}$. $K_V = k \times 10^5 \text{ m}^2 \text{ sec}^{-1}$, $H = 4 \times 10^{-7} \text{ sec}^{-1}$. The symbols are the same as those in Fig. 25.

Figures 25 and 26 show that the values of the equilibrium amplitudes attained by the fundamental disturbance through its interaction with the modification of the parallel shear flow increases with the increase in the value of wind shear (or of the amplification factor c_i) and of the order of 1 m sec^{-1} or less. The phase velocities with which these disturbances travel, c_{re} in Eq. (4.66), have also been computed and found to differ very little from those of the linearized theory.

While the values of the equilibrium amplitudes as shown in Figs. 25 and 26 define the equilibrium state at which the disturbance ultimately arrives, the values of μ_S/v_S given in Table 14 show that a greater portion of the range of ΔU_S covered in these figures, particularly in the modes (7,1) and (5,2), falls into the category in which $v_S c_i \approx \mu_S$, where the variations with time of the amplitudes are also of great interest. Numerical integrations of system (4.68) are therefore carried out for a number of cases using the fourth-order Runge-Kutta method. The results are depicted as trajectories on the $(-A_{SO}, |A_M|^2)$ -plane, shown in Fig. 27. In all of these examples the system is started with the initial value $|A_M|^2 = c_i/4$ which is greater than the equilibrium value. While vindicating the assertions made in connection with the behavior of such a system in the preceding section, these numerical studies show that the time scale in which the system undergoes the evolution is quite large. Although no general statement can be made with regard to the extreme values of the amplitudes, since they depend upon the initial state, it

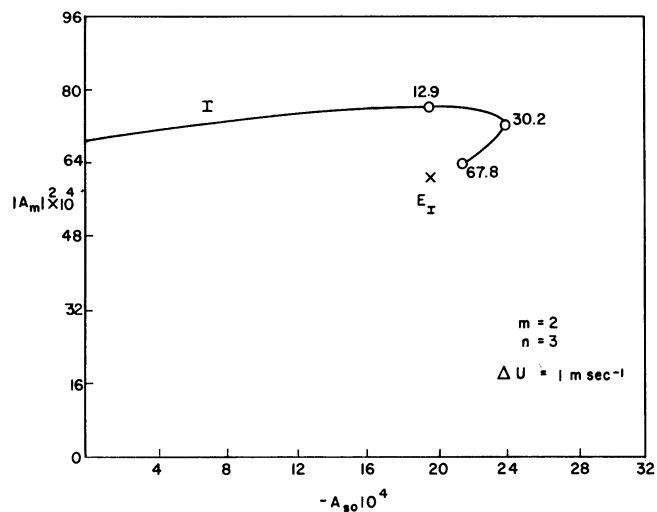
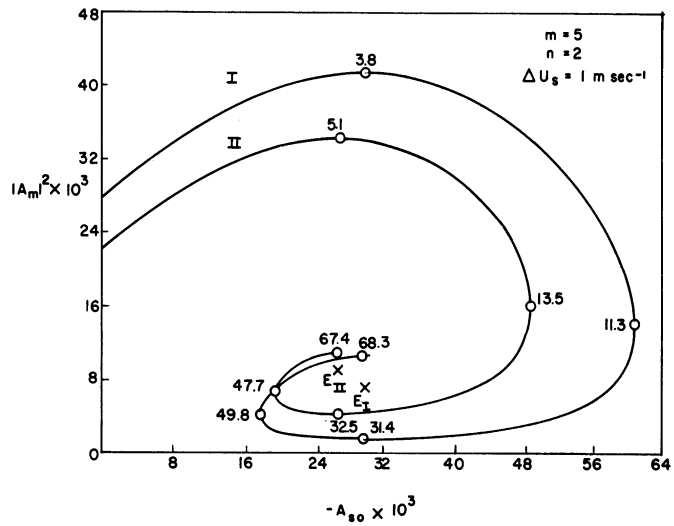
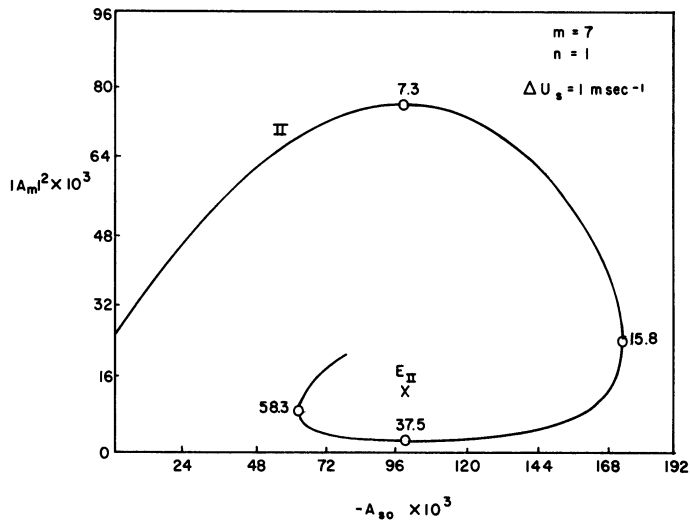


Fig. 27. Initial segments of trajectories in the $(-A_{s0}, |A_M|^2)$ -plane. I: $K_V = 1 \times 10^5 \text{ m}^2 \text{ sec}^{-1}$, $H = 0$, II: $K_V = 1 \times 10^5 \text{ m}^2 \text{ sec}^{-1}$, $H = 4 \times 10^{-7} \text{ sec}^{-1}$. The numbers next to the marked points are the times in days. E_I (or E_{II}) refers to the equilibrium state.

is nevertheless instructive to observe that the values obtained in these examples are well within the realm of the approximations employed in the present study and amount at most to several times of the equilibrium values.

5. CONCLUDING REMARKS

5.1 CONJECTURES

By combining the results of the present study, which investigates only the effects of the horizontal inertial transfer on redistribution of the atmospheric energy, with the results obtained by others, there seems to emerge what may be called the "predominant" mode of energy exchange that prevails in the real atmosphere. A qualitative description of such a mode of exchange will be given in the following.

A fraction of the zonal available potential energy which is present in the atmosphere as the result of the temperature contrast between the equator and the pole is converted largely in the troposphere into the eddy available potential energy through the eddy heat transport down the meridional temperature gradient. The distribution of this conversion on the scale of motion is such that the longer waves receive more from the zonal mean. A large part of the available potential energy entering the individual wave components is then converted into the form of kinetic energy in the same component through the vertical motion, while a small fraction of the energy received by the longer waves is redistributed in the shorter waves through the horizontal inertial transfer. The conversion from the eddy available potential into eddy kinetic energy is most intense in the troposphere and in those waves with wave numbers 2 and 4 to 10. The result of the decomposition of the exchanges in the time domains suggests that the conversion in the wave number 2 is ac-

completed mainly by the quasi-stationary wave in the scale of major continents and oceans whereas those in the wave numbers 4 to 10 are effected by the travelling cyclone waves.

A part of the kinetic energy thus converted in these waves in the troposphere is transferred to other components through the horizontal inertial transfer, but a greater portion finds its way to a higher level where development of the cyclone waves by baroclinic instability is more favorable. Nitta (1967) showed recently with a numerical experiment that this redistribution of the eddy kinetic energy is largely carried out by the convergence of the vertical flux of geopotential, while there have been indications that the vertical transport of the eddy kinetic energy itself is of a smaller consequence (Muench (1965) and Oort (1964)). Thus, the ageostrophic component of the motion plays two important roles, one being the conversion of available potential energy into kinetic energy and the other being the redistribution of kinetic energy.

As the cyclone waves grow in amplitude at the jet-stream level, their kinetic energies are then redistributed to other scales of motion through the horizontal inertial transfer. This horizontal inertial transfer of kinetic energy from the eddies into the zonal westerlies is augmented by the influx from the tropics to sustain the upper westerlies through most of the year.

On the other hand, in the lower troposphere the flux of available potential energy from the tropics helps in replenishing the zonal avail-

able potential energy which is steadily depleted through conversion into the eddy available potential energy. However, it is obvious from a comparison of the magnitudes of the conversion and the influx that a greater amount of available potential energy is created by radiation in the region.

A schematic diagram of the exchanges represented by the predominant mode described above is presented in Fig. 28, in which the energy spectra and the conversions between the available potential energies and kinetic energies are based on the studies by Wiin-Nielsen (1959,1967).

There are large fluctuations in the magnitudes of the exchanges and influxes during a year, but the predominant mode of exchange as described above persists through most of the year. The exchanges and fluxes are in general greater in winter than in summer and deviations from the predominant mode in the exchange pattern occur mainly during the summer months.

5.2 JUSTIFICATIONS

While the energetics study shows the importance of the nonlinear interactions in redistributing energy among different scales of motion in the atmosphere, the study of the effects of the nonlinear interaction on baroclinic stability illustrates the significance of such redistribution in preventing or controlling the growth of an unstable wave disturbance.

The analysis shows that the disturbance grows in amplitude by converting the energy of the parallel shear flow, that is, through a trans-

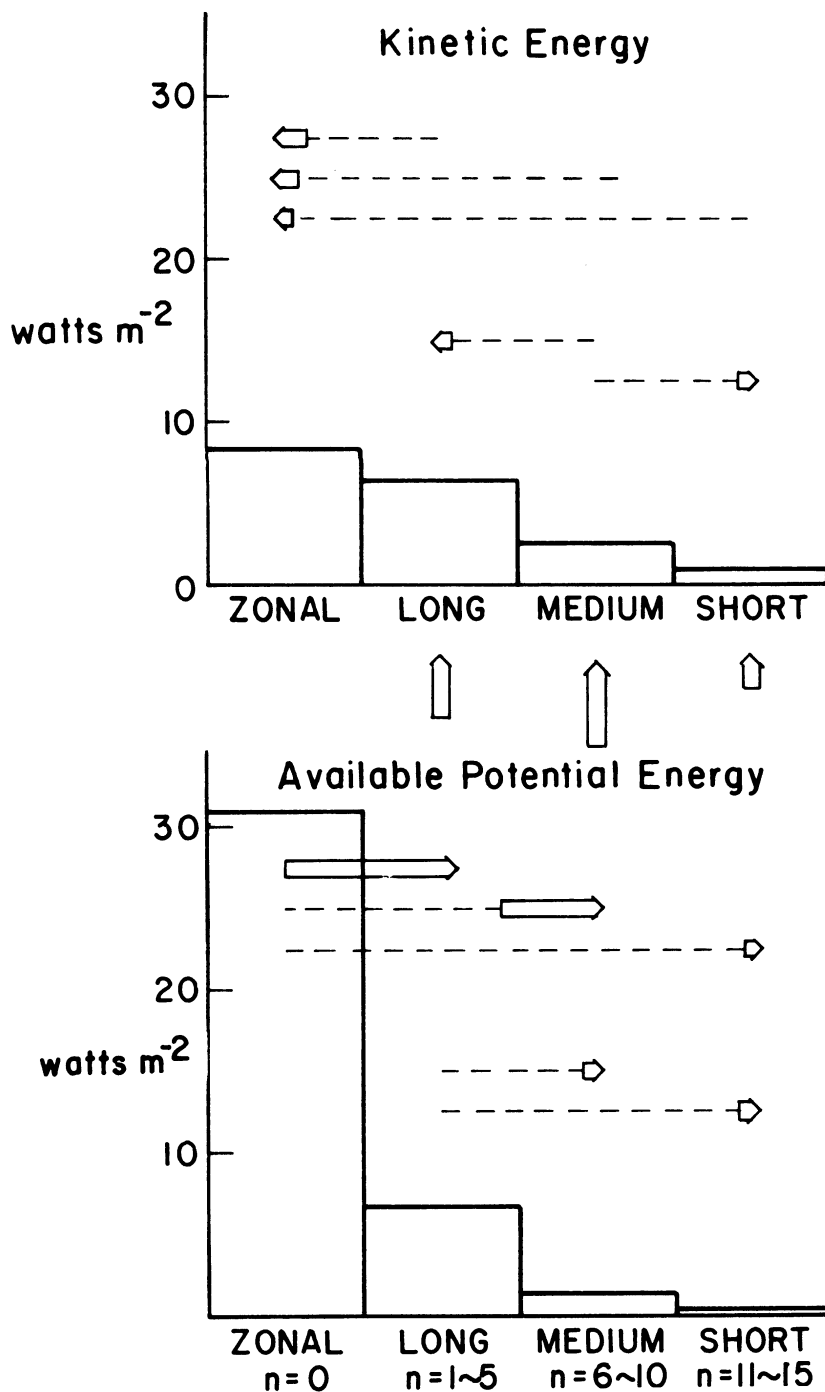


Fig. 28. A schematic diagram of the distributions of energy and energy exchanges in the atmosphere. The ordinate is energy in the unit of watt m⁻². The lengths of the arrows represent approximately the amounts of the exchanges. n is the wave number.

fer of available potential energy from the basic flow, and with its growth produces an eddy heat transport which is distributed in such a way as to modify the basic shear flow and check the energy conversion between the basic flow and the disturbance.

As crude as the model is and as rudimentary as the analysis is, the study does nevertheless point out the manner in which the nonlinear processes proceed in the course of development and their effectiveness in restraining the disturbances from becoming pathological cases.

It is also observed that the innumerable possibilities for the nonlinear interactions inherently present in the real atmosphere tend to favor the growth of baroclinic waves, if there is no external forcing imposed upon the system, precisely in the scale where the degree of instability as found by the linearized theory is greatest.

5.3 OPPORTUNITIES

Needless to say, omissions and simplifications have, of necessity, been made for the sake of economy and expediency. Among these are (i) in the study of energetics, the omission of calculation of the conversion from available potential to kinetic energy and of the vertical transfer of energies between the layers and (ii) in the study of stability, the incorporation of what Charney (1959) called "obscure and unphysical Austausch hypotheses" in the horizontal plane for the frictional mechanism.

Since most of our knowledge of the atmospheric energetics has been derived from many individuals' studies on various aspects using different data series, it would be desirable to carry out a study which takes into account all the conceivable transfer processes in a consistent manner. Though such a study may be laborious, the computing facilities presently available can certainly provide all the necessary tools. Such a study when carried out both in the real atmosphere and in the numerical experiments of the general circulation would be of a value in furthering our understanding of the atmosphere.

In the study of baroclinic stability an immediate step to improve the model can be taken by replacing the horizontal eddy diffusion by the vertical diffusion. This may increase the mathematical complexity of the problem, but the use of numerical methods might reveal important processes in the atmosphere.

BIBLIOGRAPHY

- Charney, J. G., 1960: Integration of the Primitive and Balance Equations. Proceedings of the International Symposium on Numerical Weather Prediction in Tokyo, 131-151.
- Charney, J. G., 1959: On the General Circulation of the Atmosphere. The Atmosphere and the Sea in Motion, 178-193, B. Bolin ed., The Rockefeller Institute Press.
- Coddington, E. A. and N. Levinson, 1955: Theory of Ordinary Differential Equations, McGraw-Hill, New York.
- Crutcher, H. L., 1959: Upper Wind Statistics Charts of the Northern Hemisphere. Issued by the Office of the Chief of Naval Operations.
- Fjørtoft, R., 1953: On the Changes in the Spectral Distribution of Kinetic Energy for the Two-Dimensional, Non-Divergent Flow, Tellus, 5, 225-230.
- Gates, W. L., 1960: Static Stability Measures in the Atmosphere. Scientific Report No. 3, Dynamical Weather Prediction Project, Dept. of Meteorology UCLA (AFCRL-TN-60-817).
- Goldie, N., J. G. Moore, and E. E. Austin, 1957: Upper Air Temperature Over the World. Geophysical Memoirs, No. 101.
- Haltiner, G. J. and D. E. Caverly, 1965: The Influence of Friction on the Growth and Structure of Baroclinic Waves. Quart. J. Roy. Meteor. Soc., 91, 209-214.
- Holopainen, E. O., 1961: On the Effects of Friction in Baroclinic Waves. Tellus, 13, 363-367.
- Krueger, A. F., J. S. Winston, and D. A. Haines, 1965: Computation of Atmospheric Energy and its Transformation for the Northern Hemisphere for a Recent Five-Year Period. Mon. Wea. Rev., 93, 227-238.
- London, J., 1957: A Study of the Atmospheric Heat Balance. Final Report (AFCRC-TR-57-287), Department of Meteorology and Oceanography, New York University.
- Lorenz, E. N., 1955: Available Potential Energy and the Maintenance of the General Circulation. Tellus, 7, 157-167.

- Muench, H. S., 1965: On the Dynamics of the Winter-Time Stratospheric Circulation. J. Atm. Sci., 22, 349-360.
- Murakami, T. and K. Tomatsu, 1964: Energy Cycle in the Lower Troposphere. WMO-IUGG Symposium on Research and Development Aspects of Long-Range Forecasting, Boulder Colorado, 295-331.
- Nitta, T., 1967: Dynamical Interaction Between the Lower Stratosphere and the Troposphere. Mon. Wea. Rev., 319-339.
- Oort, A. H., 1964: On Estimates of the Atmosphere Energy Cycle. Mon. Wea. Rev., 92, 483-493.
- Oort, A. H., 1964: On the Energetics of the Mean and Eddy Circulations in the Lower Stratosphere. Tellus, 16, 309-329.
- Phillips, N. A., 1954: Energy Transformations and Meridional Circulations Associated with Simple Baroclinic Waves in a Two-Layer Model. Tellus, 6, 273-286.
- Phillips, N. A., 1956: The General Circulation of the Atmosphere: A Numerical Experiment. Quart. J. Roy. Meteor. Soc., 82, 123-164.
- Saltzman, B., 1957: Equations Governing the Energetics of the Larger Scales of Atmospheric Turbulence in the Domain of Wave Number. J. Meteor., 14, 513-523.
- Saltzman, B. and A. Fleisher, 1960: The Exchange of Kinetic Energy Between Larger Scales of Atmospheric Motion. Tellus, 12, 374-377.
- Saltzman, B. and S. Teweles, 1964: Further Statistics on the Exchange of Kinetic Energy Between Harmonic Components of the Atmospheric Flow. Tellus, 16, 432-435.
- Stuart, J. T., 1960: On the Non-Linear Mechanics of Wave Disturbances in Stable and Unstable Parallel Flows. Part 1. The Basic Behavior in Plane Poiseuille Flow. J. Fl. Mech., 9, 353-370.
- Watson, J., 1960: On the Non-Linear Mechanics of Wave Disturbances in Stable and Unstable Parallel Flows. Part 2. The Development of a Solution for Plane Poiseuille Flow and for Plane Couette Flow. J. Fl. Mech., 9, 371-380.
- Wiin-Nielsen, A., 1959: A Study of Energy Conversion and Meridional Circulation for the Large-Scale Motion in the Atmosphere. Mon. Wea. Rev., 87, 319-332.

Wiin-Nielsen, A., 1964: Some New Observational Studies of Energy and Energy Transformations in the Atmosphere, WMO-IUGG Symposium on Research and Development Aspects of Long-Range Forecasting, Boulder, Colorado, WMO Technical Note 66, 177-202.

Wiin-Nielsen, A., 1967: On the Annual Variation and Spectral Distribution of Atmospheric Energy. Tellus, 19.

Wiin-Nielsen, A., A. Vernekar and C. H. Yang, 1967: On the Development of Baroclinic Waves Influenced by Friction and Heating. To be published in Pure and Applied Geophysics.

APPENDIX A

RELATIONSHIPS BETWEEN COMPLEX AND REAL EXPRESSIONS

RELATIONSHIPS BETWEEN COMPLEX AND REAL EXPRESSIONS

Since

$$F(n) = \frac{1}{2}(F_c(n) - iF_s(n))$$

$$F(-n) = \frac{1}{2}(F_c(n) + iF_s(n))$$

so that

$$\begin{aligned} F(n)G(-n) &= \frac{1}{4}(F_c(n) - iF_s(n))(G_c(n) + iG_s(n)) \\ &= \frac{1}{4}[(F_c(n)G_c(n) + F_s(n)G_s(n)) + i(F_c(n)G_s(n) \\ &\qquad\qquad\qquad - F_s(n)G_c(n))] \end{aligned}$$

$$\begin{aligned} F(-n)G(n) &= \frac{1}{4}(F_c(n) + iF_s(n))(G_c(n) - iG_s(n)) \\ &= \frac{1}{4}[(F_c(n)G_c(n) + F_s(n)G_s(n)) - i(F_c(n)G_s(n) \\ &\qquad\qquad\qquad - F_s(n)G_c(n))] \end{aligned}$$

and

$$F(n)G(-n) + F(-n)G(n) = \frac{1}{2}[F_c(n)G_c(n) + F_s(n)G_s(n)]$$

$$\text{or, } \Phi_{fg}(n) = \frac{1}{2}[F_c(n)G_c(n) + F_s(n)G_s(n)] \quad \dots(1)$$

$$F(n-m)G(-n)+F(-n-m)G(n)$$

$$\begin{aligned} &= \frac{1}{4}[(F_c(n-m)-iF_s(n-m))(G_c(n)+iG_s(n)) \\ &\quad + (F_c(n+m)+iF_s(n+m))(G_c(n)-iG_s(n))] \\ &= \frac{1}{4}[(F_c(n+m)+F_c(n-m))G_c(n)+(F_s(n+m)+F_s(n-m))G_s(n)] \\ &\quad + \frac{i}{4}[(F_s(n+m)-F_s(n-m))G_c(n)-(F_s(n+m)-F_s(n-m))G_s(n)] \end{aligned}$$

Hence $\Psi_{fg}(n,m)$

$$\begin{aligned} &= \frac{1}{4}[(F_c(n+m)+F_c(n-m))G_c(n)+(F_s(n+m)+F_s(n-m))G_s(n) \\ &\quad + i(F_s(n+m)-F_s(n-m))G_c(n)-(F_s(n+m)-F_s(n-m))G_s(n)] \\ &\hspace{20em} \dots(2) \end{aligned}$$

Consider

$$\begin{aligned} \sum_{\substack{m=-\infty \\ m \neq 0}}^{\infty} R(m) \Psi_{pq}(m,n) &= \sum_{\substack{m=-\infty \\ m \neq 0}}^{\infty} R(m) [P(n-m)Q(-n)+P(-n-m)Q(n)] \\ &= \sum_{m=1}^{\infty} R(m) [P(n-m)Q(-n)+P(-n-m)Q(n)] \\ &\quad + \sum_{m=1}^{\infty} R(-m) [P(n+m)Q(-n) \\ &\hspace{10em} + P(-n+m)Q(n)] \end{aligned}$$

Making use of the fact that

$$F(-m) = F^*(m)$$

$$\begin{aligned}
AB^* + A^*B &= \frac{1}{4}[(A_C - iA_S)(B_C + iB_S) + (A_C + iA_S)(B_C - iB_S)] \\
&= \frac{1}{4}[(A_C B_C + A_S B_S) + i(A_C B_S - A_S B_C) \\
&\quad + (A_C B_C + A_S B_S) - i(A_C B_S - A_S B_C)] \\
&= \frac{1}{2}(A_C B_C + A_S B_S)
\end{aligned}$$

Now if $A = EF$, where E, F are complex, such that

$$E = \frac{1}{2}(E_C - iE_S), \quad F = \frac{1}{2}(F_C - iF_S)$$

$$A = \frac{1}{2}(A_C - iA_S) = \frac{1}{4}[(E_C F_C - E_S F_S) - i(E_C F_S + E_S F_C)]$$

so that

$$A_C = \frac{1}{2}(E_C F_C - E_S F_S)$$

$$A_S = \frac{1}{2}(E_C F_S + E_S F_C)$$

and

$$(EF)B^* + (EF)^*B = \frac{1}{4}[(E_C F_C - E_S F_S)B_C + (E_C F_S + E_S F_C)B_S]$$

Hence

$$\begin{aligned}
&R(m)Q(n)P^*(n+m) + (R(m)Q(n))^*P(n+m) \\
&= \frac{1}{4}[(R_C(m)Q_C(n) - R_S(m)Q_S(n))P_C(n+m) \\
&\quad + (R_C(m)Q_S(n) + R_S(m)Q_C(n))P_S(n+m)]
\end{aligned}$$

$$\begin{aligned}
&= \frac{1}{4} [Q_C(n) \{R_C(m)P_C(n+m) + R_S(m)P_S(n+m)\} \\
&\quad + Q_S(n) \{R_C(m)P_S(n+m) - R_S(m)P_C(n+m)\}] \quad \dots (3)
\end{aligned}$$

For the second summation, divide the range of m into

$m \leq n-1$, $m = n$, $m \geq n+1$, and write

$$\begin{aligned}
&\sum_{m=1}^{\infty} [R(m)P(n-m)Q^*(n) + (R(m)P(n-m))^*Q(n)] \\
&= \sum_{m=1}^{n-1} [R(m)P(n-m)Q^*(n) + (R(m)P(n-m))^*Q(n)] \\
&\quad + \sum_{m=n+1}^{\infty} [R(m)P^*(m-n)Q^*(n) + R^*(m)P(m-n)Q(n)] \\
&\quad + (R(n)P(o)Q^*(n) + R^*(n)P(o)Q(n)) \\
&= \sum_{m=1}^{n-1} [(R(m)P(n-m))Q^*(n) + (R(m)P(n-m))^*Q(n)] \\
&\quad + \sum_{m=n+1}^{\infty} [(P(m-n)Q(n))R^*(m) + (P(m-n)Q(n))^*R(m)] \\
&\quad + P(o)(R(n)Q^*(n) + R^*(n)Q(n))
\end{aligned}$$

and following the same procedures as before

$$\begin{aligned}
&= \frac{1}{4} \sum_{m=1}^{n-1} [(R_C(m)P_C(n-m) - R_S(m)P_S(n-m))Q_C(n) \\
&\quad + (R_C(m)P_S(n-m) + R_S(m)P_C(n-m))Q_S(n)] \\
&\quad + \frac{1}{4} \sum_{m=n+1}^{\infty} [(P_C(m-n)Q_C(n) - P_S(m-n)Q_S(n))R_C(m)
\end{aligned}$$

$$\begin{aligned}
& + (P_c(m-n)Q_s(n) + P_s(m-n)Q_c(n))R_s(m) \\
& + \frac{1}{2}P(o)(R(n)Q^*(n) + R^*(n)Q(n))
\end{aligned}$$

so that

$$\begin{aligned}
& \sum_{m=1}^{\infty} [R(m)P(n-m)Q^*(n) + (R(m)P(n-m))^*Q(n)] \\
& = \frac{1}{4} \sum_{m=1}^{n-1} [Q_c(n) \{R_c(m)P_c(n-m) - R_s(m)P_s(n-m)\} \\
& \quad + Q_s(n) \{R_c(m)P_s(n-m) + R_s(m)P_c(n-m)\}] \\
& + \frac{1}{4} \sum_{m=n+1}^{\infty} [Q_c(n) \{R_c(m)P_c(m-n) + R_s(m)P_s(m-n)\} \\
& \quad + Q_s(n) \{R_s(m)P_c(m-n) - R_c(m)P_s(m-n)\}] \\
& + \frac{1}{2}P(o)(R_c(n)Q_c(n) + R_s(n)Q_s(n)) \quad \dots(4)
\end{aligned}$$

Consequently

$$\begin{aligned}
& \sum_{\substack{m=-\infty \\ m \neq 0}}^{\infty} R(m)\Psi_{pq}(m, n) \\
& = \frac{1}{4} Q_c(n) \left[\sum_{m=1}^{\infty} \{R_c(m)P_c(n+m) + R_s(m)P_s(n+m)\} \right. \\
& \quad + \sum_{m=1}^{n-1} \{R_c(m)P_c(n-m) - R_s(m)P_s(n-m)\} \\
& \quad \left. + \sum_{m=n+1}^{\infty} \{R_c(m)P_c(m-n) + R_s(m)P_s(m-n)\} \right. \\
& \quad \left. + 2P(o)R_c(n) \right]
\end{aligned}$$

$$\begin{aligned}
& + \frac{1}{4} Q_S(n) \left[\sum_{m=1}^{\infty} \{ R_C(m) P_S(n+m) - R_S(m) P_C(n+m) \} \right. \\
& \qquad \qquad \qquad + \sum_{m=1}^{n-1} \{ R_C(m) P_S(n-m) + R_S(m) P_C(n-m) \} \\
& \qquad \qquad \qquad + \sum_{m=n+1}^{\infty} \{ R_S(m) P_C(m-n) - R_C(m) P_S(m-n) \} \\
& \qquad \qquad \qquad \left. + 2P(o)R_S(n) \right] \qquad \qquad \qquad \dots(5)
\end{aligned}$$

APPENDIX B

MONTHLY AVERAGES AND STANDARD ERRORS OF EXCHANGES AND INFLUXES

TABLE B1
MONTHLY MEANS AND THEIR STANDARD ERRORS OF $C(K_z, K_H)$

	Wave Number, n															Σ^*	
	1	2	3	4	5	6	7	8	9	10	11	12	13	14	15	15	Σ^*
Feb. 1963	-3.6	-34.8	372.1	123.7	78.3	60.2	1.2	40.6	-54.9	-5.8	33.6	-18.1	-1.0	0.3	-12.0	579.8	
	36.4	43.1	74.2	70.4	63.8	52.3	49.6	30.1	28.5	27.0	13.8	10.5	6.9	5.2	6.1	171.7	
Mar. 1963	-25.1	-254.1	222.8	94.4	27.6	-13.8	-76.4	-19.5	-21.1	-2.8	-0.8	-18.3	4.2	-4.6	3.2	-84.3	
	18.4	46.5	73.4	62.4	34.2	25.7	30.5	27.3	12.7	12.5	11.5	9.6	5.3	4.7	3.2	100.1	
Apr. 1963	-16.6	57.4	-5.1	-55.8	-13.4	-138.3	-69.8	-47.7	-5.5	-23.2	-28.5	-9.9	-0.4	-0.9	-1.2	-473.7	
	28.5	27.1	32.8	34.1	43.2	29.3	23.6	23.5	14.2	13.7	8.5	8.6	5.4	4.1	3.8	112.7	
May 1963	-54.0	-208.6	-17.3	-124.4	-37.7	-45.4	-27.4	-30.1	-5.3	-29.2	-6.5	-7.9	-5.3	0.2	-4.7	-603.6	
	12.3	26.0	21.7	34.6	31.2	23.0	12.1	20.8	11.9	8.8	5.7	4.7	3.3	2.7	1.8	79.3	
June 1963	-105.3	-54.0	-233.3	17.7	-55.7	-94.6	-20.7	-26.7	-64.6	-63.6	-15.1	-16.9	-8.9	-8.7	-9.0	-759.3	
	23.3	23.1	30.5	25.2	33.2	27.7	23.1	17.4	19.8	16.4	8.6	8.7	5.5	4.1	3.9	86.6	
July 1963	-89.1	-139.1	-88.1	-34.7	-53.1	-82.4	-76.9	-49.4	-37.2	-69.4	-36.3	-12.9	-13.2	-7.7	-1.8	-791.2	
	28.7	28.4	32.3	25.3	24.3	25.0	36.3	16.9	14.2	15.4	10.5	6.5	9.1	5.8	3.6	96.9	
Aug. 1963	-1.2	-89.8	-60.3	-28.8	-9.9	-49.7	-28.2	-34.9	-20.5	-36.2	21.1	-2.4	-22.1	2.6	-4.8	-407.1	
	9.7	16.6	32.8	20.4	25.2	22.6	13.8	15.7	13.9	9.8	7.1	4.1	7.6	3.3	3.2	76.1	
Sep. 1963	-172.4	7.7	-69.2	-137.6	4.2	-90.2	-94.5	73.4	-47.6	-46.7	-35.2	-41.4	-16.0	-5.8	-5.4	-823.6	
	26.7	38.7	31.8	36.6	35.4	27.9	39.2	19.0	22.1	16.3	12.0	15.5	8.7	5.6	3.3	103.2	
Oct. 1963	-169.4	-200.3	-22.4	-285.7	-129.4	-17.0	-74.0	-106.7	-35.0	-45.7	-28.0	-23.7	-26.9	-12.9	-0.8	-1177.9	
	17.9	29.6	26.6	48.9	41.4	31.4	24.0	32.1	19.3	13.5	7.3	8.9	6.1	4.4	2.5	126.9	
Nov. 1963	-111.4	-311.6	-6.5	4.6	-198.1	-132.8	-174.2	-34.8	-50.1	-31.1	-21.3	-27.7	-21.6	-5.4	-6.7	-1128.7	
	23.3	55.4	30.4	34.6	51.0	46.0	34.5	24.4	20.7	14.5	9.9	11.5	7.4	5.7	2.7	111.0	
Dec. 1963	-88.2	-259.1	-30.9	-66.9	-33.1	-2.9	-49.4	-75.7	-46.7	-31.4	0.6	-8.4	-2.9	2.0	-1.7	-694.7	
	40.3	73.8	57.5	84.1	109.9	43.2	30.4	41.2	18.5	16.3	12.3	9.0	6.6	5.5	4.9	195.5	
Jan. 1964	-136.1	-194.3	160.6	-32.9	-41.3	-20.0	-88.2	-42.4	4.6	9.3	-8.7	-11.4	2.8	6.6	-3.5	-394.9	
	50.6	58.7	66.6	56.0	37.7	29.4	28.5	23.5	21.0	10.6	18.3	9.4	6.0	7.3	3.4	141.6	
Annual Average	-81.0	-149.6	18.5	-43.9	-38.5	-52.2	-64.9	-41.7	-32.0	-31.3	-13.9	-16.6	-9.3	-2.9	-4.0	-563.3	

*The rate of conversion from the zonal to eddy kinetic energy.

TABLE B2

MONTHLY MEANS AND THEIR STANDARD ERRORS OF $\sum_m C(K_m, K_n)$

	Wave Number, n															cor.*
	1	2	3	4	5	6	7	8	9	10	11	12	13	14	15	
Feb. 1963	393.9	113.2	312.3	-56.4	-446.7	67.6	-41.7	-159.6	-80.9	-84.0	-102.7	5.8	42.2	-23.1	60.1	3.3
	154.2	156.3	146.0	138.9	124.9	108.6	127.2	86.1	90.0	99.9	46.5	52.8	55.4	33.7	36.1	5.5
Mar. 1963	102.8	-342.8	63.2	138.1	110.1	-71.4	-45.3	5.7	65.3	-42.2	-25.4	-88.2	21.4	84.8	23.1	7.9
	188.7	171.6	181.9	140.4	153.5	139.2	120.5	150.7	112.5	58.0	60.4	63.4	53.8	35.4	26.8	8.9
Apr. 1963	260.3	-163.6	-64.9	-110.2	351.8	-289.2	-87.5	52.1	-31.2	-60.3	15.4	0.1	35.1	29.0	63.2	8.7
	135.6	150.7	136.7	98.1	100.5	153.1	141.1	92.9	86.9	97.5	63.9	39.7	42.1	29.2	29.9	8.5
May 1963	177.3	207.6	136.4	91.6	-161.1	-106.1	-174.5	-237.6	-64.5	-79.4	-0.8	-27.1	52.1	113.3	73.1	6.3
	64.9	124.4	72.2	92.6	87.3	80.6	79.7	76.7	74.8	81.4	53.2	37.7	28.8	25.5	21.1	5.3
June 1963	-168.5	10.8	167.7	-23.3	-235.4	109.1	-72.8	-10.7	21.0	130.6	-84.0	37.8	33.8	46.7	37.1	3.4
	63.9	65.3	69.8	56.0	71.0	85.8	65.8	54.5	49.0	48.3	45.9	43.9	20.0	17.7	16.1	3.2
July 1963	114.2	6.4	38.9	7.8	42.7	-72.4	-74.0	-70.9	-36.2	-65.7	-26.4	12.5	94.7	5.0	23.1	3.3
	55.5	59.9	63.5	52.4	63.9	63.7	71.3	79.2	52.3	55.2	38.4	27.8	26.8	28.4	14.7	4.0
Aug. 1963	6.2	-45.6	21.3	-1.9	154.6	-129.8	-31.0	-59.7	-1.5	-65.2	89.0	38.2	-3.5	-10.3	39.2	0.5
	35.7	44.8	29.7	56.1	50.6	61.9	53.7	32.4	35.7	29.5	42.0	17.2	18.7	19.7	11.1	1.4
Sep. 1963	-50.6	-175.2	96.0	50.4	-117.3	-23.5	33.2	-39.3	-52.8	102.2	14.3	-21.3	90.0	47.8	46.3	8.4
	98.1	103.6	117.5	96.5	100.9	79.5	119.8	107.3	59.0	58.1	54.3	51.0	29.1	23.5	18.0	3.7
Oct. 1963	220.9	-148.7	-180.8	102.4	-59.8	-76.5	-334.1	70.2	83.2	-26.6	10.2	115.7	41.0	110.3	72.5	-9.3
	108.6	108.6	117.3	128.0	146.5	122.8	104.7	111.6	78.2	51.1	56.8	61.1	28.6	41.2	26.3	8.1
Nov. 1963	294.5	-201.5	66.9	-60.1	20.6	18.6	-194.2	-55.6	-41.8	34.0	-37.3	25.7	43.8	30.2	56.2	-1.7
	100.6	122.3	133.8	87.5	163.5	142.9	146.4	80.3	98.7	42.8	46.7	53.3	42.0	29.4	28.8	3.5
Dec. 1963	872.2	-206.5	-231.1	-189.4	-45.6	-95.9	-156.9	-57.2	-41.2	107.6	23.2	11.0	-28.7	39.3	-1.0	-9.8
	147.2	176.6	156.3	173.0	201.5	136.8	183.5	142.2	121.2	73.6	58.2	47.0	43.6	45.8	41.3	6.0
Jan. 1964	738.2	-400.9	156.8	154.1	-323.1	-3.5	-132.2	-215.8	-170.7	-20.4	47.4	24.3	56.9	17.9	80.1	-29.1
	167.2	144.7	189.0	204.9	153.4	112.8	153.0	155.0	123.9	85.8	67.2	61.6	42.0	47.5	38.6	6.1
Annual Average	246.7	-112.2	48.5	8.6	-59.1	-56.1	-109.3	-64.9	-29.3	-5.8	-6.5	11.2	39.9	40.9	47.7	0

* The amount of correction added to $\sum_m C(K_m, K_n)$ in each wave component.

TABLE B3
MONTHLY MEANS AND THEIR STANDARD ERRORS OF $F(K_E)$

	Wave Number, n															$\sum \frac{F}{n}$
	1	2	3	4	5	6	7	8	9	10	11	12	13	14	15	
Feb. 1963	-10.9 47.7	-12.5 43.4	-31.6 29.8	-7.9 22.6	22.4 22.1	-22.6 37.5	-17.8 26.1	21.4 18.5	19.8 18.0	4.2 15.4	0.7 9.7	13.1 12.6	-9.4 12.4	23.4 9.7	17.5 11.5	9.8 158.1
Mar. 1963	-14.0 35.9	-5.7 44.9	-3.8 44.5	-83.2 81.4	63.6 27.0	0.0 46.8	40.7 37.5	49.8 41.9	-8.3 17.6	-9.6 28.5	-10.7 28.8	39.4 19.9	-6.9 13.3	-38.6 16.6	-16.8 16.9	-4.1 282.3
Apr. 1963	-32.6 34.0	51.6 62.1	-33.4 15.8	-12.8 30.8	35.7 39.1	45.3 32.0	72.1 45.7	-5.8 15.9	29.3 26.8	-29.6 12.6	20.5 15.9	17.2 9.5	10.1 9.8	11.1 12.5	-2.1 7.0	176.6 254.4
May 1963	-23.0 16.3	-6.6 27.8	-70.2 15.0	-9.3 20.9	31.8 18.7	-49.9 24.7	14.2 15.2	10.5 14.7	-20.4 15.2	10.7 16.0	-12.3 12.0	14.6 12.1	-15.8 8.8	-22.6 9.4	-5.5 6.7	-153.9 117.2
June 1963	-16.3 22.0	-15.1 14.3	-12.8 18.1	-13.9 12.1	19.0 9.1	-54.6 18.0	39.7 16.1	16.8 13.0	-25.5 13.7	23.4 9.3	8.3 7.8	-9.3 10.0	-11.1 4.6	-6.1 7.0	-16.3 6.6	-73.8 91.4
July 1963	-2.6 19.3	37.6 17.2	37.0 14.3	12.5 8.4	36.3 15.8	15.9 13.5	73.6 26.6	18.3 9.0	19.4 11.4	-8.7 14.8	-17.4 13.8	-0.4 8.3	-32.7 9.6	6.7 13.4	0.3 7.2	195.7 90.1
Aug. 1963	-12.7 14.4	19.6 13.4	22.0 9.1	6.7 4.7	1.9 10.6	0.0 8.3	14.0 8.7	4.6 5.8	-16.5 5.5	2.7 6.9	-6.0 5.5	6.8 6.2	-3.1 4.9	5.1 6.2	7.1 2.7	52.2 36.9
Sep. 1963	53.0 20.7	66.3 15.3	28.9 14.6	55.8 19.4	26.5 14.0	14.1 15.1	50.7 16.3	16.4 13.7	-25.9 14.9	3.4 11.4	2.3 10.1	11.1 15.2	-29.2 9.2	-1.4 8.9	6.4 6.9	278.3 92.7
Oct. 1963	10.5 23.6	-99.2 43.6	29.2 19.6	1.6 17.0	48.7 18.4	-16.9 37.8	-20.9 23.1	-31.1 20.1	-25.2 22.0	-33.2 15.1	0.6 13.6	-24.8 30.9	-27.1 10.0	-14.6 15.4	-10.1 11.1	-212.3 206.0
Nov. 1963	-8.1 19.1	-33.5 28.9	-6.5 18.8	-28.0 17.9	52.9 36.9	-17.4 21.6	41.3 24.5	16.9 13.8	-30.3 16.6	-33.5 14.5	-31.3 9.9	30.5 15.2	-18.5 9.3	-4.1 7.8	-13.2 7.3	-82.9 108.6
Dec. 1963	-151.0 43.5	-156.1 45.0	43.9 34.8	-8.7 60.7	66.3 34.3	-34.5 32.3	-21.3 36.6	5.5 29.4	16.2 27.0	-15.0 14.0	-35.1 21.2	-0.5 15.4	-2.6 9.8	17.8 11.6	-16.0 7.8	-291.3 182.0
Jan. 1964	-87.0 56.2	20.7 45.9	-6.2 46.0	-145.2 54.3	-24.9 39.0	-91.2 35.1	92.5 27.7	-105.1 25.8	-85.3 23.9	-29.2 22.9	-82.3 20.2	-4.1 12.7	-9.4 14.4	-23.3 10.2	20.3 10.2	-785.3 177.2
Annual Average	-24.5	-11.1	-0.3	-19.4	31.7	-17.6	16.1	1.5	-12.7	-9.5	-13.7	7.8	-13.0	-3.9	-5.7	-74.3

* The total influx of the eddy kinetic energy.

TABLE B4

MONTHLY MEANS AND THEIR STANDARD ERRORS OF $C(E_z, E_n)$

	Wave Number, n															Σ_n^*
	1	2	3	4	5	6	7	8	9	10	11	12	13	14	15	
Feb. 1963	1035.9	1500.2	1671.4	554.1	681.5	163.5	406.5	320.3	124.5	160.5	63.4	47.6	44.7	6.3	18.4	6798.8
	171.1	281.7	283.1	159.1	171.1	78.5	84.9	48.5	40.1	52.2	24.2	18.6	16.0	13.7	9.8	357.1
Mar. 1963	165.9	383.6	1040.8	708.8	783.3	486.4	600.7	402.9	126.1	90.9	84.7	41.2	16.9	1.7	0.9	4934.8
	61.7	71.9	193.6	141.2	195.2	112.5	97.1	94.8	44.5	43.6	30.1	19.5	18.5	11.5	9.7	271.2
Apr. 1963	73.9	310.1	357.8	309.7	615.2	813.9	612.5	255.9	114.6	111.6	59.6	23.2	10.1	1.6	3.3	3673.0
	85.0	73.3	55.5	90.3	99.0	164.5	124.6	55.8	33.1	38.4	26.7	15.7	10.6	8.0	5.7	206.9
May 1963	361.7	748.7	230.9	-117.9	291.3	343.5	249.7	197.1	109.1	83.9	27.3	28.2	8.5	-10.4	6.1	2557.7
	38.2	77.8	58.6	49.2	55.4	56.8	43.1	47.7	21.0	12.7	12.0	10.5	7.3	6.5	4.4	171.2
June 1963	-278.5	-318.7	116.4	84.2	255.2	293.6	238.2	86.0	135.2	60.7	29.8	18.3	21.7	-8.0	9.0	743.1
	89.3	95.0	50.4	57.4	51.3	46.1	42.2	26.0	19.9	12.9	10.6	8.4	7.8	8.7	5.4	153.6
July 1963	-480.1	-103.4	-36.8	225.4	130.3	190.1	184.3	77.4	55.4	16.8	-25.3	-15.7	-21.7	-11.9	4.3	189.1
	57.4	71.0	23.9	32.7	35.5	43.7	39.3	25.7	16.0	16.4	13.8	7.6	13.1	8.9	5.5	113.3
Aug. 1963	-294.4	207.1	-42.3	75.3	107.7	183.5	218.1	97.1	5.4	73.0	21.0	41.1	18.3	-7.0	1.8	705.7
	73.8	41.4	30.4	30.5	26.3	37.5	40.3	23.0	18.6	22.5	7.1	9.1	7.1	9.1	6.7	116.0
Sep. 1963	249.1	466.8	166.1	323.4	189.1	75.8	208.3	214.5	54.8	17.1	15.5	34.9	10.0	2.9	-6.3	2022.1
	61.4	34.6	37.1	83.1	56.6	30.5	36.7	47.7	14.4	13.5	12.1	15.0	7.3	5.6	3.7	155.5
Oct. 1963	365.4	168.6	398.9	623.1	442.4	349.3	363.8	245.7	128.4	20.1	42.4	34.2	1.6	-9.9	-7.5	3166.5
	70.6	47.5	67.6	130.6	90.4	52.6	87.4	58.4	31.8	21.1	12.3	11.7	10.4	6.8	4.3	233.1
Nov. 1963	362.1	423.3	348.1	310.4	862.5	756.6	676.8	325.6	169.2	95.4	47.4	4.9	39.3	13.2	-0.5	4434.2
	60.7	75.5	88.5	84.9	195.0	123.3	100.3	58.4	48.1	30.0	19.0	13.4	13.5	14.2	6.8	331.1
Dec. 1963	710.8	992.0	981.6	652.5	1284.8	507.0	382.6	308.1	266.1	23.5	45.0	32.4	27.0	11.5	13.7	6238.5
	102.3	193.8	170.3	203.7	235.6	130.7	109.3	91.6	66.7	27.6	23.6	20.0	12.0	11.3	7.5	380.9
Jan. 1964	942.1	353.3	1563.4	885.4	290.0	579.0	552.4	367.7	221.8	74.6	11.2	43.6	22.8	20.7	11.6	5939.6
	163.9	162.0	129.9	168.1	88.2	120.9	124.7	76.0	54.5	23.7	23.6	15.8	11.5	11.0	11.8	337.0
Annual Average	267.8	427.6	566.4	386.2	494.4	395.2	391.2	241.5	125.9	69.0	35.2	27.8	16.6	0.9	4.6	3450.3

*The rate of conversion from the zonal to eddy available potential energy.

TABLE B5

MONTHLY MEANS AND THEIR STANDARD ERRORS OF $\sum_{m,n} C(E_m, E_n)$

	Wave Number, n															Cor.*
	1	2	3	4	5	6	7	8	9	10	11	12	13	14	15	
Feb. 1963	2.8 101.9	-558.5 92.7	-256.4 107.7	95.8 94.5	77.6 77.7	254.1 66.9	38.3 49.2	56.0 49.7	35.4 37.6	152.8 20.8	28.8 25.0	24.5 15.9	7.5 18.5	27.8 15.0	13.4 12.8	0.1 4.5
Mar. 1963	373.3 93.7	-201.6 122.5	-438.0 115.6	-189.9 70.5	-53.3 94.0	51.9 86.4	36.5 73.4	68.7 65.8	109.6 44.5	52.5 27.9	64.4 24.1	17.6 18.9	42.1 18.7	38.0 15.3	28.0 12.4	1.7 6.4
Apr. 1963	214.1 61.0	-292.8 84.9	36.8 69.1	-121.4 79.8	-58.7 50.3	-43.6 71.2	-120.4 55.3	42.1 54.7	95.7 33.1	82.0 28.0	38.3 19.1	18.6 16.3	39.2 12.6	39.9 11.3	30.1 10.2	7.2 4.2
May 1963	221.8 60.4	-515.4 67.1	52.1 46.9	88.2 42.6	-161.2 32.3	12.9 45.9	-78.4 35.9	90.8 39.5	137.1 27.5	32.4 26.1	46.7 14.8	29.7 14.5	11.2 16.0	16.8 14.6	15.7 6.3	2.0 4.9
June 1963	100.6 61.7	-154.9 89.0	37.5 53.0	83.2 57.3	-12.9 49.6	39.4 57.7	-119.5 50.4	65.7 27.0	142.7 38.1	-9.2 26.4	-44.5 31.1	-15.8 22.4	-61.9 31.5	-30.7 15.9	-19.7 13.4	-3.3 10.1
July 1963	-78.1 72.5	186.7 63.2	37.8 90.3	-18.7 43.0	58.2 66.7	-14.2 72.8	-149.2 79.4	-4.7 46.4	-47.1 41.0	0.3 34.0	-26.8 43.4	25.7 37.5	49.5 35.8	-18.5 31.3	-0.8 25.1	-4.9 25.7
Aug. 1963	30.5 48.5	-271.6 49.9	216.2 62.8	-15.2 39.6	104.9 65.1	-119.1 45.0	-53.0 49.9	62.2 40.4	-44.1 35.3	24.9 31.5	55.3 32.9	-6.2 34.3	13.5 22.7	-4.3 30.5	6.1 17.1	-13.1 12.7
Sep. 1963	65.8 47.9	-439.7 49.4	45.5 40.7	-137.9 47.1	-0.5 58.4	64.6 26.4	47.4 37.3	45.4 32.2	53.8 24.6	51.2 16.8	78.2 17.2	19.0 17.5	39.0 10.1	46.7 9.2	21.5 7.8	12.2 3.8
Oct. 1963	-115.1 88.1	-328.3 78.1	150.9 54.9	10.1 93.4	-56.1 57.6	-56.2 43.3	-12.2 50.1	86.6 37.2	55.9 21.6	55.1 21.0	44.3 17.8	65.3 21.2	31.5 12.5	34.0 7.5	34.2 9.8	9.3 4.0
Nov. 1963	63.5 78.2	-151.2 86.2	-14.9 60.5	78.8 76.9	-198.8 84.9	-138.4 64.7	-27.4 47.0	13.3 23.9	97.7 22.8	45.3 24.3	88.1 15.2	50.3 17.3	19.6 12.2	34.4 12.3	39.7 11.3	5.3 2.2
Dec. 1963	-155.3 96.1	-166.9 83.7	-206.0 98.7	252.6 76.2	-235.2 115.1	-35.4 59.6	120.8 69.0	38.7 33.0	81.2 33.6	143.5 28.6	70.2 23.3	29.8 23.2	24.8 11.2	12.0 11.8	25.1 9.2	9.8 4.4
Jan. 1964	158.1 128.6	-346.2 101.0	-220.1 95.2	-360.8 77.2	21.7 91.4	6.2 71.0	-11.5 57.4	142.5 44.4	203.5 46.1	88.1 31.0	140.2 29.3	26.3 18.8	53.1 13.3	41.4 15.6	57.5 10.8	15.9 3.5
Annual Average	73.5	-270.0	-46.6	-19.6	-42.9	1.9	-27.4	58.9	76.8	59.9	48.6	23.7	22.4	19.8	20.9	0

* The amount of correction added to $\sum_{m,n} C(E_m, E_n)$ in each wave component.

TABLE B6

MONTHLY MEANS AND THEIR STANDARD ERRORS OF $F(E_n)$

	Wave Number, n															$\sum_{n=1}^{15}$
	1	2	3	4	5	6	7	8	9	10	11	12	13	14	15	
Feb. 1963	38.2	6.5	24.8	-46.5	-65.0	-61.8	-32.7	15.0	-28.2	-11.2	-5.8	13.7	1.4	1.6	3.5	-146.5
	93.3	58.1	39.6	27.2	36.6	32.9	31.7	20.5	16.4	8.0	6.8	7.4	5.6	3.5	4.3	123.3
Mar. 1963	-183.6	164.8	-129.8	77.6	15.7	144.1	-35.8	-42.7	-7.7	35.5	-14.1	32.5	-7.1	-3.7	-3.7	42.0
	56.4	75.4	59.5	46.5	39.4	48.4	29.2	27.7	15.0	22.8	14.4	10.6	12.2	5.5	5.9	194.7
Apr. 1963	-30.6	151.2	-44.9	75.1	-17.6	-48.2	43.8	2.0	-4.9	-18.3	-3.3	2.4	5.7	-8.6	-3.6	100.4
	36.8	34.7	37.7	26.7	29.4	14.3	27.2	21.4	18.3	10.8	9.0	7.5	5.9	5.3	4.1	121.0
May 1963	-68.1	21.3	-98.3	9.0	60.6	-56.9	95.1	-37.7	-18.2	9.9	-10.7	1.1	-0.9	8.3	-4.2	-89.8
	52.1	42.9	32.3	27.0	29.3	20.9	23.5	18.5	17.3	16.0	10.2	9.4	7.2	9.6	3.3	153.8
June 1963	-384.5	-146.0	-235.7	-46.1	-127.1	-133.5	-4.2	-67.1	-104.3	5.7	35.0	22.7	41.8	16.5	-6.9	-1133.8
	106.3	60.6	61.5	49.4	48.2	53.1	35.1	22.1	23.7	16.9	18.0	20.0	24.0	13.6	8.0	329.5
July 1963	-394.9	-163.1	-285.0	22.7	-150.7	-125.0	-72.6	-21.7	62.4	16.0	-3.2	-41.9	-72.3	-21.0	-26.2	-1276.6
	193.6	114.5	96.9	69.5	94.8	109.4	78.9	61.9	54.5	44.8	42.1	39.7	31.6	22.3	14.0	873.3
Aug. 1963	41.7	129.4	-263.2	42.9	-155.3	10.9	-23.3	-5.6	88.1	-16.3	-28.8	1.4	5.8	16.8	1.6	-153.9
	119.8	65.3	59.0	35.2	50.2	42.0	41.0	32.6	36.9	23.6	29.2	22.8	13.3	27.5	14.8	383.3
Sep. 1963	102.0	226.5	-18.4	-5.9	-32.3	1.6	1.4	-7.1	23.9	5.8	10.6	3.7	2.3	-2.7	-9.0	302.5
	54.2	30.5	23.1	20.3	18.1	15.4	17.0	14.4	13.8	9.9	12.4	13.2	6.7	4.3	4.5	116.0
Oct. 1963	-42.1	82.5	-163.5	-5.8	35.5	95.3	118.7	-5.7	8.7	-5.4	22.8	-28.2	-2.4	-12.8	-11.0	86.5
	36.4	46.2	26.0	22.5	19.9	21.4	29.0	22.5	13.0	10.9	16.1	13.5	7.7	5.0	6.6	129.2
Nov. 1963	-25.8	107.9	-48.4	33.3	13.1	-26.6	9.9	8.6	-11.8	6.4	-20.2	11.4	10.5	-2.3	-2.7	63.2
	23.8	29.2	19.8	18.3	23.3	16.8	17.9	12.6	11.1	9.1	9.0	7.1	7.3	3.4	2.7	63.0
Dec. 1963	3.0	245.2	-6.1	-97.1	20.0	67.3	-24.6	49.4	-5.8	5.3	-12.4	18.7	-9.6	5.2	-6.1	252.6
	45.5	42.6	42.6	59.2	29.7	27.6	32.3	20.8	12.1	10.9	12.9	10.3	4.3	5.2	2.7	141.7
Jan. 1964	31.6	483.8	-320.4	153.2	78.8	65.2	-20.4	0.0	-7.8	-9.4	-18.1	0.8	0.3	-4.3	-5.6	427.7
	77.5	56.2	42.7	58.2	37.6	21.6	30.9	16.1	14.1	11.9	12.7	8.8	4.5	5.0	4.4	103.4
Annual Average	-76.1	109.2	-132.4	17.7	-27.0	-5.6	4.6	-9.4	-0.5	2.0	-4.0	3.2	-2.0	-0.6	-6.2	-127.1

* The total influx of the eddy available potential energy.

TABLE B7

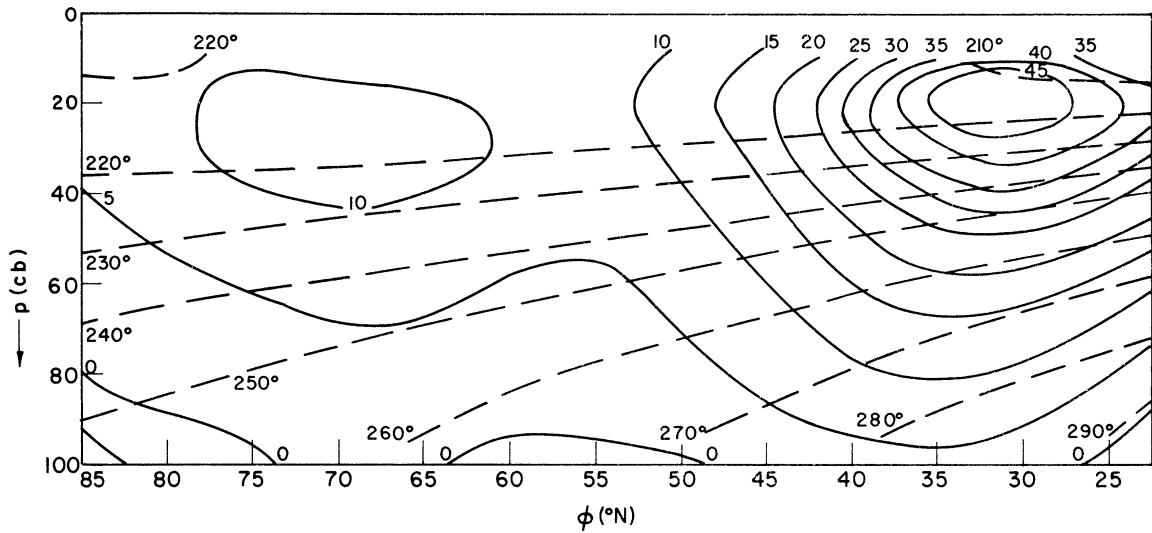
MONTHLY MEANS AND THEIR STANDARD ERRORS OF $F(K_Z)$ AND $F(E_Z)$

	$F(K_Z)$	$F(E_Z)$
Feb. 1963	1228.2 154.1	2053.0 249.6
Mar. 1963	667.3 131.0	450.4 251.3
Apr. 1963	513.6 74.8	752.7 141.9
May 1963	217.5 60.7	431.4 162.3
June 1963	62.2 23.2	-391.2 112.8
July 1963	-44.6 18.2	-387.9 80.4
Aug. 1963	-31.9 13.4	58.8 80.4
Sep. 1963	-15.1 12.9	735.1 110.7
Oct. 1963	87.6 23.7	39.0 101.5
Nov. 1963	584.8 78.9	1070.0 150.2
Dec. 1963	625.0 118.3	1245.0 214.8
Jan. 1964	1288.1 194.1	134.4 348.4
Annual Average	431.9	515.9

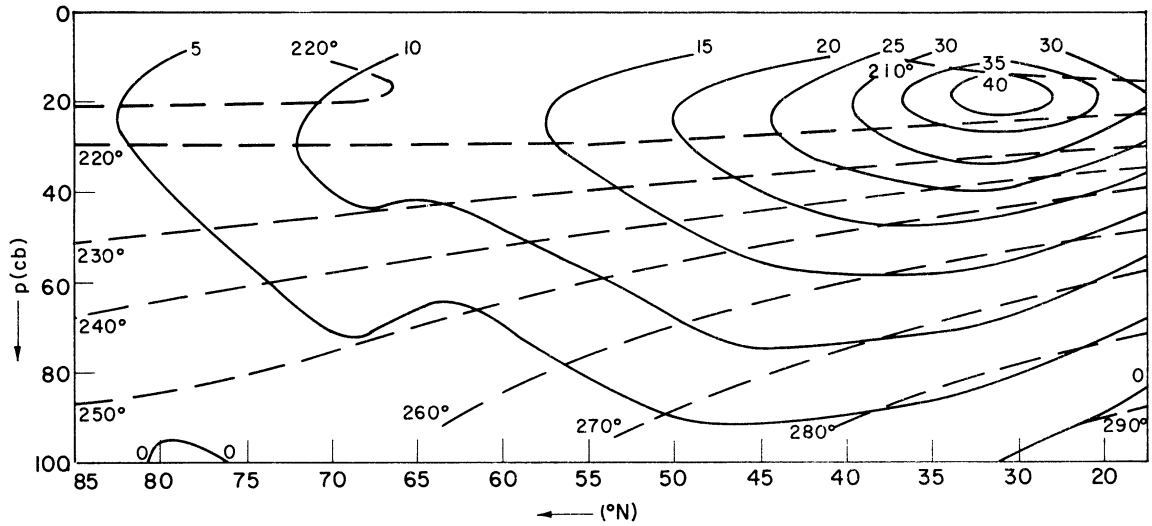
APPENDIX C

MONTHLY MEANS OF ZONAL WIND AND ZONAL TEMPERATURE

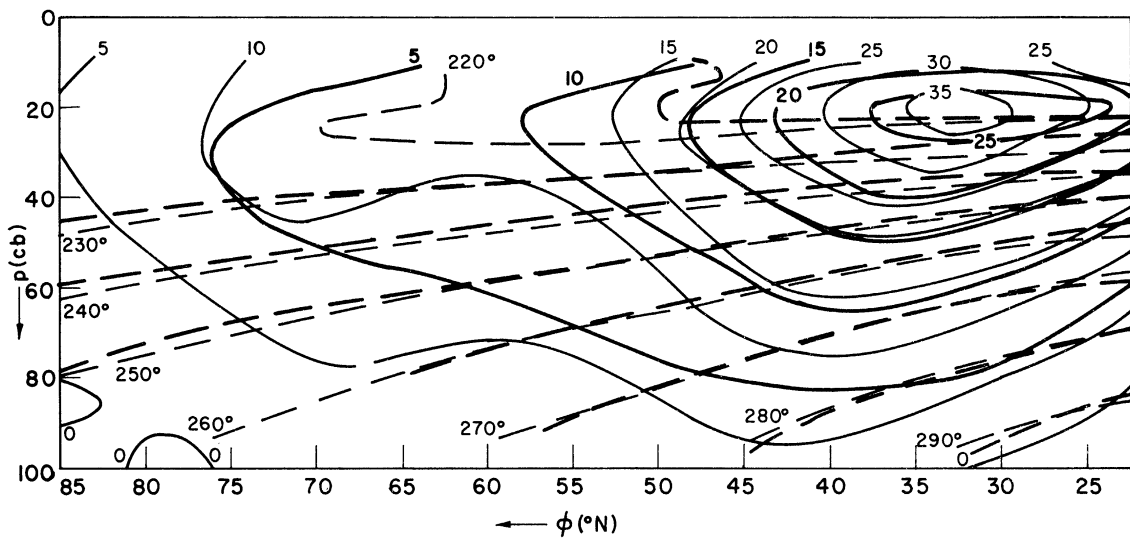
(Thin solid curves are the monthly mean isotachs and the thin dashed curves are the monthly mean isotherms. The corresponding thick curves are the seasonal means.)



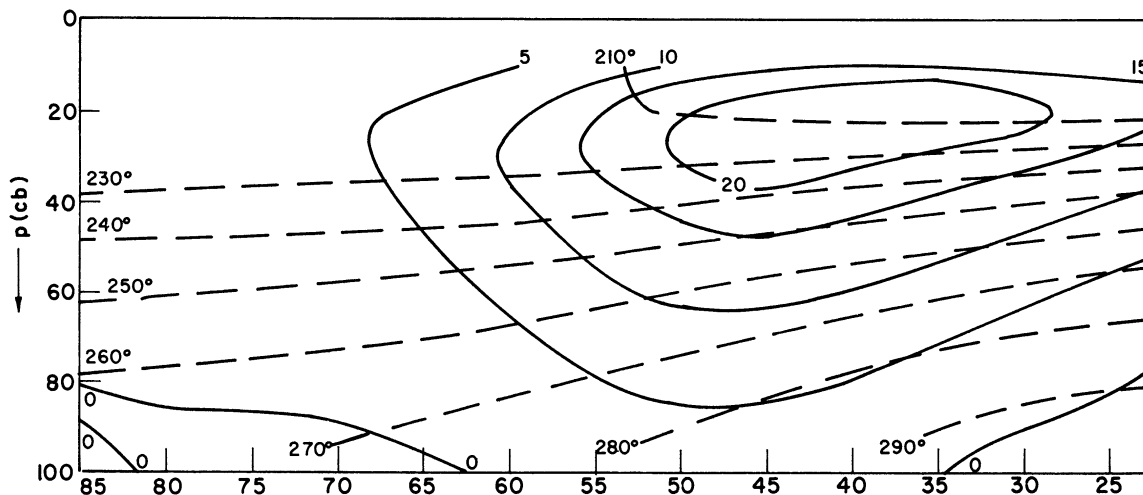
PROFILES OF ZONAL WIND AND ZONAL TEMPERATURE, FEB 1963



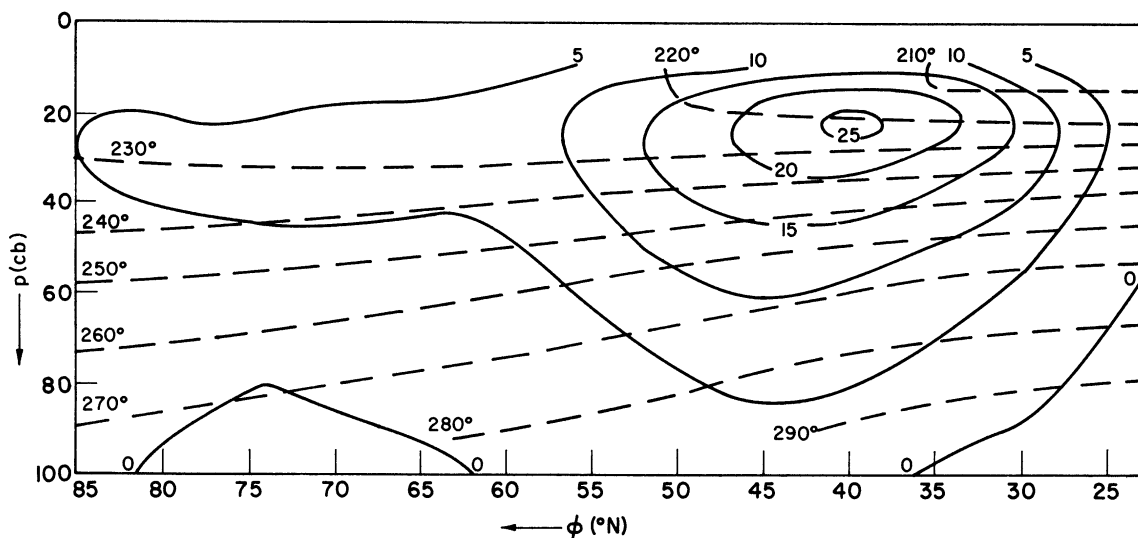
PROFILES OF ZONAL WIND AND ZONAL TEMPERATURE, MAR 1963



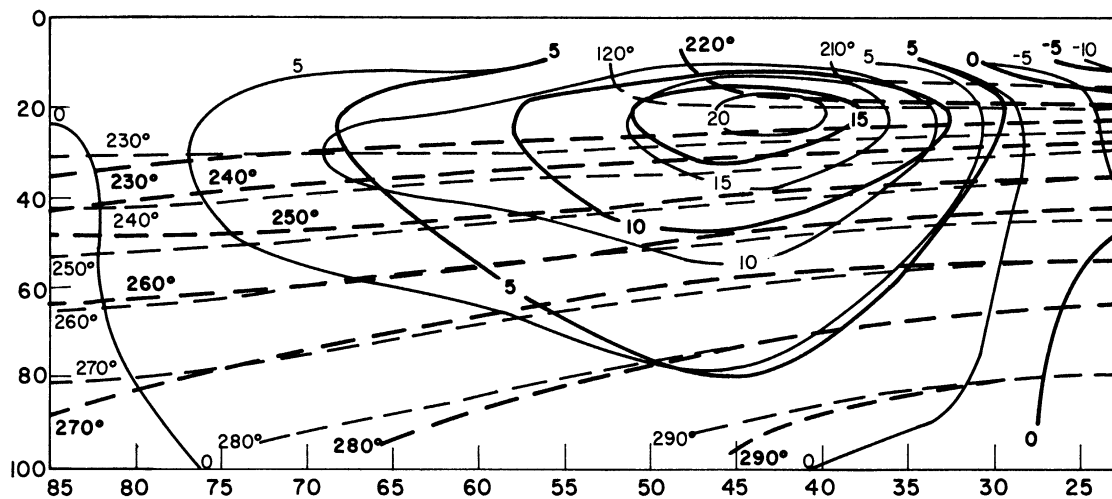
PROFILES OF ZONAL WIND AND ZONAL TEMPERATURE, APR 1963



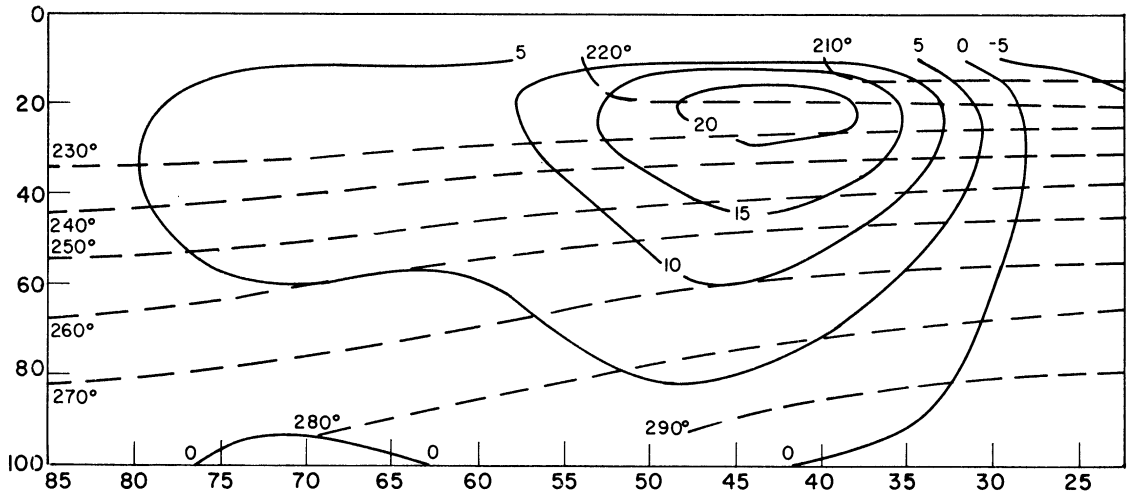
PROFILES OF ZONAL WIND AND ZONAL TEMPERATURE, MAY 1963



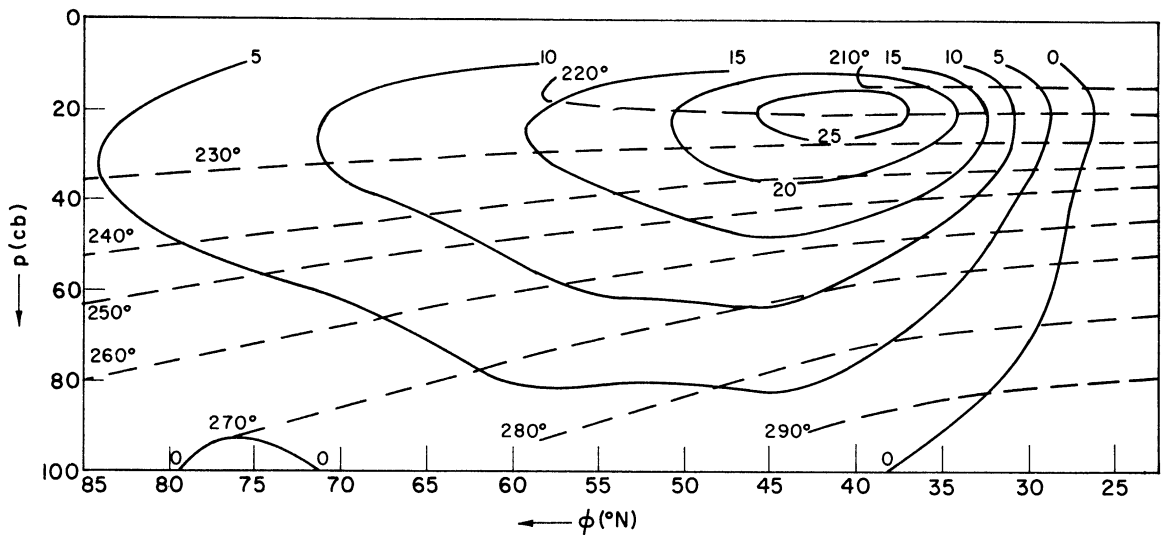
PROFILES OF ZONAL WIND AND ZONAL TEMPERATURE, JUNE 1963



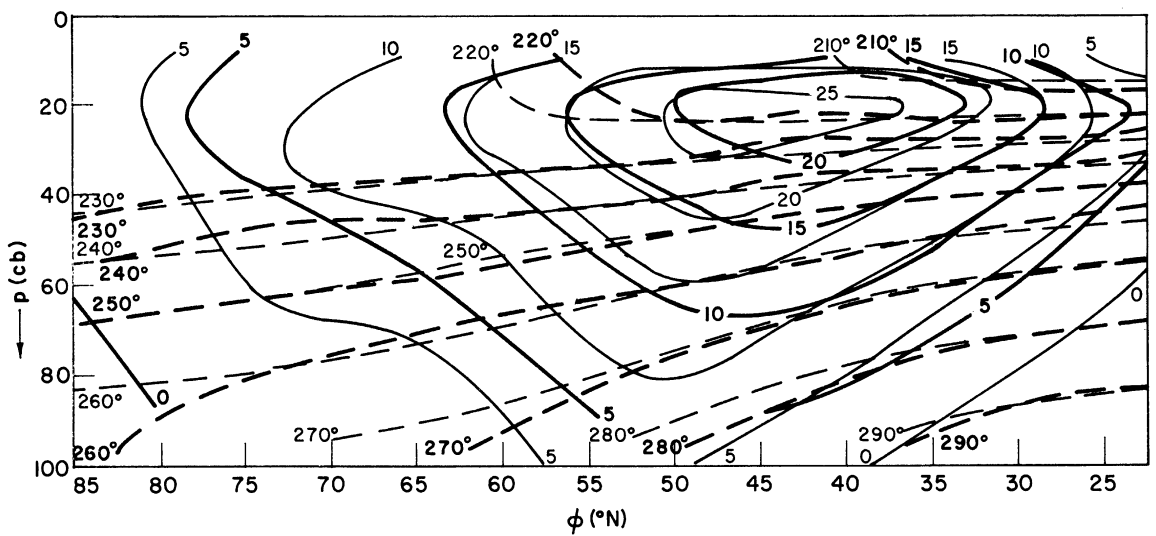
PROFILES OF ZONAL WIND AND ZONAL TEMPERATURE JULY 1963



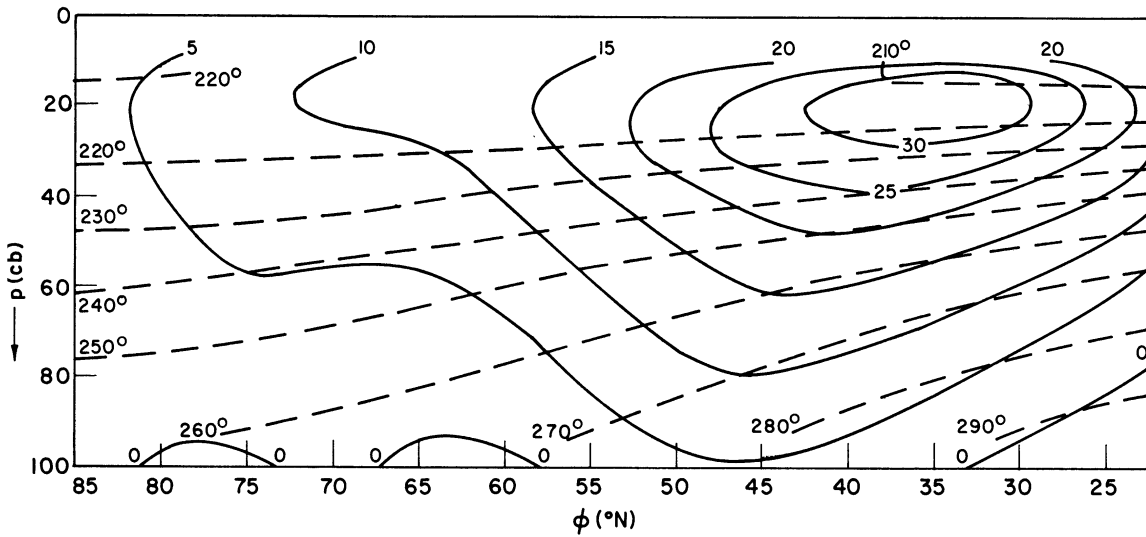
PROFILES OF ZONAL WIND AND ZONAL TEMPERATURE, AUG 1963



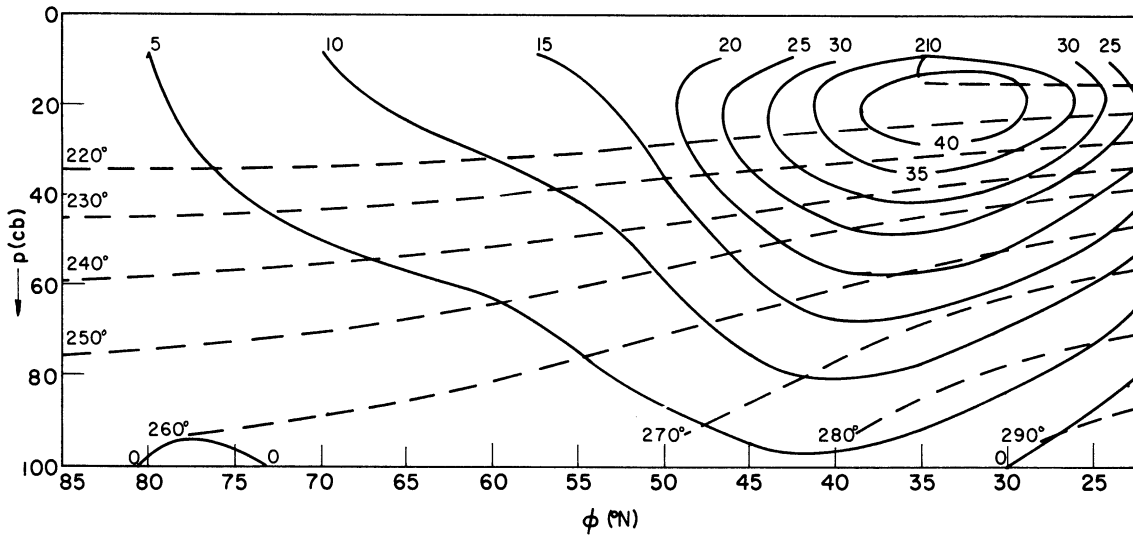
PROFILES OF ZONAL WIND AND ZONAL TEMPERATURE, SEPT 1963



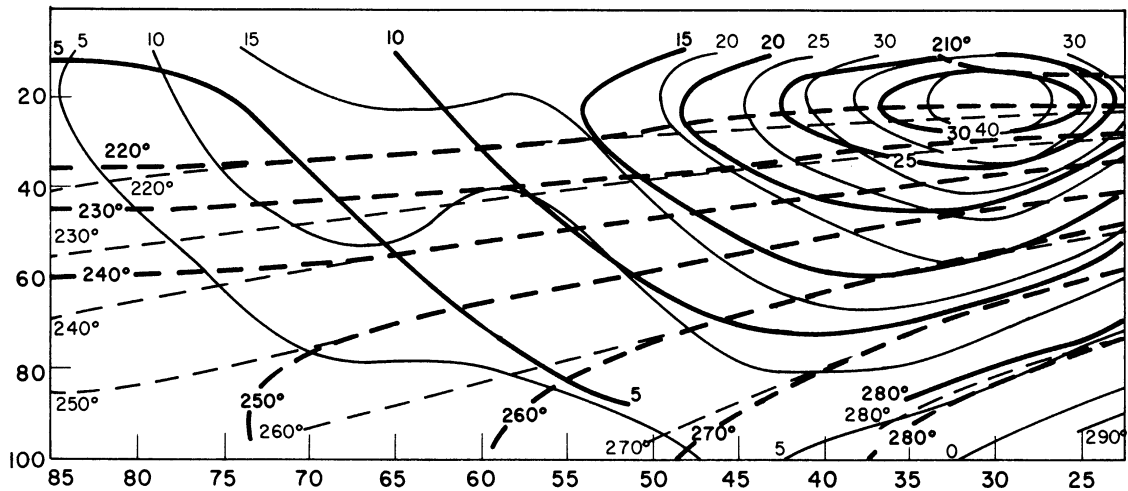
PROFILES OF ZONAL WIND AND ZONAL TEMPERATURE, OCT 1963



PROFILES OF ZONAL WIND AND ZONAL TEMPERATURE, NOV 1963

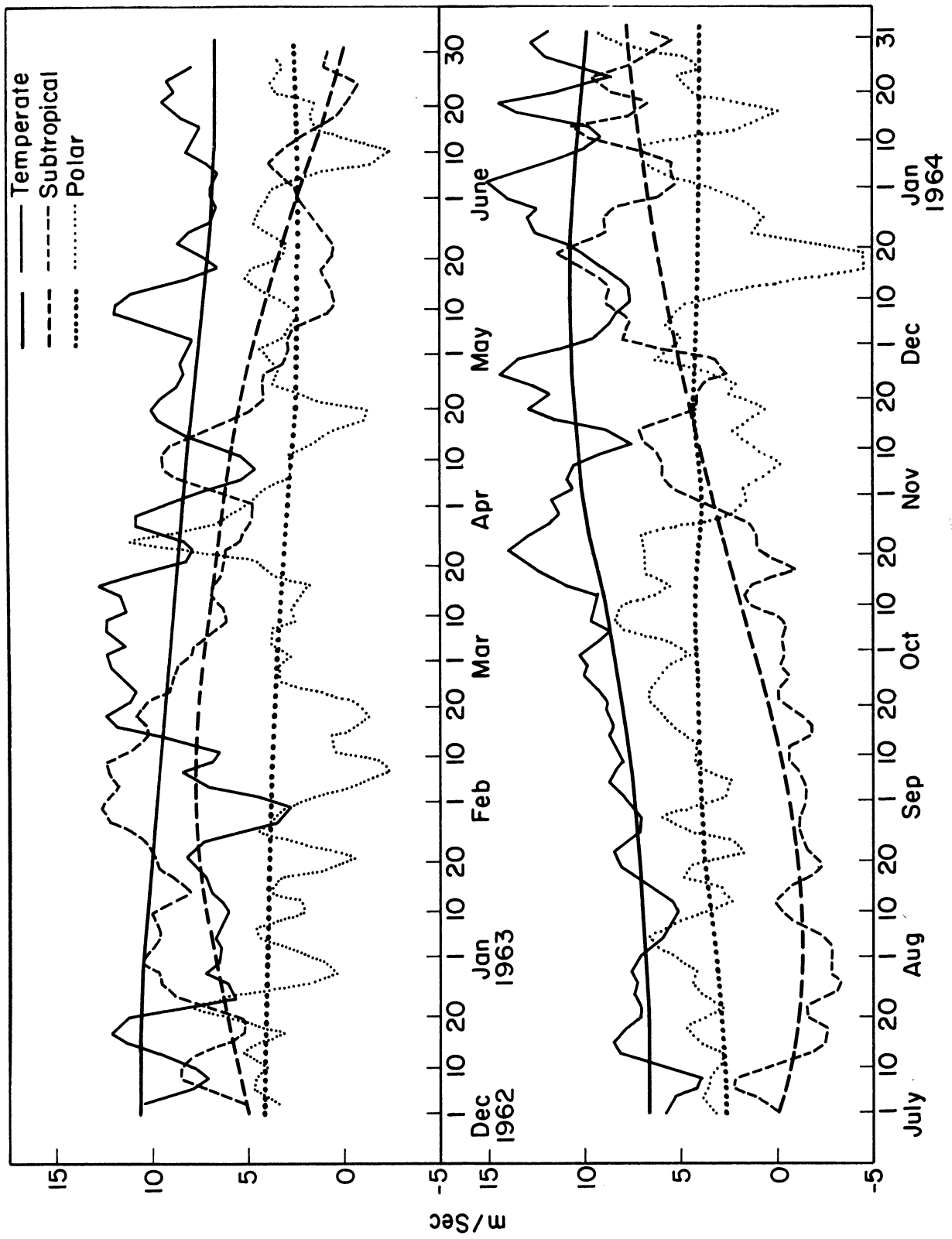


PROFILES OF ZONAL WIND AND ZONAL TEMPERATURE, DEC 1963



PROFILES OF ZONAL WIND AND ZONAL TEMPERATURE, JAN 1964

APPENDIX D
ZONAL INDICES



UNIVERSITY OF MICHIGAN



3 9015 03527 5778